ARMY RESEARCH LABORATORY

A Review of Biological Communication Mechanisms Applicable to Small Autonomous Systems

by Kesshi Jordan, Daniel Calderone, Alexandra Rubin, and Alma E. Wickenden

ARL-TR-5340 **September 2010**

NOTICES

Disclaimers

The findings in this report are not to be construed as an official Department of the Army position unless so designated by other authorized documents.

Citation of manufacturer's or trade names does not constitute an official endorsement or approval of the use thereof.

Destroy this report when it is no longer needed. Do not return it to the originator.

Army Research Laboratory
Adelphi, MD 20783-1197

ARL-TR-5340 **September 2010**

A Review of Biological Communication Mechanisms Applicable to Small Autonomous Systems

Kesshi Jordan, Daniel Calderone, Alexandra Rubin, and Alma E. Wickenden
Sensors and Electron Devices Directorate, ARL

REPORT DOCUMENTATION PAGE

Form Approved
OMB No. 0704-0188

1. REPORT DATE *(DD-MM-YYYY)*	2. REPORT TYPE	3. DATES COVERED (From - To)
September 2010	Final	June 2009 to September 2010

4. TITLE AND SUBTITLE
A Review of Biological Communication Mechanisms Applicable to Small Autonomous Systems

5a. CONTRACT NUMBER

5b. GRANT NUMBER

5c. PROGRAM ELEMENT NUMBER

6. AUTHOR(S)
Kesshi Jordan, Daniel Calderone, Alexandra Rubin, and Alma E. Wickenden

5d. PROJECT NUMBER

5e. TASK NUMBER

5f. WORK UNIT NUMBER

7. PERFORMING ORGANIZATION NAME(S) AND ADDRESS(ES)
U.S. Army Research Laboratory
ATTN: RDRL-SER-L
2800 Powder Mill Road
Adelphi, MD 20783-1197

8. PERFORMING ORGANIZATION REPORT NUMBER
ARL-TR-5340

9. SPONSORING/MONITORING AGENCY NAME(S) AND ADDRESS(ES)

10. SPONSOR/MONITOR'S ACRONYM(S)

11. SPONSOR/MONITOR'S REPORT NUMBER(S)

12. DISTRIBUTION/AVAILABILITY STATEMENT
Approved for public release; distribution unlimited.

13. SUPPLEMENTARY NOTES

14. ABSTRACT
The field of biomimetics has grown in recent years as interest in using biology as an inspiration for technology has grown. Biology constantly optimizes mechanisms, materials, and integrated systems through natural selection. These systems and materials can be incorporated into a variety of applications, using the technology that nature has already developed as a launch point for novel solutions to engineering problems. Nature's mechanisms accomplish a variety of sensory, communications, and processing functions in low signal-to-noise ratio environments on the millimeter- to centimeter-scale, using very limited amounts of power. Many of these biological analogs function more reliably and are more sophisticated than the engineered systems that current technology can provide. This survey of selected biological analogs for low-power communication suggests mechanisms that biology has used to communicate and that could be realized in millimeter- to centimeter-scale engineered autonomous systems, with the objective of providing biomimetic inspiration for future technologies.

15. SUBJECT TERMS
Bio-inspired, biomimetic, bio-engineered, low power communications.

16. SECURITY CLASSIFICATION OF:			17. LIMITATION OF ABSTRACT	18. NUMBER OF PAGES	19a. NAME OF RESPONSIBLE PERSON
a. REPORT	b. ABSTRACT	c. THIS PAGE			Alma E. Wickenden
Unclassified	Unclassified	Unclassified	UU	108	19b. TELEPHONE NUMBER (*Include area code*) (301) 394-0094

Contents

List of Figures

List of Tables

INTENTIONALLY LEFT BLANK.

1. Introduction

Natural selection is a powerful experiment that is constantly gathering vast amounts of data and repeating trials to optimize the "fitness" of a species for their given environment. Biological organisms have evolved to optimize power because as the efficiency of an organism increases, so does the amount of excess energy available to the organism for the goals of survival and propagation. Through the study of these highly optimized systems, researchers can channel natural selection in the development of biomimetic technologies, saving time and resources by taking advantage of nature's experimentation.

In the development of communication systems, the parameters by which living systems are constrained lend themselves to general trends (Fletcher, 2005). Larger species generally have a lower population density, so they must communicate over longer distances to reach other members of their species. For this reason, the frequency of their acoustic communication is usually very low so that the signal will not attenuate before it reaches the other organism. Smaller animals usually have a higher population density because they consume fewer resources, so a smaller zone of the environment can support the population. These species generally cannot produce low frequency signals due to the size constraint on their emitter geometry, and rarely need to because their communications are typically over short distances. When organisms such as these need to send signals over large distances without the ability to generate low frequency signals, they can use chemical communication to accomplish the data transfer (Johnson, 2010). Table 1 summarizes the advantages and disadvantages of different communication channels.

Table 1. Characteristics of different biological channels of communication (Wyatt, 2003).

Characteristics of Different Biological Channels of Communication

Feature of Channel	Chemical	Acoustical	Visual	Tactile
Range	Long	Long	Medium	Very short
Transmission rate	Slow	Fast	Fast	Fast
Flow round barrier?	Yes	Yes	No	No
Locatability of sender	Difficult	Medium	High	High
Energetic cost to sender	Low	High	Low to moderate	Low
Longevity (fade-out)	Variable, potentially high	Instantaneous	Instantaneous	Short
Use in darkness	Yes	Yes	No (unless make own light)	Yes
Specificity	Potentially very high	High	More limited	Limited

Table: Alcock (1989)

The following review examines a wide variety of biological analogs for low-power communication. Specific examples of biological mechanisms and their applications are organized into sections by mode of communication employed. These sections include acoustic, chemical, tactile, electromagnetic, and optical sensing.

2. Acoustic

Most animals use auditory transmitters and receivers in some form, whether in predation, escaping predation, or for intra-species communication. Species have evolved to suit their environment and to best complete the tasks that ensure their survival. For this reason, trends across species, caused by natural selection pressures, appear in many areas of biological study. Organisms typically want to maximize the distance that they can communicate, which depends on both power and frequency. These dependencies have strong trends across air-breathing animals in which (Fletcher, 2005)

$$d \propto m^{-0.6} \text{and } f \propto m^{-0.4} \tag{1}$$

where

m = mass of animal's body

f = dominant frequency

d = communication distance

Figure 1 illustrates this calculation, showing the distribution of dominant frequencies for a range of air-breathing animals (Fletcher, 2005).

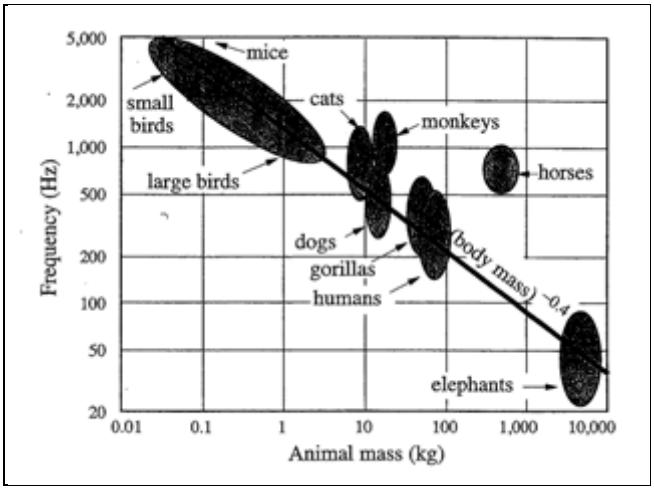

Figure 1. Distribution of dominant frequencies for a range of air-breathing animals (Fletcher, 2005).

The mammalian vocalization mechanism is generally consistent. The lungs compress the air and the vocal organ controls the frequency of the sound produced using muscle tension. This method is very inefficient (at high sound levels its maximum efficiency is 1%), but advantageous in its wide frequency range. A general output maximum is on the order of 10 μW per kg of body mass (For 90 dB at 1 m: human ≈10 mW and elephant ≈1 W). Birds and insects are much more efficient. Birds have two valves that share the work of producing sound, and insects use other methods, discussed later, to improve their efficiency. A cicada weighing less than 1 g can produce up to a milliwatt (80 dB at 1 m) of sound energy, which is comparable to an opera singer's output (Fletcher, 2005). The cicada can produce a sound output comparable to a human roughly 70,000 times its size (assuming m_{cicada} = 1 g and m_{singer} = 70 kg).

2.1 Bat Echolocation

Some of the best understood acoustic sensory systems in the animal kingdom are those that bats use for echolocation systems. Many species of bat emit high frequency sound pulses and then analyze the echoes to map their environment. In general, bats use two types of calls typically within the range of 30–80 kHz (*Encyclopædia Britannica*, 2010a) to obtain different types of information about the environment. When scanning for objects at long range in the open air, bats use long duration, constant, low frequency pulses with long time delays between each pulse. These lower frequency pulses do not attenuate as quickly, giving the bat a longer viewing range. The longer time delay between pulses also gives them more time to analyze the returning echo (Holderied, Baker, Vespe, and Jones, 2008). When flying in a cluttered environment or catching an insect at close range, bats use shorter, high frequency calls that sweep over a range of frequencies. Shorter calls help the bat to distinguish between the initial pulse and the echo, and higher frequency sweeping pulses provide a more accurately detailed picture of their surroundings (Simmons and Stein, 1980). Looking at the ear as a system, a large structure called the pinna acts as a resonator for the high frequency signals (*Encyclopædia Britannica*, 2010a). Some bats also emit additional tones at higher harmonics to provide even more accurate localization information (Simmons and Stein, 1980). In order to avoid confusion with the calls of other nearby bats, echolocating bats can adjust their call frequencies, duration, bandwidth, and sweep rate (Chiu, Xian, and Moss, 2009). In some cases, they actually call to each other to coordinate group formation and foraging (Boughman, 1998). When a large swarm exits a cave, for example, only the few bats on the perimeter will echolocate in order to ensure that the individual calls can be distinguished.

Bats create ultrasonic pulses with their vocal chords, with most species also modulating their signal. For example a *Myotis lucifugus* or *Eptesicus fuscus* bat might start a signal at 70 kHz and decrease it to 33 kHz after approximately 0.2 s. Subsequent signals may have different starting and ending frequencies as well, though the energy peak is usually in the middle of the range (approximately 50 kHz in the previous example) (*Encyclopædia Britannica*, 2010a). These signals must be extremely loud to counteract the high attenuation rate of ultrasonic sound in air. Some species of bat can even range up to 137 dB (Milius, 2000). To keep the bat from

deafening itself, the animal has a special muscle called the stapedius attached to its eardrum that holds the drum fixed while the bat is calling. This muscle is able to expand and contract extremely quickly in order to accommodate the 200-Hz duty cycle of the bat call, the highest duty cycle rate in the animal kingdom (Hill and Smith, 1984). It has been observed that bats time their pulses with their wing beats in order to conserve energy. This may be one of the reasons that echolocation is most common among flying animals (Speakman, Anderson, and Racey, 1989). This is not always possible when navigating in high clutter environments because the bat must emit more pulses in order to avoid obstacles (Moss, Bohn, Gilkenson, and Surlykke, 2006). Megachiropteran (*Rousettus aegyptiacus*), the one species of the *Pteropodidae* family to use echolocation, is able to echolocate using signals with a much lower energy content (approximately 4E-8 J/m^2, an order of magnitude lower than other bats), but the mechanism for this ability is unknown (Holland, Waters, and Rayner, 2004).

Electrophysical studies of cochlear potentials of the *Myotis lucifugus* indicate that the bat's sensitivity to an acoustic signal is poor at low frequencies, improves as frequency increases until approximately 2–5 kHz, levels off until 15 kHz, and then generally decreases. The peak sensitivity range for *E. fuscus* is between 4 and 15 kHz, above which sensitivity diminishes quickly. In behavior studies of *E. fuscus*, sensitivity increases between 2.5 and 10 kHz with a sensitivity peak from 10 to 30 kHz and another between 50 and 70 kHz (*Encyclopædia Britannica*, 2010a).

2.2 Insect Acoustic Transmitters

Insect sound-producing mechanisms are as varied as the insects themselves. In general, insects produce sounds in five different ways: by rubbing two body parts together (stridulation), by hitting the ground with their feet, abdomens, or heads (percussion), by vibrating a body part such as a wing, by expelling air out through an opening, and by vibrating a drum-like tymbal membrane (Alexander, 1957). Table 2 shows examples of insects that use different types of sound-producing mechanisms.

Table 2. Insect sound-production methods (Alexander, 1957).

Method	Examples
Stridulation	Crickets, katydids, grasshoppers, beetles, moths, butterflies, ants, caterpillars, beetle larvae
Hitting the ground	Band-winged grasshoppers, cockroaches, death-watch beetle
Body vibrations	Mosquitoes, flies, wasps, bees, others
Expelling air (whistling)	Cockroaches, sphinx moths, short-horned grasshoppers
Tymbal membranes	Cicadas, leafhoppers, treehoppers, spittlebugs

2.2.1 Stridulation: Crickets and Katydids

Stridulation is the process of creating sound by rubbing two rough surfaces together. This method is the most common method of insect sound production. Many insects use stridulation to create sounds and then use secondary resonators to amplify them. A common means of stridulation is running a scraper (or plectrum) across over a more complicated ridge (or file). The plectrum and file can be located on many different parts of the insect's body including the wings, the legs, and abdomen (Bailey, 1991).

Crickets (*Gryllidae*) and katydids (*Tettigonidae*) produce stridulations by rubbing their wings together. In general, the plectrum is located on the costal margin of the right wing and a toothed file is located on the cubital vein on the left wing (Bailey, 1991). The rubbing action is powered by flight muscles, though in some cases the movements can be even quicker than those involved in flight (Josephson and Halverson, 1971). Resonating regions in the wings vibrate and produce sound as the plectrum of the right wing is rubbed along the teeth of the file on the left wing (for wing diagram, see figure 2). The teeth of the file act as a clock escapement with the wing muscles acting as springs (Elliott and Koch, 1985).

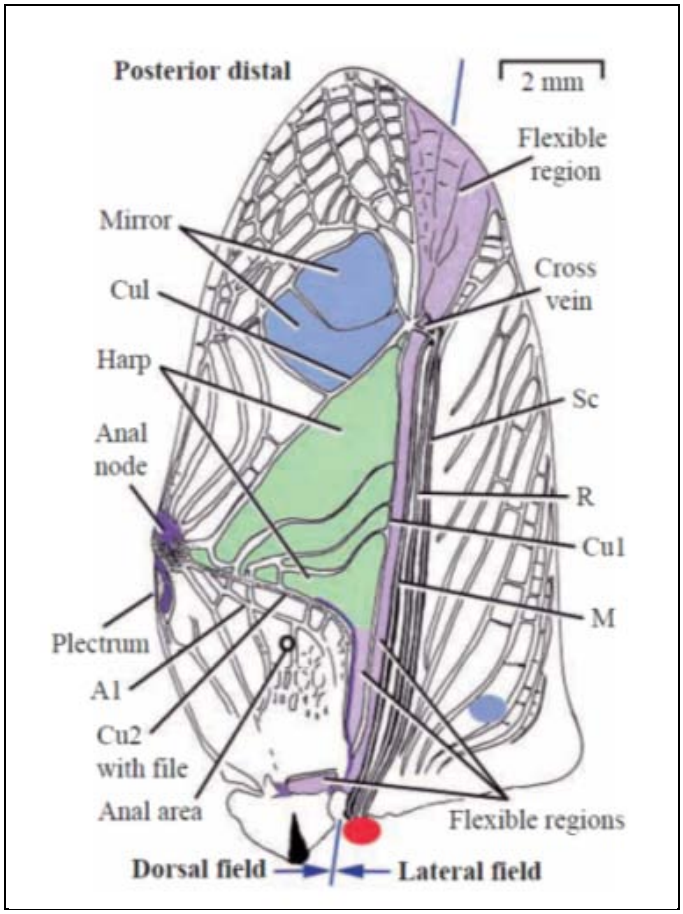

Figure 2. Diagram of a field cricket wing showing the location of the plectrum, file, and harp (Bennet-Clark, 2003).

In tettigonids, the resonating region, called the "mirror," is only located in one wing (Bailey, 1970). As the tettigonid's wing strikes a tooth (figure 3), the edge or "frame" of the mirror is put under tension, deforming the shape of the mirror, and then released. This plucking action causes the mirror to vibrate at its natural frequency, creating the sound (Bailey, 1991). In tettigonids, these vibrations decay rapidly between each tooth strike. The frequency spectrum of these pulses contains many overtone ultrasonic frequencies because of the transient nature of the pulses (Keuper, Weidemann, Kalmring, and Kaminski, 1988; Bailey, 1991). In crickets, the resonating regions, called the "harps" (Michelsen and Nocke, 1974), are slightly larger and are located on both wings. The cricket controls the speed at which it rubs its wings together so that the teeth strike the opposite wing almost perfectly in time with the natural frequency of the harps. This causes the individual pulses from each tooth striking to join together into one longer swelling tone (Bailey, 1991).

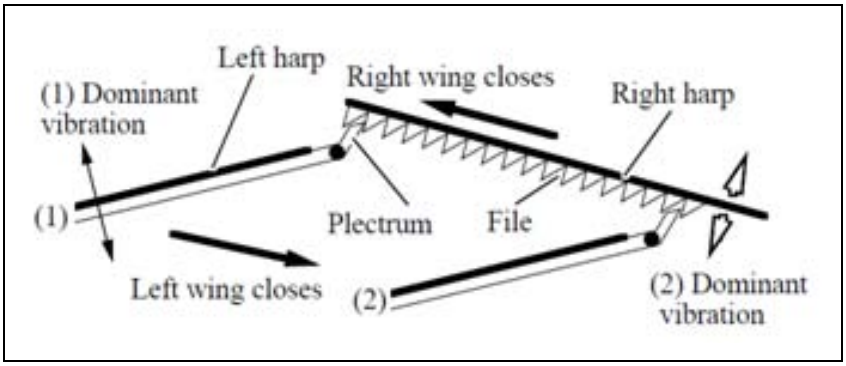

Figure 3. Diagram of a cricket stridulation mechanism (Bennet-Clark, 2003).

2.2.2 Percussion

2.2.2.1 Agaristid Moth

Some insects strike their wings or legs together to produce percussive sounds. Striking wings together is especially common in butterflies and moths (*Lepidoptera* and *Noctuidae*). The Agaristid moth (e.g., *Hecatesia exultans* and *Hecatesia thyridion*) has castanet-like structures on the leading edges of its forewings. These structures consist of hard knobs, each surrounded by a band of pleated, pliable cuticle (figure 4) that resonates with a very pure tone of 30 kHz. To produce sound, the moth claps the heavy castanets together and cups its wings to amplify the sound. The cupped cavity formed by the wings is almost exactly one quarter the wavelength of a 30 kHz sound wave, making a perfect resonator. The *H. exultans* moth produces a very pure tone of 30 kHz, where as the *H. thyridion* produces a broad-band signal in both the ultrasonic and audible ranges (Bailey, 1978; Alcock and Bailey, 1995; Conner, 1999; Bailey, 1991).

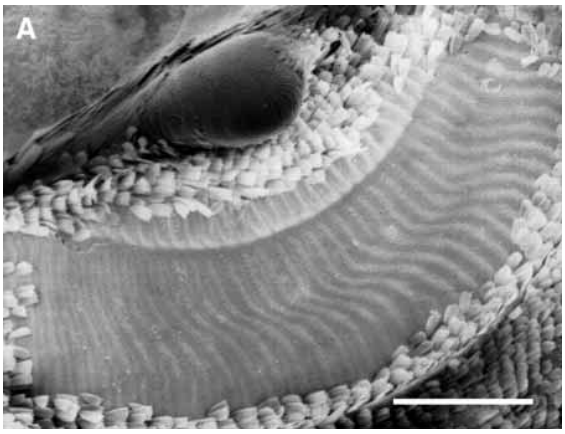

Figure 4. The castanet on the wing of a *H. thyridion* moth showing the hard knob and the pleated cuticle structure. The scale bar is 0.5 mm. (Alcock and Bailey, 1995)

2.2.2.2 Water Strider

Water striders (*Gerridae*) (figure 5) create ripples on the surface of the water by slapping the water with their middle leg or by shaking a larger piece of debris in the water. The surface tension of the water that allows the water striders to walk on the surface also allows them to create these capillary surface waves (Wilcox, 1989). To transmit a mating call, the male uses a frequency range of 17–29 Hz. The females respond to signals in this range and discriminate between signals with an accuracy of 1.5–2 Hz. These signals can propagate as far as 20 to 35 cm and still be understood by females. (Wilcox, 1972). Along with calling for females, males use their signals to warn other males away once they have attracted a mate. These warning signals have the same base frequency as the calls to attract females, but use a different pattern (Wilcox, 1972).

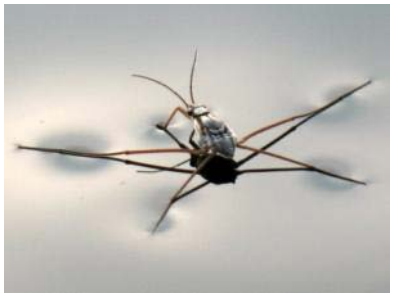

Figure 5. Water strider (TrekNature, 2008).

This form of acoustic communcation is categorized as vibrational waves; a signal that is produced by percussion that can propagate across a medium other than air. Such an idea has been applied to sensors in the siesmic field, using accelerometers to receive a seismic signal and calculate its strength in the form of siesmographs.

2.2.2.3 Applications

Based on the water strider, a research group has built a controllable tethered biomimetic device that is capable of walking on the surface of water using surface tension forces. This biomimetic water strider weighs about a gram with each of the four supporting legs able to support approximately 0.5 g (Song, 2006). The biomimetic water strider is also capable of moving at 2.3 cm/s and turning at 0.5 rad/s. It uses piezoelectric actuators to create an elliptical motion at the tips of two 0.33-mm Teflon-coated stainless steel legs to move across the water. The biomimetic water strider also creates waves on the surface of the water, as the real one does to communicate. Further research into using these waves for novel communication has been recommended (Suhr, 2005).

The same group has also performed further research on the design of water-walking robotic legs. They built a platform with 12 support legs, each able to support 0.8 g. This model is capable of lifting 9.3 g (Song, 2006). Using 12 of these legs for support, with two additional motorized legs, the researchers have built a non-tethered water strider robot, the Surface Tension Robotic Insect Dynamic Explorer (STRIDE), which weighs only 6.3 g, leaving 3.7 g for a payload (figure 6). This robot is also capable of moving at 8.7 cm/s and turning 0.8 rad/s (Song, 2007). Unlike the smaller first water strider robot, this robot uses a lithium-polymer battery for power, micro-switches to change direction, and two miniature DC motors for locomotion (Didel MK04S-24), creating a paddle-wheel type motion.

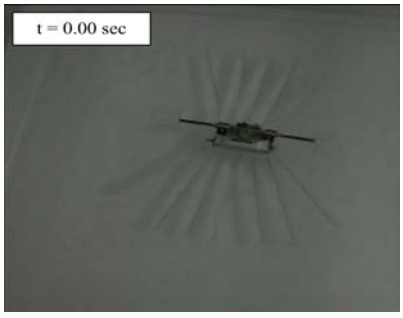

Figure 6. STRIDE robot (Song, 2007).

2.2.3 Tymbals

The sound producing mechanism of the cicada (*Cyclochila australasiae*), one of the loudest insects (Young, 1990), consists of a large tymbal plate parallel to a series of vertical ribs, surrounded by a springy pad of resilin (an elastic protein found commonly in arthropods) (*Encyclopædia Britannica*, 2010b). Figure 7 shows a diagram of the cicada tymbal resonator and its location on the insect's body.

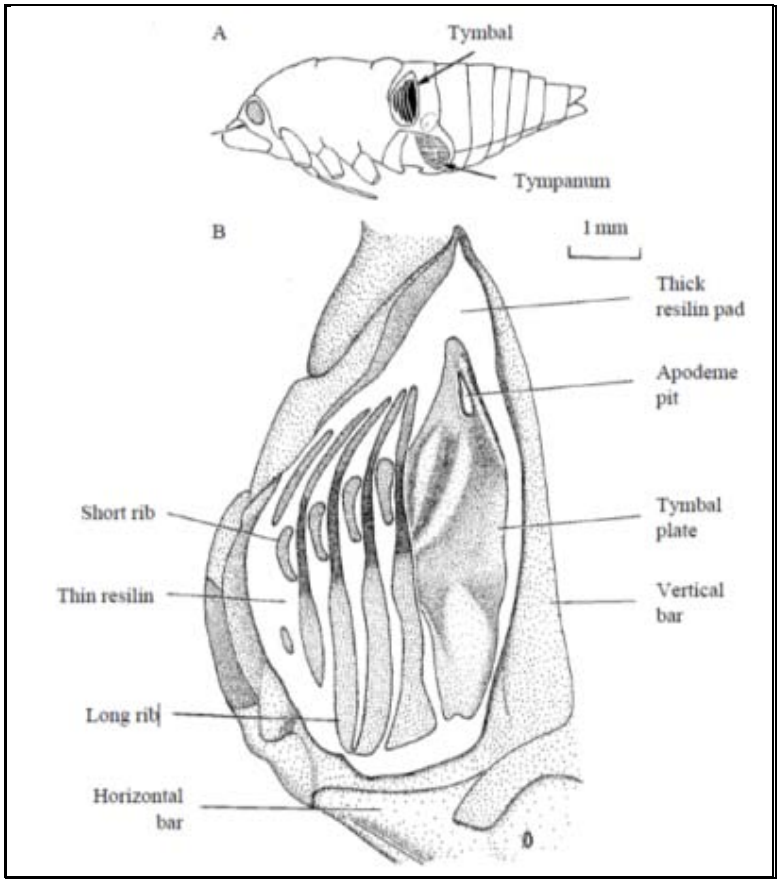

Figure 7. Diagram of the cicada tymbal resonator and its location on the insect's body (Young and Bennet-Clark, 1995).

To initiate sound, muscles around the tymbal contract, axially loading the ribs and plate. As the force increases, the ribs buckle in succession, with about 2 ms in between each buckling event (Bennet-Clark, 1999). As each rib buckles, the tymbal plate also buckles inward sharply, and then snaps back out due to the springy counter force of the resilin pad, producing a loud click (Young and Bennet-Clark, 1995). As each rib buckles, it becomes loosely coupled to the tymbal plate, vibrating with it and increasing the mass of the resonator (figure 8). This increase in mass decreases the frequency of the vibration from an initial frequency of 4.4 to 4.2 to 3.9 kHz as the three main ribs are coupled to the membrane (Bennet-Clark, 1999). The vibrations from the buckling tymbal plate create pressure waves that resonate the air inside a large abdominal air sac. The air sac acts as a Helmholtz resonator with the tympanal membrane (the cicada's ear-drum) on the side of the sac acting as the neck of the resonator. The majority of the sound appears to be radiated out through this tympanal membrane (Young, 1990). Peak pressure values in the air sac can reach 155–159 dB SPL (sound pressure level). The sound is radiated out of the air sac through tympanic membranes on the side of the abdomen. Outside the tympana, peak pressures reach approximately 149 dB SPL (Young and Bennet-Clark, 1995). Figure 9 illustrates the tymbal, air sac, and tympanum.

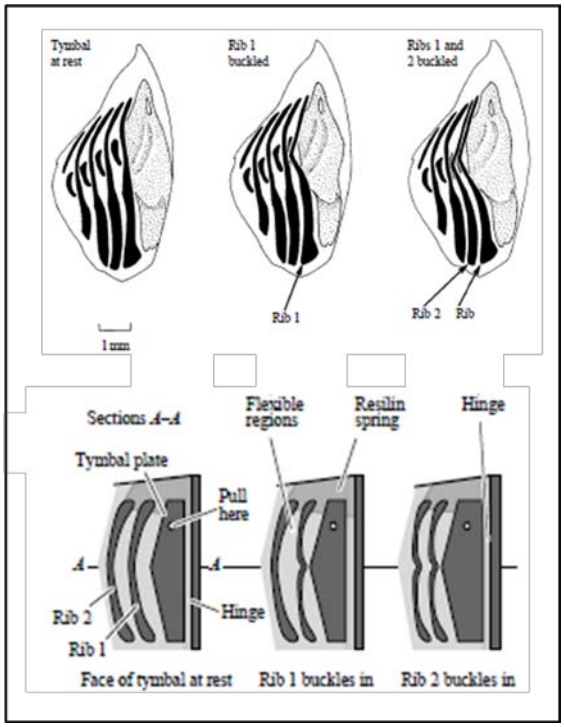

Figure 8. Schematic of how the tymbal resonator works (Bennet-Clark, 1999; Young and Bennet-Clark, 1995).

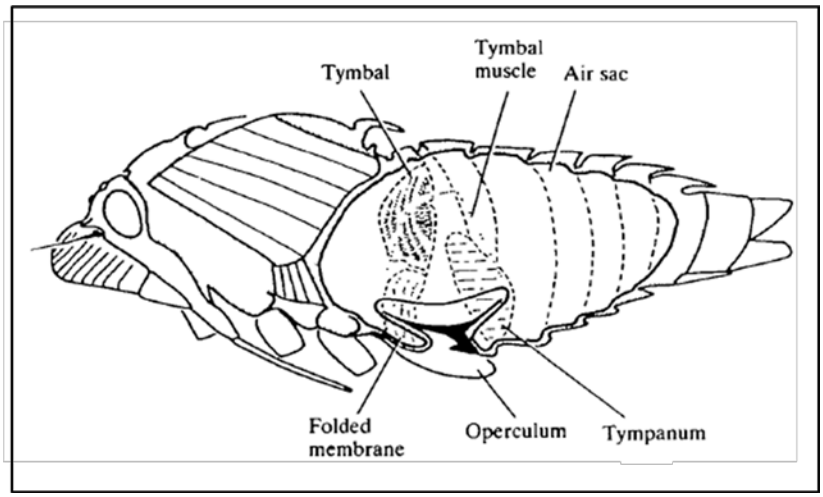

Figure 9. Diagram of the tymbal, air sac, and tympanum (Young, 1990).

2.2.4 Resonators

One challenge with insect acoustic communication is the small size of the sound-producing mechanism. Typically, for good impedance matching between the sound producing organ and the surrounding air, the diameter of the resonator must be greater than one-third the wavelength of the sound. To enable effective sound production, many small insects that produce loud sounds have larger secondary resonators driven by the smaller primary resonators that actually

produce the sound. In the cicada, a large abdominal air sac, which can be modeled as a Helmholtz resonator, serves this purpose. The mole cricket (*Gryllotalpa vineae)* digs out a tunnel with a cavity at the end to serve as its resonator. When these secondary resonators are used, insect sound systems can be very efficient. The cicada appears to have a sound transduction efficiency of 18–46% and the mole cricket is estimated to have efficiencies of 17–34% (Bennet-Clark, 1999).

2.2.5 Expelling Air

Some cockroaches whistle through breathing holes in their abdomen called spiracles. The giant Madagascar cockroach (*Gromphadorhina portentosa)* (figure 10) has an especially large horn-shaped structure (1 cm in length for the average adult male) connecting its tracheal tube to one of its spiracles (Nelson, 1979). The tube is thinner where it connects to the trachea and widens out to the place where it connects to the spiracle. The opening of the spiracle is covered with a flap, which can be opened and shut by opposing muscles. The cockroach makes a hissing sound by forcing air through the thin opening between the trachea and the tracheal horn. The sound is then resonated in the larger horn volume. The hiss is a relatively broadband signal, but the most pronounced frequency falls at 8.5 kHz, consistent with the resonant frequency of the horn. There are also less pronounced higher harmonics. To distinguish between signals in various social contexts, cockroaches amplitude modulate the signal. The amplitude of the hiss is affected by several things, including the amount of air moving past the tracheal constriction, the initial tracheal volume, the cockroach's expiration rate, and the degree and rate of opening of the spiracle valve. The movement of the valve is probably the most important factor, since it allows the cockroach to change the amplitude of the pulse during one expiration cycle (Nelson, 1979). Along with hissing, the *Elliptorhina chopardi* cockroach (a similar species to the *G. portentosa*) can also create pure tone whistles consisting of two independent harmonic tones emitted together (Sueur and Aubin, 2006). These hisses and whistles propagate both through the air and through the ground simultaneously. In the signals propagating through the ground, some of the harmonics are filtered out, focusing the acoustic signal in a narrower frequency band. Along with having two independent voices, the cockroach's signal is fast frequency modulated, making it one of the most complicated signals in insect communication. Currently, the sound receiving mechanism in the cockroach is not fully understood. Lacking a tympanum on its body, some species of cockroach do have vibration sensors in their legs, but these are only known to respond to lower frequency vibrations (Sueur and Aubin, 2006).

Figure 10. A giant Madagascar cockroach (*G. portentosa*) (Myers, 2008).

2.3 Insect Ears

Insect ears are some of the smallest, most efficient acoustic receivers in the animal kingdom. Developed separately in many different species, these organs have a wide variety of uses from detecting predators or prey to finding a mate. Many of these tiny organs display novel approaches to acoustic signal reception and processing. Mechanical analogs of these simple sound receivers may enable simple yet powerful acoustic receivers that could be used in a wide variety of applications, such as frequency selective microphones or power efficient echolocation systems.

Insect ears come in two forms, hair-like structures such as those found on some antennae, and membranes. Hairs respond to displacement in air molecules caused by sound or nearby motion of an object (Bailey, 1991) and membranes are similar to the human ear drum, sensing the changes in pressure caused by sound waves (Bailey, 1991). Hairs are ideal for sensing low frequency sounds (e.g., the male mosquito antenna resonant frequency $\approx$0.38 kHz) and membranes are adapted to sense high frequency ultrasonic signals (e.g., the moth tympanic membrane resonant frequency $\approx$50 kHz [Bailey, 1991]).

2.3.1 Antennae

Insect antennae can be extremely sensitive to air flow and displacement. Many arthropods, including crickets, cockroaches, caterpillars, spiders, mosquitoes, and flies, use antennae or hairs to “listen” to movements of predators, prey, a potential mate, or their own body. The following discussion considers mosquitoes and flies. A discussion of spider hairs with relevance to acoustics is covered in section 4.1 on tactile sensing.

A mosquito antenna is a very sensitive and specialized hair acoustic sensor. The antennae of the yellow fever mosquito (*Aedes aegypti*) can sense deflections as small as 7 nm and are still robust enough to withstand the rigors of flight and hard landings. Mosquito antennae have up to 16,000 neurons, comparable to the number contained in the human ear (Robert and Jackson, 2006).

The acoustic sensitivity of the male and female *Toxorhynchites brevipalpis* mosquitos' antennae (figures 11 and 12) has been investigated by simultaneously examining acoustically induced antenna vibrations and neural response (Gopfert and Robert, 2000). As sound waves of a given frequency come in contact with one of the mosquito's antennae, they cause both the main shaft and the smaller hairs to vibrate at that frequency. The main shaft of the female's antennae resonates at 230 Hz and the main shaft of the male's antennae resonates at 380 Hz, the fundamental frequency of the female's wing beats (shown at the top of figure 13). This allows males to listen specifically for the females in order to find a mate. The hairs of the male's antennae are tuned to 2600–3100 Hz (shown in the bottom of figure 13) and are stiffly coupled to the main antennae shaft in such a way that movements of the hairs are transmitted to the neurons at the base of the main shaft. This is thought to improve the acoustic sensitivity of the antennae (Gopfert, Briegel, and Robert, 1999). The organ at the base of the mosquito's antennae is called the Johnston organ. Johnston organs in male mosquitoes can respond to the antennae tip moving as little as ±7 nm. The female's antennae are slightly less sensitive responding to ±11 nm (Gopfert and Robert, 2000). This is thought to be one of the most sensitive motion receivers among arthropods (Gopfert, Briegel, and Robert, 1999).

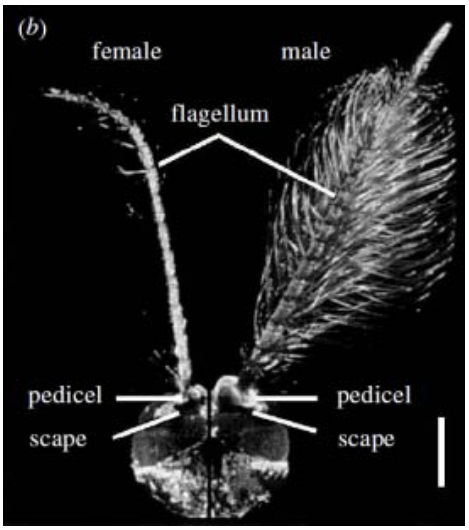

Figure 11. Antenna of a male (right) and female (left) mosquito (*T. brevipalpis*). The scale bar is 0.5 mm (Gopfert and Robert, 2000).

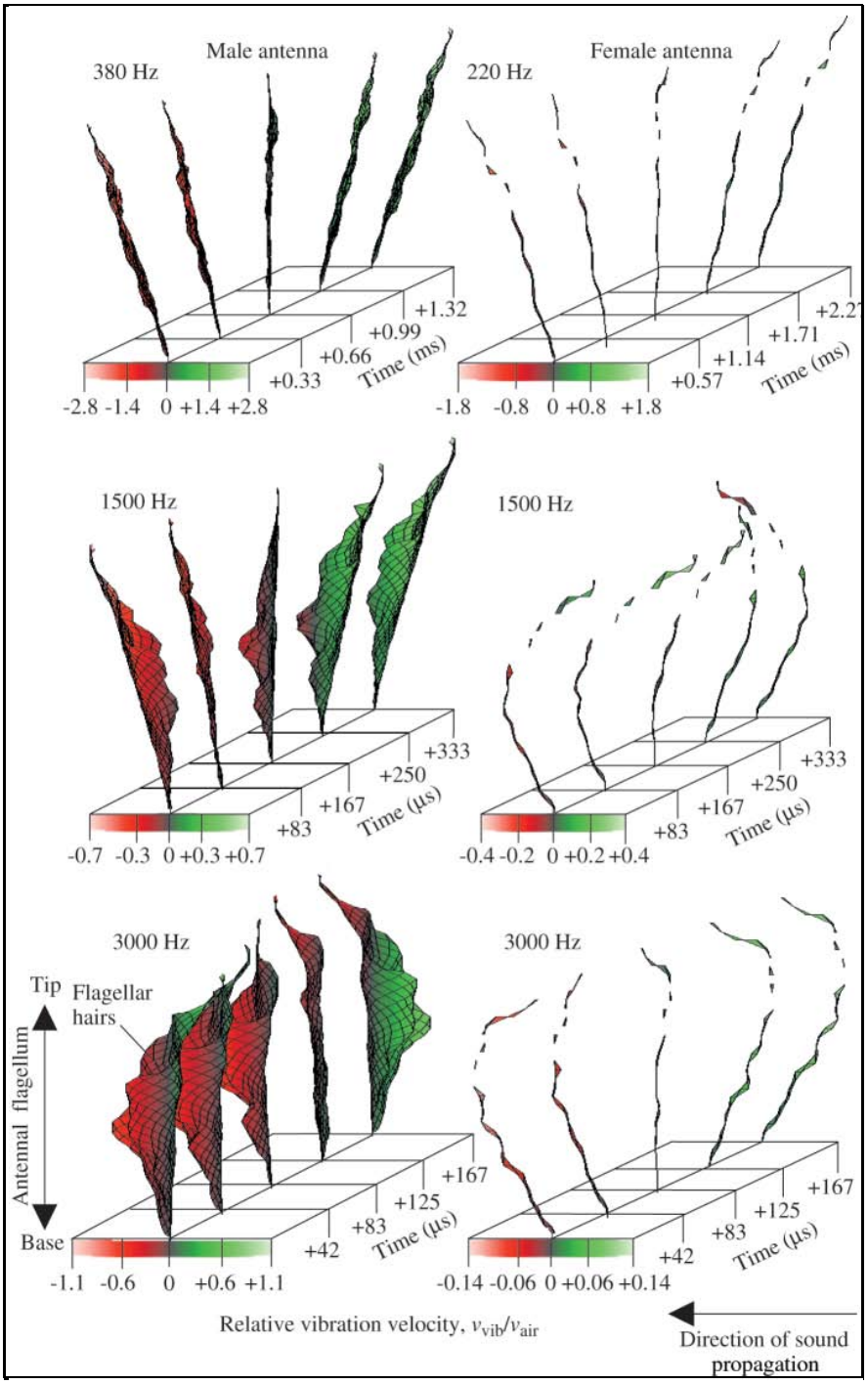

Figure 12. Deflection shapes of male and female antennae at different frequencies. The top figure shows the resonance pattern of the center shaft alone while the lower figures show the resonance patterns of the hairs coming off the central shaft. Notice the greater excitation of the male's antennae compared to the female's antennae. The scale bars is 0.5 mm. (Gopfert, Briegel, and Robert, 1999).

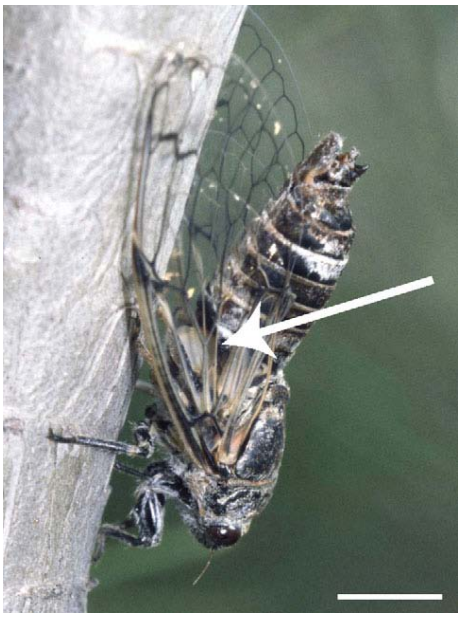

Figure 13. Male *C. atra*. The arrow indicates the location of the ear. The scale is 5 mm. (Picture by Stéphane Puissant/OPIE-LR; Sueur, Windmill, and Robert, 2006).

The mosquito's antenna also exhibits active control, quality factor control, and nonlinear responses (Gopfert and Robert, 2001). When the male hears the sound of a nearby female mosquito, he actively tunes his antennae to sense that frequency more clearly. This tuning is hysteretic, meaning the antennae stays tuned to this frequency for a period of time even after the sound disappears (Robert and Jackson, 2006).

Like mosquitoes, flies (*Calliphora*) also actively move their antennae to amplify specific sounds (Gopfert, Humphris, Albert, Robert, and Hendrich, 2005). Males listen for female's wing beats and females listen for male's courtship songs. Some flies also use their antennae to estimate flight speed by the amount of air flowing past them. Currently, researchers are investigating how flies might listen to the air currents generated by their own wings. It is possible that flies use the echoes from these "self-generated flight tones" during landing maneuvers and to avoid approaching obstacles (Robert and Gopfert, 2002; Robert, 2009).

2.3.2 Membranes

Tympanic membranes are very common acoustic sensors in the insect class. They vary widely in shape, location on the insect's body, function, and operation, and many employ power efficient techniques to receive signals and perform simple analysis on them.

2.3.2.1 General Form

Tympanic membranes usually consist of a thin layer of tissue stretched over an air-filled cavity that allows the tissue to resonate. Unlike insect hair sensors that sense movement of air

molecules, tympanic membranes respond to pressure waves in the air. Some membranes are open to the air, while others can only be reached through slits in the carapace (upper section of exoskeleton) or surrounding tissue that can be widened when hearing is more critical. Some are even covered by special resonating cavities (Bailey, 1991). The nerve receptors that measure the vibration of the membrane are attached in a variety of places depending on the membrane. Some are attached to the back of the membrane with a nerve connected, while others are attached to the edges of the membrane. Sometimes, the main membrane does not contain the sensors, but instead interacts with other associated membranes with sensors on them. The sensory cells respond to shearing stresses created by the stretching and relaxing of the membrane (Bailey, 1991).

2.3.2.2 Frequency Tuning

An insect's tympanic membranes are tuned to listen to specific frequencies that are relevant to its environment, such as the call of a mate or the sound of an approaching predator. While some membranes are tuned to only one frequency, others resonate at multiple frequencies. Some membranes can even distinguish between different frequencies mechanically.

2.3.2.3 Mediterranean Cicada

The ear of the Mediterranean cicada (*Cicadatra atra*) (figure 13) uses the deflection of a special ridge on the tympanic membrane to sense acoustic signals. This ridge (figure 14) is located at the site where the neurons connect to the back of the membrane.

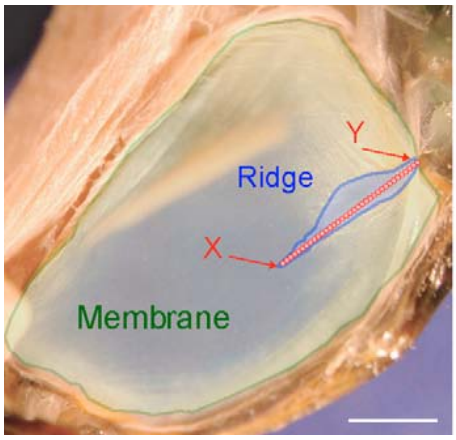

Figure 14. Right tympanum of the male cicada with the ridge labeled. (Sueur, Windmill, and Robert, 2006).

When the membrane is excited, surface waves form on the flat part of the membrane and travel along the ridge. As the frequency of the signal changes, the shape of the ridge deflection also changes. In particular, the location of maximum deflection along the ridge changes as a function of frequency (Sueur, Windmill, and Robert, 2006). Figure 15 shows several high-resolution

scans of the surface waves on the membrane and figure 16 shows the envelope of mechanical deflection of the ridge at several different frequencies.

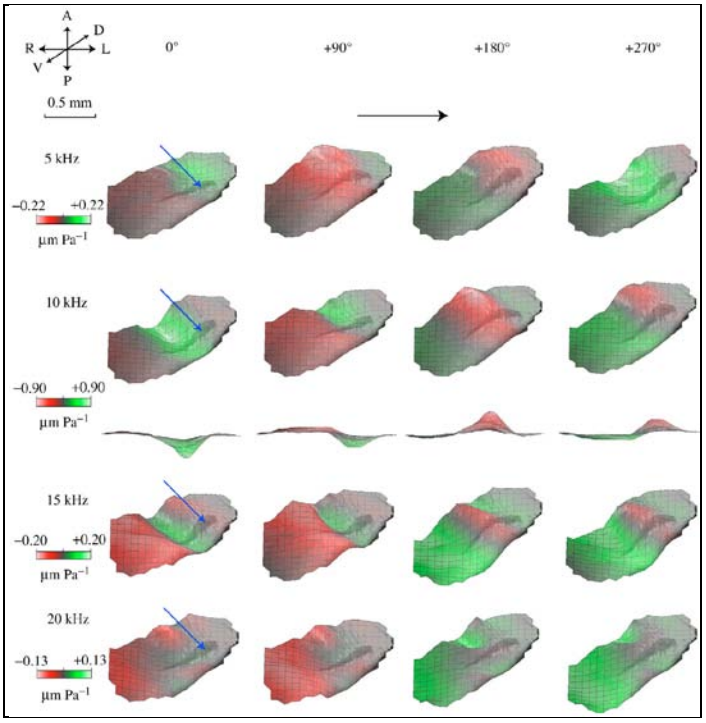

Figure 15. Deflection shapes of a male left tympanal ridge at different frequencies. (Sueur, Windmill, and Robert, 2006).

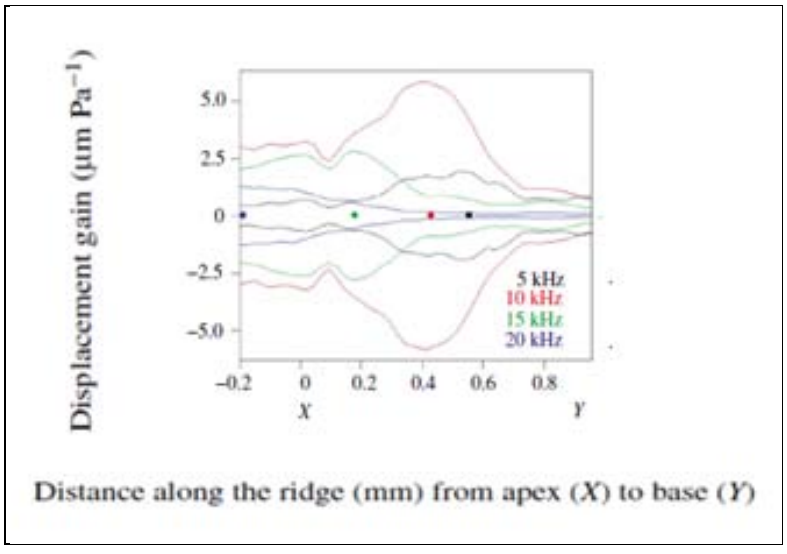

Figure 16. Envelopes of mechanical deflections along the tympanal ridge for different frequencies (labeled by color). The dots indicate locations of maximum deflection for a given frequency. (Sueur, Windmill, and Robert, 2006).

2.3.2.4 Migrating Locust

The migrating locust *(Schistocerca gregaria)* has a different membrane that actually decomposes a sound wave into component frequencies on its surface (figure 17). As travelling waves of different frequencies form on the surface of the membrane, they propagate to unique locations on the membrane, depending on their frequency, where correspondingly tuned neurons are located (Windmill, Gopfert, and Robert, 2005). Figure 18 shows a magnified view of the locust ear and figure 19 shows the deflection shapes of the locust ear at different frequencies.

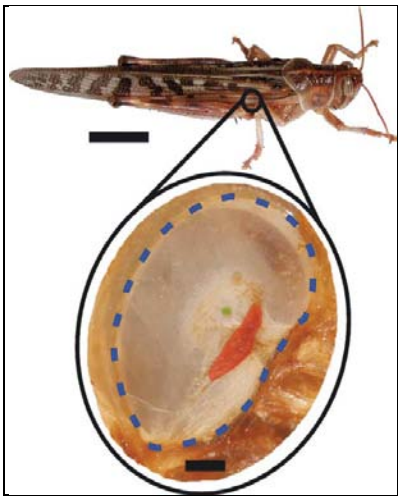

Figure 17. The tympanal membrane of the locust ear and the position on its body. The body scale bar is 12 mm; the membrane scale bar is 200 µm. (Windmill, Bockenhauer, and Robert, 2008).

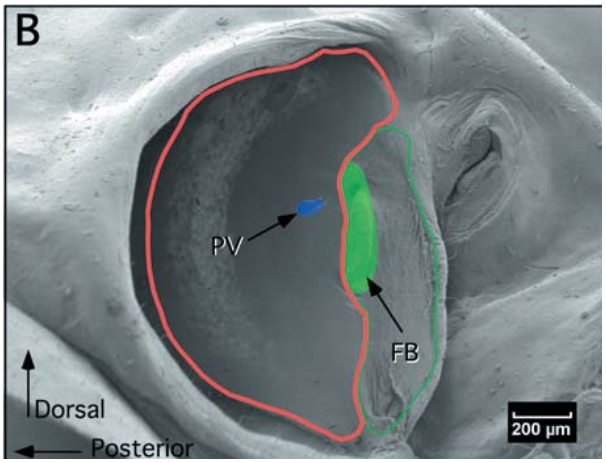

Figure 18. Magnified view of the locust ear. The thin part of the membrane is outlined in red. The thicker part where most of the neurons are located is outlined in green. The blue highlighted region marks the location of the high frequency mechanoreceptors. The green highlighted region marks the location of the low and mid frequency mechanoreceptors. (Windmill, Gopfert, and Robert, 2005).

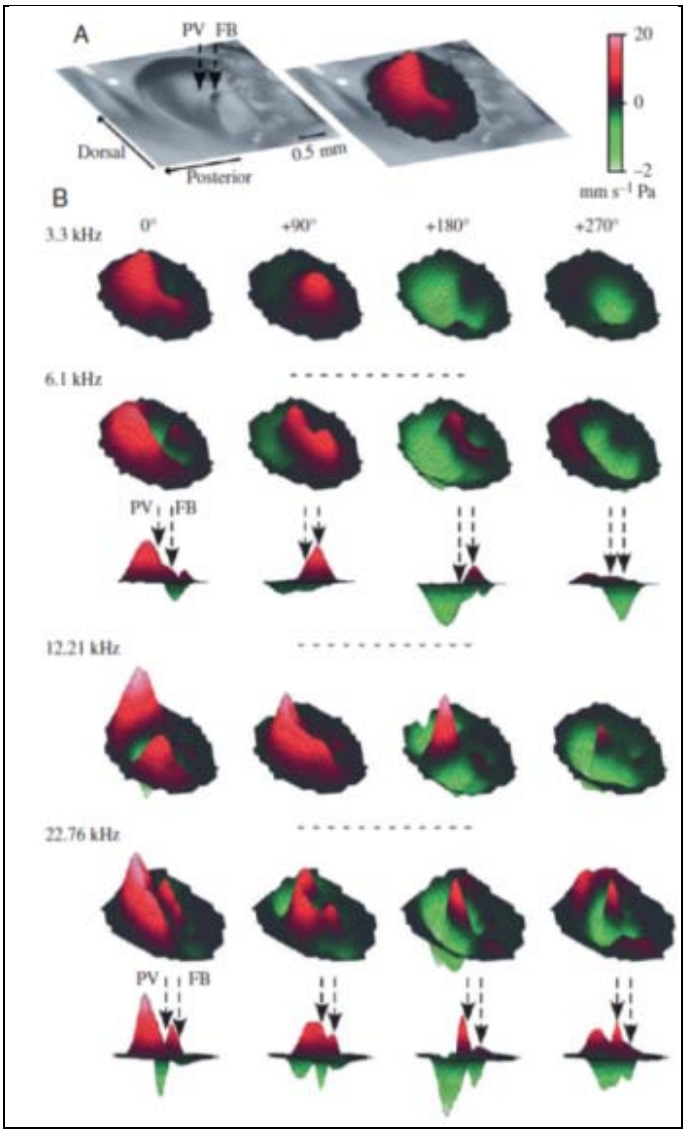

Figure 19. Deflection shapes of the locust ear at different frequencies. Red = positive velocities (outward tympanal deflections), Green = negative velocities (inward tympanal deflections). (Windmill, Gopfert, and Robert, 2005).

Along with being tuned to specific frequencies, some insect membranes have the ability to amplify a signal of interest. Moths are thought to have some of the simplest ears in the insect class. The ear of the noctuid moth has only three receptor cells and the ear of the notodontid moth has only a single auditory neuron (Surlykke, 1984). The moth ear's sensitivity is exceptional, with a suprathreshold vibration amplitude below one nanometer. Recent research, however, has shown that moth ears do not vibrate like simple drums. The noctuid moth has a tympanic membrane (maximum dimensions ≈0.5 mm x 1.5 mm and resonant frequency ≈50 kHz) that deflects mainly at the opaque zone (figure 20), the location where the receptor cells are attached. This might be due to non-uniform thickness of the membrane or non-uniform

tension across it. The tympanic membrane is attached to a larger membrane, the conjunctivum, whose function is no yet determined. The conjunctivum has a resonant frequency much lower than that of the tympanic membrane and moves in anti-phase with membrane (figure 21). It is also possible that other mechanisms surrounding the membrane contribute to the vibrations (Windmill, Fullard, and Robert, 2007). These moths also dynamically tune their ears to bat echolocation calls. The membranes are usually most sensitive to 20–40 kHz frequencies, the lower range of bat ultrasound, but when a moth is attacked by a bat, the ear adjusts its frequency response to hear the higher frequencies of the attacking bat. This tuning up to a higher resonant frequency is hypothesized to be due to a stiffening of the tympanic system. Even after the bat leaves, the moth's ear remains tuned to these higher frequencies for several minutes as the membranes slowly relax again. This hysteretic tuning allows the moth to be ready if the bat should attack again (Windmill, Jackson, Tuck, and Robert, 2006).

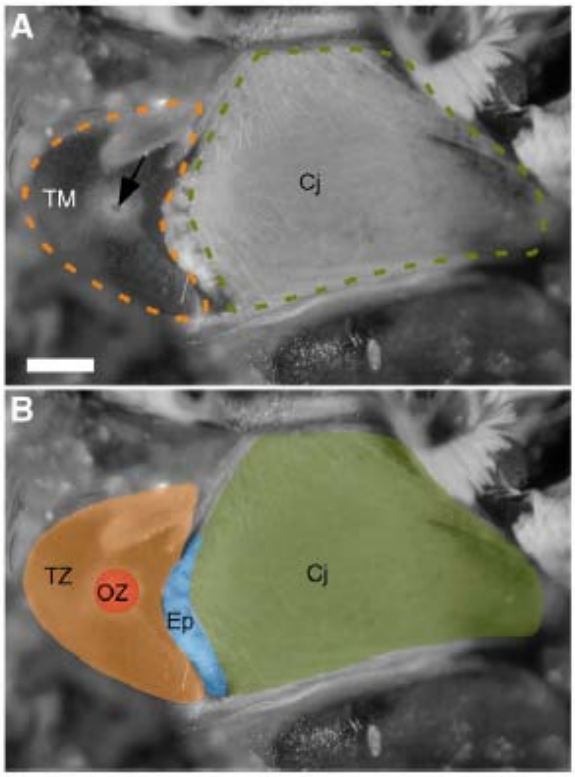

Figure 20. The tympanum (TM) is attached to a larger membrane, the conjunctivum (Cj), and separated by the epaulette (Ep). The transparent zone (TZ) surrounds the opaque zone (OZ), which is the region of the membrane that deflects the most. The arrow in A shows where the auditory chordotonal organ attaches to the TM. The scale bar is 0.25 mm (Windmill, Fullard, and Robert, 2007).

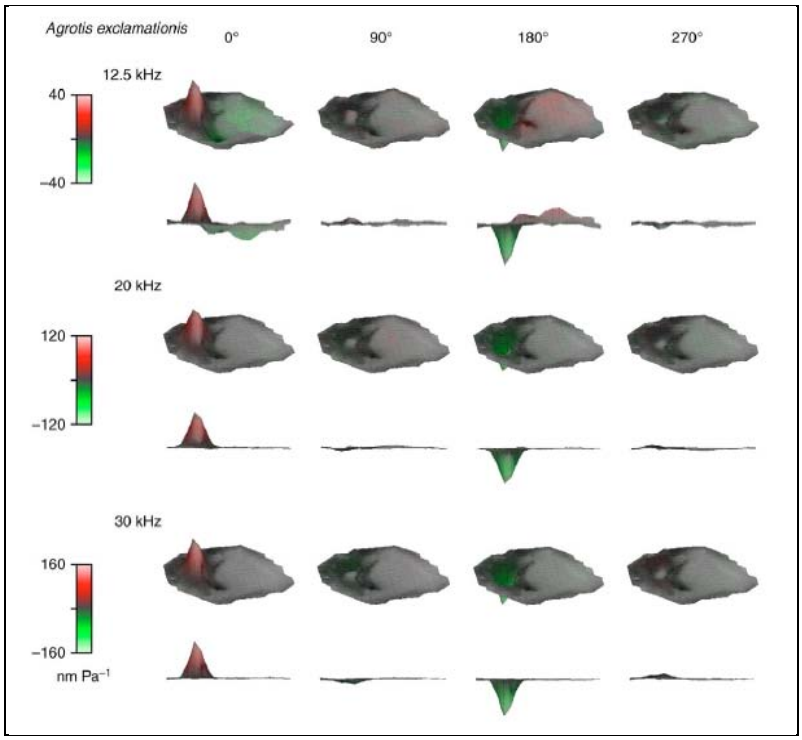

Figure 21. This image shows an area scan and the deflection shapes of the *Agrotis exclamationis* tympanic membrane as it undergoes nonlinear vibration. Red = positive displacement/outward tympanal deflections, Green = negative displacement/inward tympanal deflections (Windmill, Fullard, and Robert, 2007).

2.3.3 Directional Hearing

The parasitoid fly, *Ormia ochracea*, has a unique coupling mechanism between two tympanic membranes that helps it to determine from which the direction that a sound is coming. In larger creatures, directionality of sound can easily be determined by interaural amplitude and time differences between sound waves arriving at two different tympanic membranes. This is not possible for the fly because its small size forces the two membranes to be less than 1 mm apart, so these differences would ordinarily be impossible to distinguish. To solve this problem, the fly is equipped with a small bridge-like structure that couples the two membranes together (figure 22). This coupling bridge increases the difference in vibrations between the two membranes, giving the fly the ability to sense the differences in the incident sound waves, which in turn allows it to determine the direction from which the sound is emitted (Robert, 2001).

A team of researchers at the University of Maryland at College Park and the U.S. Army Research Laboratory have been able to mimic this fly ear in a micro-electromechanical systems (MEMS) microphone. Similar to the actual fly ear, the microphone consists of two circular membranes coupled together with a small beam that serves to amplify the difference between the magnitude and phase of sound waves hitting the two membranes at an angle (figure 23). During the initial tests, the microphone was able to produce amplification factors up to 7 times at an angle of 90°

(directly from the side of the fly's head) (Liu, Currano, Gee, Yang, and Yu, 2009; Currano, Liu, Gee, Yang, and Yu, 2009).

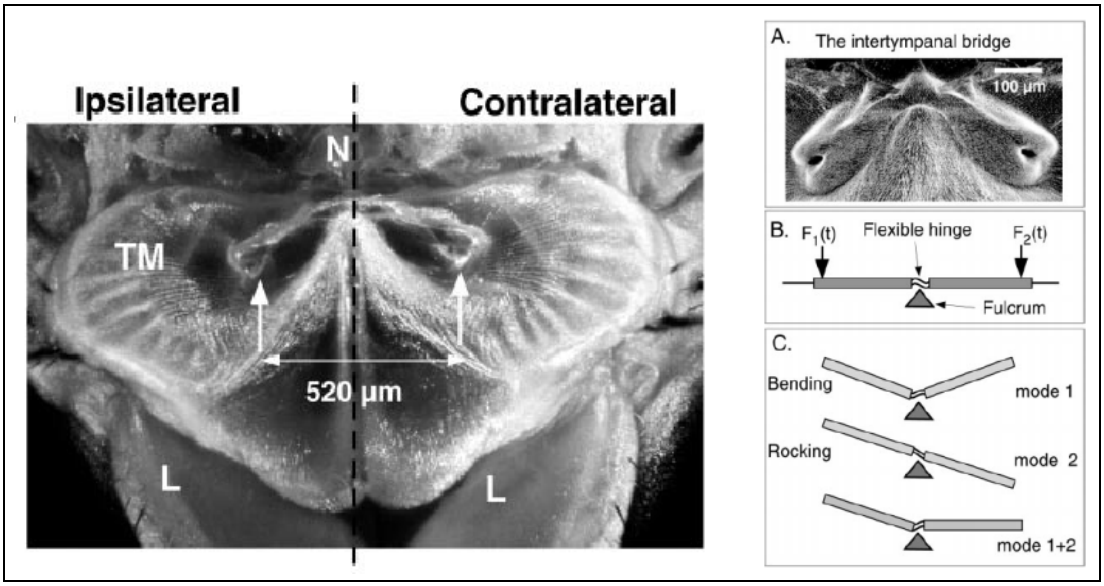

Figure 22. Two fly membranes connected by the intertympanal bridge along with a close-up and schematic of the bridge (Robert, 2001).

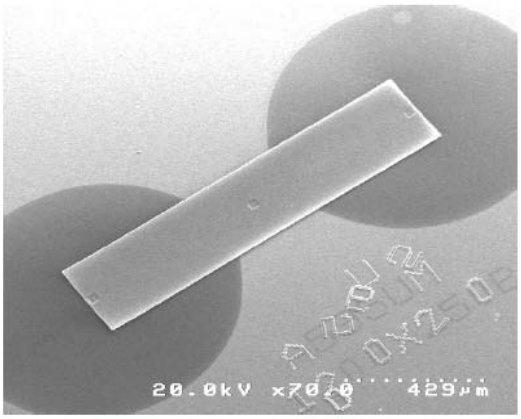

Figure 3: Coupled membrane acoustic localization microphone.

Figure 23. Coupled membrane directional microphone inspired by fly ear (Currano, Liu, Gee, Yang, and Yu, 2009).

3. Chemical

A variety of highly application-specific chemical communication mechanisms are discussed in this section. The airborne release of chemicals by moths are contrasted with the mechanisms of ground-based species like ants that deposit chemicals on the ground to provide a signal after the

organism has left. Mammalian olfaction senses an exceptionally wide variety of chemicals and mixtures, and quorum sensing is a communication performed over an entire colony of bacteria. Snakes use their tongue to transfer molecules sampled form the external environment to a chemosensory organ in their mouth. Also discussed is an analogous pheromone robotics concept that has borrowed concepts from biological organisms without using actual chemicals.

3.1 Pheromones: Moths

Biological organisms use specified organic molecules called pheromones to chemically communicate with their environment and other organisms. This mode of communication is very popular among smaller organisms because the distance-to-power ratio is very high (Wyatt, 2003). Chemical communication can reach over great distances, is not impeded by barriers (unless they are air-tight), can convey a range of complexities of information, and does not require the presence of the organism to continue transmission. In general, an inverse relationship exists between the distance that the signal can travel with accurate reception and the complexity of the signal. A simple signal containing one to a few different types of molecules has a few distinct peaks on a gas chromatograph. This type of signal is easy to distinguish from background noise and thus travels far without distortion because there are only a few components to be accounted for. A complex signal containing many varied molecules has many more peaks on a gas chromatograph and conveys a great deal of information, but only travels short distances before the information is distorted by breezes separating the mixture of molecules and ambient noise (Wyatt, 2003). The disadvantages of chemical communication are that the transmitter generally has little control over the direction of the signal and that the signal, compared to other modes of communication, takes a long time to reach the receiver (Wyatt, 2003). These factors lead to a great deal of disagreement in the ranges and sensitivities of natural chemical communication systems, which may be impacted by wind currents and other environmental interactions.

Pheromones have certain general characteristics that make them ideal for chemical communication. Pheromone molecules typically contain 5 to 20 carbon atoms and have a molecular mass between 80 and 300 amu. Staying above the lower bound allows for an acceptable amount of diversity in the molecules that can be produced, and in some insects, enables greater olfactory detection efficiency. The upper bound exists when the size of the molecule enables molecular diversity beyond utility, thus the energy cost of producing these large molecules exceeds the benefit of extra diversity in signal molecules (Hölldobler and Wilson, 1990). Additionally, pheromones need to be small enough to volatilize, but large enough that they will not dissipate before the signal is received (Walsh, 2000). Alarm pheromones do not require specificity beyond the fact that they are a warning, so their molecular weights are low (between 100 and 200 amu in ants) and often can be received by a number of species, especially if they share a common predator. Pheromones used for mating calls require a greater specificity, thus their molecular weights are higher (often between 200 and 300 amu) (Wyatt, 2003). Different moth species use slightly different molecules for their mating pheromone (figure 24).

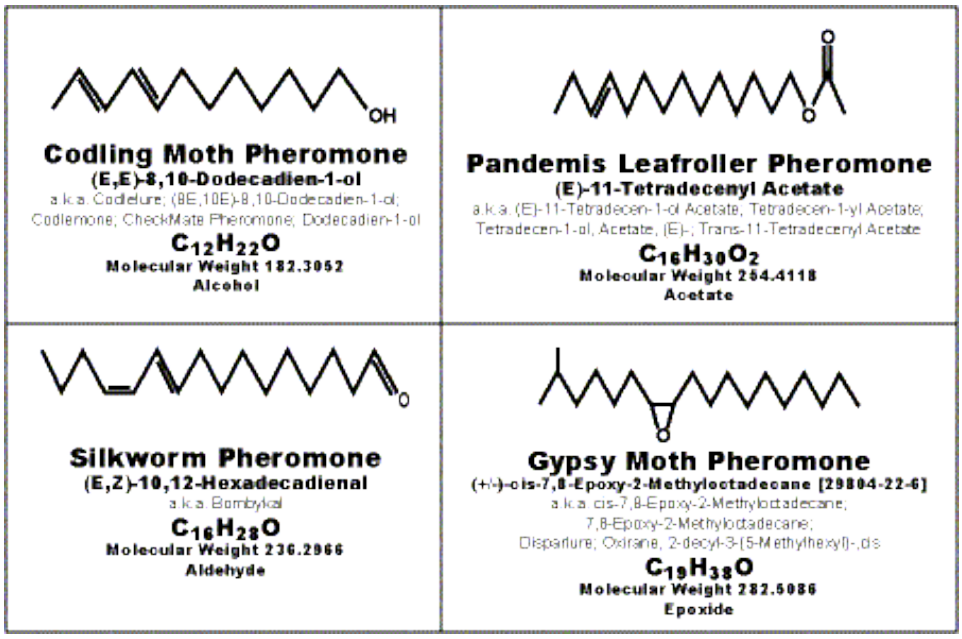

Figure 24. Four variations of the moth pheromone used by different species (Walsh, 2000).

These specific characteristics lead to pheromone structures that are shared by many species with similar purposes for chemical communication, though different species may use the same compound for uses unique to their needs (table 3) (Wyatt, 2003).

Table 3. A summary of compounds used for chemical communication, the organisms that use them, and the specific functions that they are used for (Wyatt, 2004).

		Occurrence	
Compound	Function	Family	Genus
Benzaldehyde	Trail pheromone	Bee, Apidae	*Trigona*
	Defence	Ant, Formicidae	*Veromessor*
	Male sex pheromone	Moth, Amphipyrinae	*Pseudaletia*
2-Tridecanone	Alarm pheromone	Ant, Formicidae	*Acanthomyops*
	Defence	Termite, Rhinotermitidae	*Schedorhinotermes*
Dehydro-*exo*-brevicomin	Male sex pheromone	Mammal	Mouse, *Mus*
Exo-brevicomin	Aggregation pheromone	Insect	Bark beetle, *Dendroctonus*
(Z)-7-Dodecen-1-yl acetate	Female sex pheromone	Mammal	Asian elephant *Elephas maximus*
		Insect	~140 species of moth (as one component of a multi-component pheromone)

After Blum (1982), with additional information from Kelly (1996).

Pheromones released for short-range communication depend on diffusion. The movement of these pheromones can be modeled based on the molecule released, the transmitter, and the receiver. Bossert and Wilson have developed models that represent the active space (the area over which the signal can be detected) of these diffusing signals (equation set 1). These models are based on the diffusion constant of the molecule, the threshold sensitivity of the receiver, the quantity of pheromone, and the time of diffusion (Wyatt, 2004).

The following discussion on diffusion models for pheromones at close range is taken from Wyatt (2003) for contextual reference:

> Bossert and Wilson (1963) developed models to calculate the active space of diffusing pheromone signals, given that there were no fluid currents and that the entire system was small-scale. The following equations assume that the pheromone is diffusing from the ground, so the shape of the cloud is a hemisphere.
>
> Note: This scenario uses 2Q because the molecules can only diffuse away from the ground, but if a model of three-dimensional (3-D) space were required, 2Q would be replaced by Q.
>
> Q = the quantity of pheromone (#molecules released in burst or #molecules/time),
>
> K = threshold sensitivity(#molecules/volume)
>
> D = diffusion constant (cm^2/s)
>
> R = radius of active space
>
> t = time

$$R(t) = \sqrt{4Dt \log\left(\frac{2Q}{K(4\pi Dt)^{3/2}}\right)} \tag{1}$$

For $0 \leq t \leq \frac{1}{4\pi D}\left(\frac{2Q}{K}\right)^{2/3}$

$$R(t) = 0 \; otherwise \tag{2}$$

Equation 2 provides an upper limit on time and radius when the intensity (concentration) is below threshold everywhere.

The radius of the threshold hemisphere increases through time to a maximum R_{max}:

$$R_{max} = \sqrt{\left(\frac{2Q}{K}\right)^{2/3} \times \frac{3}{2\pi e}} = 0.527\left(\frac{Q}{K}\right)^{1/3} \tag{3}$$

At time t_{Rmax},

$$t_{Rmax} = \frac{1}{4\pi De}\left(\frac{2Q}{K}\right)^{2/3} = \frac{.0464}{D}\left(\frac{Q}{K}\right)^{2/3} \tag{4}$$

It then fades out completely:

$$T_{\text{fade-out}} = \frac{1}{4\pi D}\left(\frac{2Q}{K}\right)^{2/3} = e.t_{Rmax} = \frac{0.126}{D}\left(\frac{Q}{K}\right)^{2/3} \quad (5)$$

The equations can be rearranged to give estimates of K or Q as required from the data available (Wyatt, 2003).

Long-range chemical signals are often carried in plumes, which are clouds of molecules carried away from the transmitter by wind currents. The motion of these plumes is not dependent on diffusion, but on the ambient fluidic environment (Wyatt, 2004). Wind, temperature, vapor pressure, and topography all play a role in plume movement (Walsh, 2000).

Olfactory systems in nature are very similar in mechanism, even between mammals and arthropods. The moth olfactory system is extremely sensitive and is a good case to study. To sense these minute quantities of chemicals, the sensory system has olfactory sensory neurons, usually gathered into a nose, antennae, or other sensory organ, that extend from the outside environment directly to the brain. Olfactory receptor proteins are located in the cell membrane, on the surface of small hair-like structures called cilia that reach from the dendrite of the neuron through the mucus layer to the environment (Pyk et al., 2006). The signal molecule is brought to the receptor protein by an odorant binding protein, where it attaches to a receptor protein. Then, proteins in the membrane cause a reaction cascade that sends an action potential down the axon, signaling the antennal lobe of the brain in insects and olfactory bulb in vertebrates (Wyatt, 2003). The action potential from the soma (the end of the neuron where the nucleus resides) signals the brain when the concentration of calcium in the dendrite exceeds a threshold and the membrane is depolarized. The frequency of the action potential depends on the concentration of the signal molecule (Pyk et al., 2006). When the signal reaches the brain, it is received by 100–200 μm diameter balls of nerve cells called glomeruli. Each molecule type signals a different combination of glomeruli, telling the brain what chemical is being sensed. This information is sent from the glomeruli to other parts of the brain where the information is further processed and a response generated (Wyatt, 2003). These olfactory systems can sense a large variety of molecules using combinations of signals from several olfactory receptors. Each molecule has a particular set of characteristics, called odotopes, to which the olfactory receptors bind. A particular molecule will bind to several receptors, and from this combination, the brain will be able to determine the identity of the molecule. Arrays comprised of hundreds of slightly different receptors make these biological systems very sophisticated chemical sensors (Pyk, et al., 2006).

Moths use chemical communication to transmit a mating call. The female silk moth *(Bombyx mori)* emits a bombykol (figure 25) pheromone beacon, called an odor plume, that can be sensed by males at reported distances of hundreds of meters (Pyk et al., 2006) to roughly 10 km (Cotton, 2009). This is remarkable, given that the adult *B. mori* only has a wingspan of 40–50 mm (*Encyclopædia Britannica*, 2010c). There is a large disparity in the reported sensory distance

results due to the uncertain nature of the plume movement. If there is a steady breeze in one direction, the plume may travel a great distance, but if the plume is broken up or stays local to the transmitter from lack of air currents, the communication distance is much shorter. The male silk moth senses the chemical signal using olfactory hairs on its antennae (figure 26) and has a behavioral threshold of 1,000 molecules/mL before it pursues the signal (Kaissling, 2009). The male silk moth can sense a single molecule of bombykol (the female sex pheromone) in 10^{17} air molecules, but current knowledge suggests that the male must sense between 200 and 300 molecules per second in order to follow the signal (Cotton, 2009). The male has been observed to fan his wings when in pursuit of a signal, which may be a mechanism enabling detection of the direction of the signal's origin (Ishida, Nakamoto, Moriizumi, Kikas, and Januka, 2001).

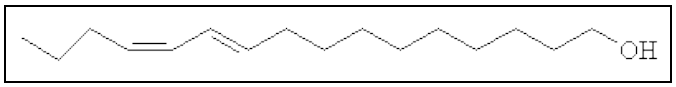

Figure 25. The molecular structure of bombykol (10*E*,12*Z*)-hexadeca-10,12-dien-1-ol.

Figure 26. The silk moth (Kaissling, 2001).

At long distances, the male moth cannot track a concentration gradient back to the female. The signal attenuates significantly as it spreads from the source, and the moth's size in relation to the diffusion of the molecules is too small to sense the gradient. Also, the signal can be distorted by environmental conditions such as breezes. The search pattern that the male silk moth uses is highly effective in a unidirectional wind environment. When the male senses bombykol, it flies upwind until it cannot sense the molecules anymore. Then, it flies in a crosswind pattern, an action known as casting, until it again detects the bombykol molecule. At this point, the moth flies upwind again, continuing this system until he reaches the female. This tracking pattern is illustrated in figure 27. This method ensures that the male is constantly moving toward the female's continuous signal, but will not miss her by following an incorrect trajectory (Kaissling, 1997).

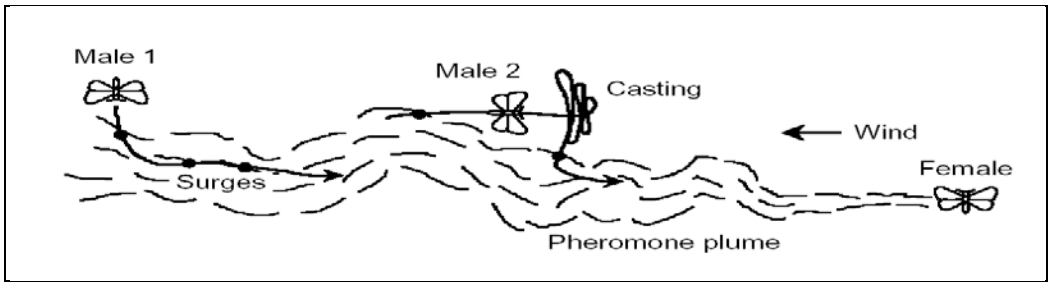

Figure 27. Male moth tracking pattern (Parmentola, 2008).

The silk moth's high sensitivity to bombykol is a direct result of the receptor protein and pheromone binding protein's customization for this target molecule, as well as the exceptionally large number of olfactory sensory neurons. Each antenna has approximately 17,000 sensilla (hairs) with two neurons leading to each one. The hairs channel the bombykol molecule, and of the two neurons on each hair, one is customized for bombykol (Wyatt, 2003). The hydrophobic bombykol molecule enters the sensilla through microscopic pores in the waxy cuticle that envelops the hair, and is then encapsulated and brought through the aqueous sensillary lymph by a hydrophilic pheromone binding protein (figure 28). Given that air currents often carry the pheromone molecules quickly away, this sensory system's response time of 0.5 s enables the moth to follow a constantly moving signal (Sandler, Nikonova, Leal, and Clardy, 2000). The male moth can then fly upwind, searching for the female (Greenfield, 2002). This is an example of a basic type of pheromone that has a very simple gas chromatograph (Wyatt, 2003).

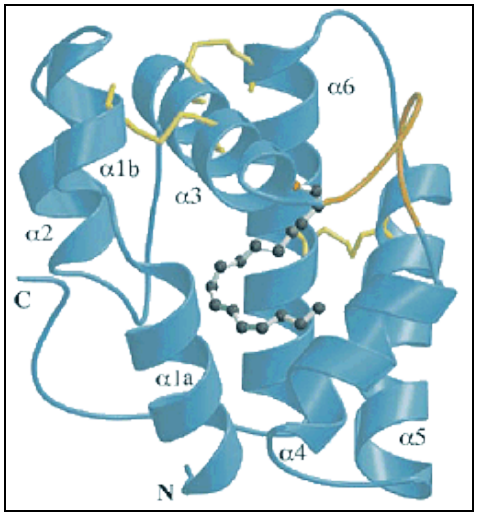

Figure 28. The moth pheromone bombykol is represented with a ball and stick model in the middle of a pheromone binding protein (Cotton, 2009).

Applications

The amoth (artificial moth) is a robot (diameter 20 cm, height 16 cm) with wind direction and chemical sensors whose behavior was modeled after the cast-and-surge pheromone tracking system of the moth, discussed previously (figure 29). The purpose of the system is to search for and localize target chemicals. In the experiment, the system was demonstrated to successfully track ethanol using the male moth casting pattern under varying airflow conditions, including turbulence. A 6-grid array thin-film metal oxide chemosensor was used, which only requires about 270 mW and is very small in size (0.18×0.2 mm). A diagram, schematic, and picture of the printed circuit board are shown in figure 30. The robot, when the chemical sensing system was combined with an optomotor lobula giant movement detector (LGMD) based collision avoidance system, was able to localize the source of the ethanol in the presence of obstacles, but did not find the shortest path-length (Pyk et al., 2006).

Figure 29. The artificial moth robot (diameter = 20 cm) (Pyk et al., 2006).

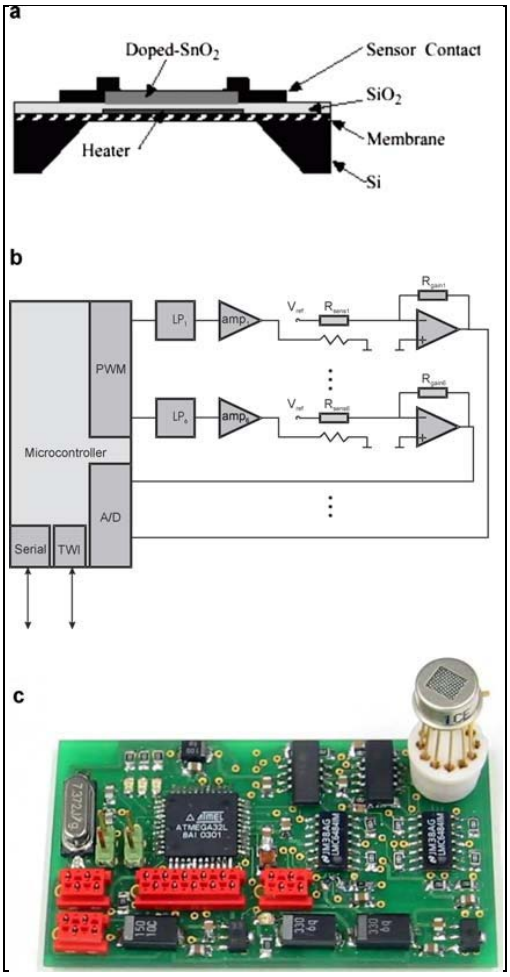

Figure 30. A diagram (a), schematic (b), and picture (c) of the printed circuit board (dimensions ≈7cm x 5cm) (Pyk et al., 2006).

Another group added an "odor compass," mimicking the moth fanning feature, to their robot by attaching a small fan to two sensors. Depending on the direction of the signal, each sensor has different outputs. By rotating the odor compass, the direction of the signal's origin can be determined much more successfully than the simpler model (Ishida, Nakamoto, Moriizumi, Kikas, and Januka, 2001).

3.2 Pheromones: Ants

Ants use chemical communication in two ways. They release a chemical into the environment to signal their location and status, or they leave a chemical trail to be followed by other members of the colony. These small arthropods manage a communication system over a large area using very small amounts of chemical. The Florida harvester ant (*Pogonomyrmex badius*) stores, on average, 16 µg of its primary alarm pheromone, which is a 0.53% payload assuming a 3-mg ant (Hölldobler and Wilson, 1990).

The town ant (*Atta texana*) lays a pheromone 4-methylpyrrole-2-carboxylate on the ground to create trails for other members of the colony (figure 31). To gain a perspective of the potency of this molecule, 0.33 mg of this pheromone would lay a detectable trail around the Earth's circumfrence (USDA-Forest Service, 2010).

Figure 31. Town ants following a diluted trail of their pheromone (USDA-Forest Service, 2010).

Pharaoh ants use chemical communication to transmit to the other members of the colony the location of food and which trails should not be followed (Jackson and Ratnieks, 2006). An ant that finds a food source brings some back to the nest while leaving a trail of pheromones (Brown, 2009). If it is a valuable trail, other ants follow and lay down more pheromones, reinforcing the signal in a positive feedback loop, and attracting other ants to follow (Klarreich, 2006). Pharaoh ants lay down three types of pheromones. Two types are used to lay trails, one of which lasts for 20 min and is used for short-term trails; the other lasts for days and is used leading to longer-term food sources (Jackson and Ratnieks, 2006). If there is a trail that should not be followed, then a different chemical signal is left.

Malaysian ponerine army ants use different types of pheromones with different levels of volatility to send specialized signals. A more volatile compound is a signal for prey because the prey will be gone before the 5-min signal expires. These ants use a less volatile compound that lasts for about 25 min to find their way back to the nest and to communicate with other members of the colony to search the area for prey in a systematic manner (Jackson and Ratnieks, 2006).

Another chemical signal that ants employ is an alarm beacon that calls for other ants when one is in danger. The threatened ant releases a chemical that attracts other ants to come and fight. Different species use unique combinations of molecules for these alarm signals. The species *Phodilus badius* releases the single molecule 4-methyl-3-heptanone, which diffuses a short distance, signals ants close enough to fight, and then fades rather quickly. The African weaver ant (*Oecophylla longinoda*) uses a combination of four molecules: 2-butyl-2-octenal,

3-undecanone, 1-hexanol, and hexanal to send specific messages to ants that are varying distances away (figure 32). This is controlled by the volatility of the molecules released, each of which elicits a different response from neighboring ants (Wyatt, 2004).

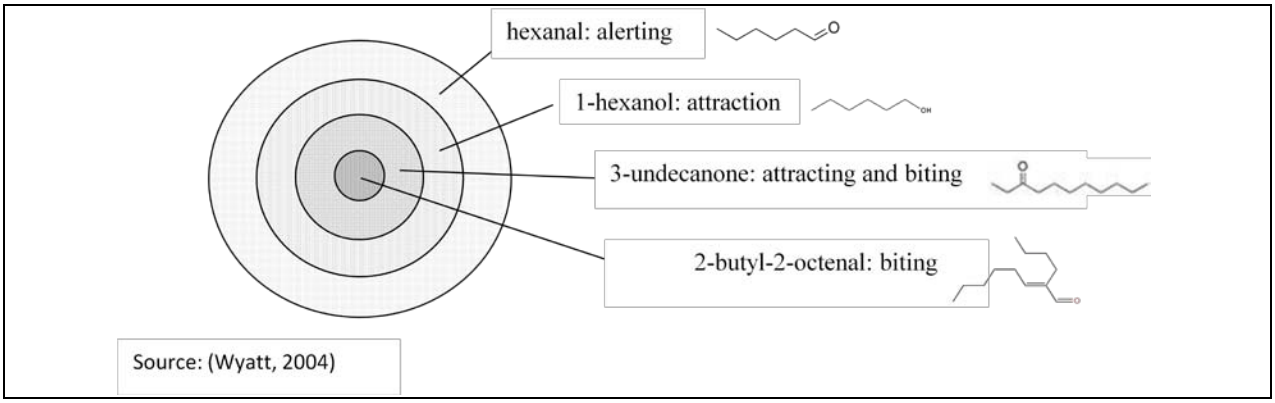

Figure 32. Different layers of signals are created by releasing a mixture of variably volatile molecules. Hexanal is the most volatile molecule and diffuses the farthest to warn other ants. 2-butyl-2-octenal is the least volatile molecule and stays local to the ant, inducing ants in the immediate vicinity to attack (Wyatt, 2004).

Pheromone marks evaporate relatively quickly, so house mice and other mammals that mark their territory often leave waste products containing proteins that gradually release pheromones into the environment. This leaves a longer-lasting chemical signal that does not require the presence of the organism for long periods of time. To maintain the signal, the organism must return to mark the territory again when the proteins are depleted. This signal has a higher energy cost than basic pheromone secretion because the proteins must be produced, and more so because the animal must maintain the signal (Wyatt, 2003). This is an example of a complex signal, informing the receiver on the attributes of the transmitting organism (Wyatt, 2003).

3.3 Air-Breathing Mammalian Olfaction

Mammalian noses use an array of sensors to distinguish between nuances in odors. Each nerve cell has a dendrite, which extends into the nasal cavity and is covered with small hair-like organelles called cilia. Molecules in the air enter the nasal cavity and are dissolved in the mucus coating the dendrites (Kimball, 2009). The molecules then bind to shape-discriminating receptor proteins, which fit with these molecules akin to a lock-and-key scenario. This bond changes the shape of the receptor protein, causing a chemical cascade that sends an action potential to the brain. All of the individual signals together allow the brain to distinguish the nature of the smell and compare it against others in its memory (*Encyclopædia Britannica*, 2010d).

Application

Many different research groups are developing the biomimetic technology for what is called an electronic nose, or ENose, which is modeled after the mammalian nose. The devices that have been tested are very sensitive. They can detect the difference between Pepsi and Coke, sensing a

change of 1 ppm (Miller, 2004). This technology uses an array of sensors (figure 33), the combination of which provides a distinctive "smellprint" that identifies a particular odor. The sensors are made of polymer films, which consist of an organic insulator with conductor dispersed throughout the material. The molecules of the target odor cause the organic insulator to swell, increasing the resistance of the material by increasing the distance between conductor particles. Each sensor is made of a different polymer, and swells differently when exposed to different molecules (NASA Jet Propulsion Laboratory, 2010a). The polymers respond well to organic compounds, bacteria, and natural products (WooriSystems, 2001). The combination of the different polymer swellings creates the smellprint that uniquely defines the odor (Lewis Research Group, 2010) and a software analysis program (pattern recognition or a neural network) can be used to analyze the data (Frequently Asked Questions). The device will take a baseline reading to eliminate noise, and then subtract that reading from the sample it takes to determine the exact smellprint of the target odor (Lewis Research Group, 2010).

Figure 33. ENose Sensor Array (Shope and Fisher, 2000).

The ENose technology was originally developed by NASA to monitor the air in inhabited spacecraft in real time. The device was designed to act in the capacity of a toxic gas alarm, alerting against chemical leaks and spills. The ENose can also detect the molecules that are released preceding an electrical fire and warn astronauts of the danger (Miller, 2004). The third generation device developed by the NASA Jet Propulsion Laboratory (JPL) at CalTech consists of 32 polymer carbon black composite sensors (Dutta, Hines, Gardner, and Boilot, 2002). It is 15 cm long, has a volume of 820 cm^3, has a mass of 840 g, and can be used in conjunction with a personal digital assistant (PDA), laptop, or interface unit to record and analyze data in real time (NASA Jet Propulsion Laboratory, 2010b). The components to the device are the senor unit, microprocessors, power conditioning, and input/output connections for data and power (NASA Jet Propulsion Laboratory, 2010c).

The device underwent a successful 6-month field test in 2009, when it was put into full-time use monitoring the International Space Station (ISS) (figure 34). The device monitored 10 contaminants continuously and identified harmless amounts of formaldehyde, Freon 218, methanol, and ethanol during the course of the test (NASA Jet Propulsion Laboratory California Institute of Technology, 2009).

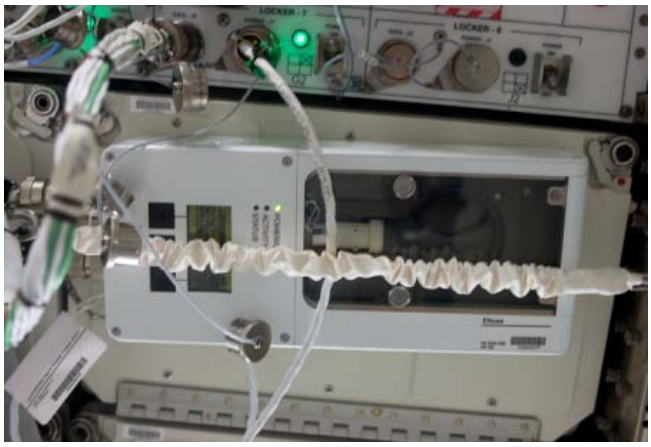

Figure 34. The JPL ENose being used on the (ISS) (NASA Jet Propulsion Laboratory, 2010d).

Using JPL's ENose technology, Cyrano Sciences created the Cyranose 320 for commercial use (figure 35). The specifications are summarized in table 4. This handheld device learns a particular smell, stores that pattern, and can later identify the odor. Caltech has a large ENose technology research group headed by Dr. Nate Lewis. The Lewis Group's current device contains approximately 20–50 different polymeric sensors on 1-mm to 1-cm substrates with the electronics integrated with the sensor elements. The handheld device controls the sensor temperature, collects data form 32 channels, and records the data to a laptop. This ENose functions at atmospheric pressure in a variety of temperatures and humidities. It can track vapors in the air and gives close to real-time data. The device has demonstrated the ability to detect odors in an ordinary room, and then direct a robot toward the source of the odor without the aid of other devices like pumps and carrier gases. To reduce the sensor time, the polymer film thickness could be decreased (Lewis Research Group, 2010).

Figure 35. The Cyranose 320 (WooriSystems, 2001).

Table 4. Specifications for the Cyranose 320 (WooriSystems, 2001).

Weight	< 32 ounces (0.91 kg)
Sensors	32-channel Polymer Composite Sensor Array
Battery Type	NiMH, 4 AA Battery Pack or 4AA Alkaline
Battery Life (Normal Operating Conditions)	3 hours
Battery Charging	< 3 hours with External Adapter
Dimensions	10 x 22 x 5 cm
Universal Power Adapter	110–240 V AC external power adapter
Display	320 x 200 Graphic w/LED Backlight
Response Time	10 seconds
Field Calibration	TBD
Inlet Probe	2- and 4-in needle interchangeable with any standard female Luer Lock or slip adapter.
Keypads	5 Buttons - Scroll Up/Down Select, Cancel, and Run
Communication*	RS-232 Link, 9600 bps
Sampling Pump	50–180 cc/min
Algorithms	KNN, Kmeans, PCA, CDA.
Operating Temperature	0 to 40 °C (32 to 104 °F)
Humidity	0–95%, non-condensing
Storage Temperature	–20 to 50 °C (–4 to 122 °F)
Data Storage Capacity	
Number of Methods	2 onboard Cyranose 320, infinite on PC
Number of Classes per Method	6
Number of Training Exposures per Class	10
Number of Saved Identifications	Upto 100 logged on Cyranose 320, can be downloaded to PC and deleted from Cyranose.

The ability of these devices to localize an odor and identify a chemical is useful in a variety of fields. In the food industry, ENoses are used for quality control and to detect spoiling. In environmental fields, they could identify organic acids in waste water streams and sense gasoline and other contaminants in recycled containers. Many workplaces could use the ENose to profile a chemical environment so that customized safety measures and equipment can be provided, locate any leaks that may occur (WooriSystems, 2001), and then monitor the progress of clean-up efforts (NASA Jet Propulsion Laboratory, 2010b). Medical professionals are working on ways that ENose technology could be used to diagnose patients (Marconi, 2004). Other applications include auto-emissions detection, chemical detection, and location of landmines (WooriSystems, 2001).

3.4 Quorum Sensing

Large colonies of single-celled bacteria use a type of chemical communication system called quorum sensing to coordinate group behavior. These groups act in such synchrony as to resemble a single multi-cellular organism (Bassler, 2008). Each individual communicates chemically with other bacteria, coordinating biofilm construction and synchronized expression of virulence factors, bioluminescence, and sporulation (Higgins, Pomianek, Kraml, Taylor, Semmelhack, and Bassler, 2007).

Each bacterium in the colony sends out a chemical message by producing an autoinducer (a bacteria pheromone) molecule, while simultaneously sensing the local environmental concentration of the molecule. As the number of bacteria in the colony increases, so does the molecular concentration of the autoinducer (figure 36). When the population density reaches a critical point, all of the cells sense the critical concentration at the same time and begin the coordinated group behavior, whatever that may be (Bassler, 2008).

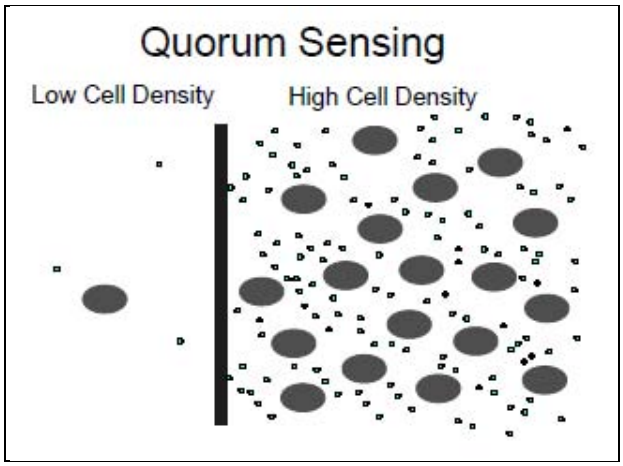

Figure 36. Quorum sensing (Bassler, 2008).

Some bacteria, like *Vibrio fischeri*, use quorum sensing to decide when the group will exhibit bioluminescence. This species of bacteria has a symbiotic relationship with the nocturnal Hawaiian bobtail squid (*Euprymna scolopes*) (figure 37). The bacteria reside in glowing lobes in the squid's light organ, where they are fed by the amino acids and nutrients within. The bacteria colony grows in size, producing an autoinducer, until a concentration of about 10^{11} or 10^{12} cells/mL. When the bacteria reach their critical population size, they begin to luminesce and the squid uses their light to match the moonlight intensity so that they do not create a shadow for predators to track. When the squid burrows into the sand each morning, a pump expels about 95% of the bacteria so that the population is below the threshold, and the light turns off. The remaining bacteria reproduce until they reach they reach the critical population, and then the light turns on again (Bassler, 2008).

Figure 37. Hawaiian bobtail squid (*E. scolopes*) (Bassler, 2008).

One of the most common demonstrations of quorum sensing is the infections of a body by bacteria. Most bacteria repress virulence (turn off the genes that produce toxins) to hide from the immune system until they have a large enough population to overwhelm it. Once the bacteria, using quorum sensing, have established that they have a large enough population, they express pathogenicity in a coordinated effort (Howard Hughes Medical Institute, 2007).

Vibrio cholerae (figure 38), the pathogen that causes cholera, communicates chemically using two molecules: Cholerae Autoinducer 1 (CAI-1) and Cholerae Autoinducer 2 (CAI-2). CAI-1 is used for intra-species communication and is species specific, while CAI-2 is a molecule that many bacteria species share, facilitating inter-species chemical communication (Bassler, 2008).

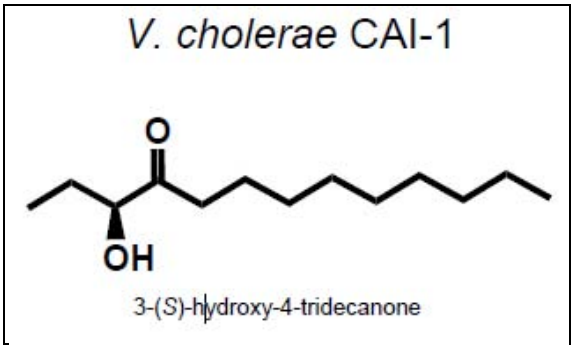

Figure 38. (Bassler, 2008).

When there is a low concentration of autoinducer, expression of virulence factors releases toxins into the body and a biofilm forms to protect the bacteria as their population grows (Higgins, Pomianek, Kraml, Taylor, Semmelhack, and Bassler, 2007). When the bacteria population has

reached its critical point, indicated by the critical concentration of autoinducer, the virulence factors are repressed and genes for an enzyme that detaches the colony from the small intestine turn on. This allows the colony to exit the body en masse and infect other organisms (Bassler, 2008).

3.5 Snakes

Snakes live all over the world and as a result of varying environmental pressures, species in different areas have evolved very differently. One trait that has remained constant across all snakes is the chemoreceptor found on the roof of the mouth called Jacobson's organ (*Encyclopædia Britannica*, 2010e) or the vomeronasal organ (VO), which senses moisture-borne odors (*Encyclopædia Britannica*, 2010f). The snake collects molecules from the external environment with its tongue and then transfers them directly to the VO. The arrangement of the snake's basic chemosensory components is pictured in figure 39.

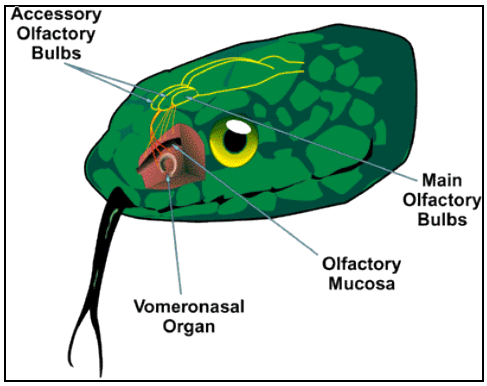

Figure 39. The snake's chemosensory system (Meredith, 2010).

This sense is mainly used in hunting, but is also applied to sensing enemies, tracking other members of the species, and engaging in courtship (*Encyclopædia Britannica*, 2010e). The courtship is accomplished using pheromones as a mating call, and there is also evidence to support the claim that a similar pheromone communication occurs between competing animals in aggressive and territorial signals (*Encyclopædia Britannica*, 2010f). The snake's chemoreception is an integral part of their hunting. When a venomous snake does not have VO sensitivity, the number of strikes they attempt is halved, and they do not follow their prey after striking them (Kardong and Berkhoudt, 1999). With VO sensitivity, a venomous snake will usually strike their prey and then let it go to die. After several minutes, the snake will begin flicking its tongue at a greatly increased frequency as it searches for the prey. The snake can identify, and will choose to follow, the chemical signature of struck prey, even when presented with scents of siblings who were raised under the same conditions (environment and food were consistent). It appears that the snake can both distinguish an envenomated animal from a healthy one, and that it notes the chemical signature of its particular prey when it strikes (Furry, Swain, and Chiszar, 1991).

The nerve that connects VO to the brain is a part of the olfactory nervous system. The main VO's sensory projections that are responsible for carrying chemical information to the snake's brain is depicted in figure 40.

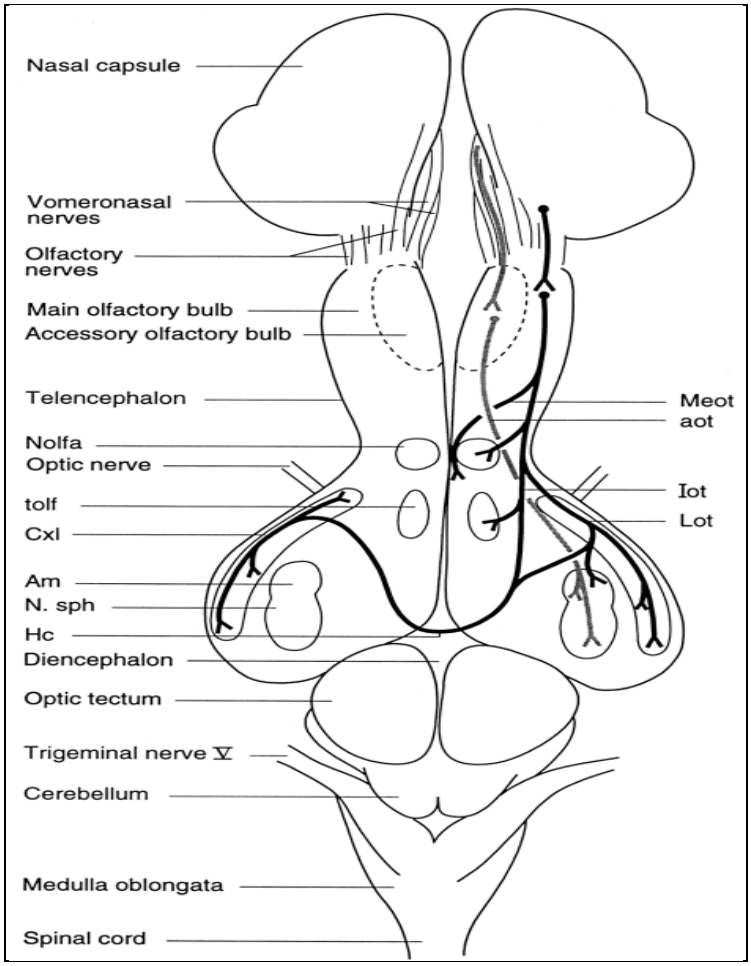

Figure 40. Dorsal view diagram of the vomeronasal (gray) and olfactory sensory (black) projections in a rattlesnake brain (Kardong and Berkhoudt, 1999).

Note: Am = Amygdaloid complex; aot = accessory olfactory tract; Cxl = cortex lateralis; Hc = habenular commissure; lot = intermediate olfactory tract; Lot = lateral olfactory tract; Meot = medial olfactory tract; Nolfa = nucleus of the lateral olfactory tract; N. sph. = nucleus sphericus; tolf = tuberculum olfactorium.

The vomeronasal system mechanism is similar to that of an olfactory system. When odor molecules are brought to the VO, they bind to receptor molecules, which send a signal to the brain (*Encyclopædia Britannica*, 2010f). In the VO, there are olfactory receptor cells to which the odor molecules bind. These receptor cells are bipolar neurons with axons that go to the accessory olfactory bulb in the brain (Halpern, Cinelli, and Wang, 2006).

3.6 Design Constraints in Creating Pheromone Robotics

Many research groups have tried to create a viable chemical communication system, but there are a number of problems impeding the use of this technology. The sensors in use are not nearly as sophisticated as their biological counterparts, being larger both in size and power requirement, than is practical for small platforms. The biological sensors of interest filter background noise, can sense very small signals, and are very small in size (Pyk et al., 2006)—attributes that, given current technology, cannot be mimicked to the same degree of quality in manmade objects. Also, the chemical in use should have minimal environmental impact, which severely restricts the chemicals that can be employed.

Application

A group at Hughes Research Laboratories (HRL) is investigating the use of infrared (IR) signals as a pheromone robotics system to coordinate swarm behavior. These "virtual pheromones" are transmitted and received by a simple transceiver (figure 41) that is mounted on each robot. Much less onboard processing is required as a result of the pheromone system structure (Payton, Daily, Hoff, Howard, and Lee, 2001). A comparison of chemical and virtual pheromones is summarized in table 5.

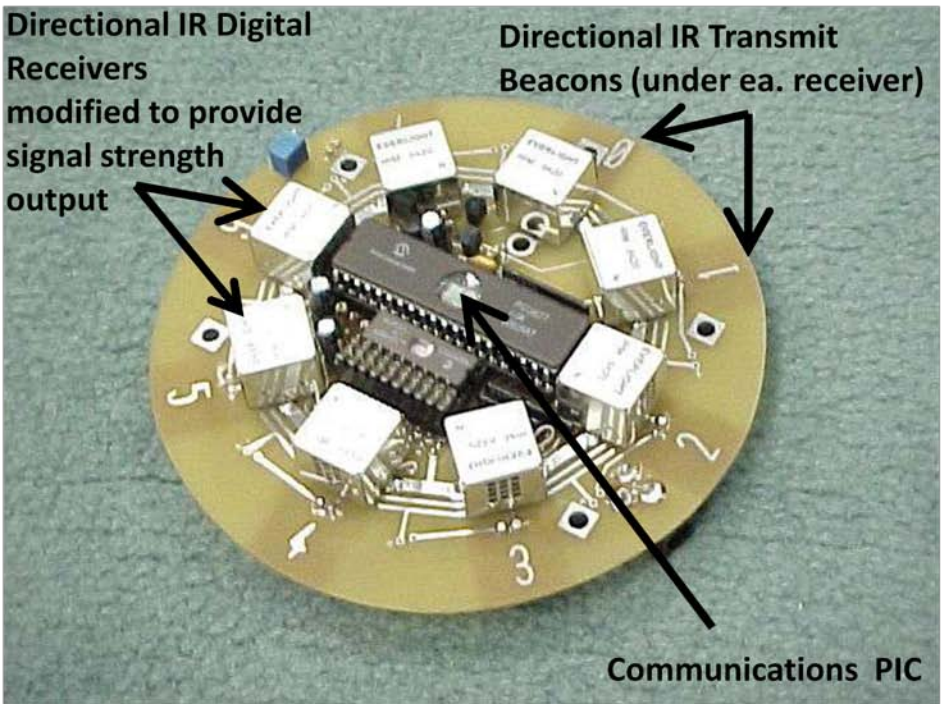

Figure 41. The transceiver mounted on the HRL Pherobot (Payton, Pheromone Robotics).

Table 5. A comparison of chemical and virtual pheromones (Payton, Pheromone Robotics).

Chemical Pheromones	Virtual Pheromones
Facilitates emergent coordinated activity of thousands of cooperating agents	yes
Sender needs not know identity of recipient	yes
Sender needs no acknowledgement of message receipt	yes
Information conveyed through intensity gradients	Yes, but by using intensity-tagged message packets
Propagation is sustained passively through the environment	Propagation is sustained by active relaying between robots
Different chemical types needed for different messages	Messages may be tagged with additional data

When a swarm of robots (figure 42) is released into an area, they quickly disperse in their search patterns (figure 43). The robots, instead of communicating with a central system or with all of the other robots, only maintain contact with the few bots in their vicinity, saving significantly on power. When a robot finds the object of interest, for example, a survivor in a disaster area, it emits a specific “object found” beacon signal to the robots in its vicinity. The message, which includes a field-of-view field (sets the angular width of the beam), a type field, a hop-count field (the number of times the signal has been relayed), and a data field, is then passed from unit to unit, with each transmission of the message adding to the hop count. Each robot knows the direction from which the signal came, and thus is able to follow the shortest route to the origin of the signal. If more than one signal is received by a single robot, the one with the lowest hop count is followed. The aggregate set of robots form an embedded computing grid and an embedded display for finding the shortest path to a survivor, which eliminates the need for a map (Payton, Daily, Hoff, Howard, and Lee, 2001). An overlay in the field of view of a head-mounted display allows a human to read information from the IR signals emitted by each robot.

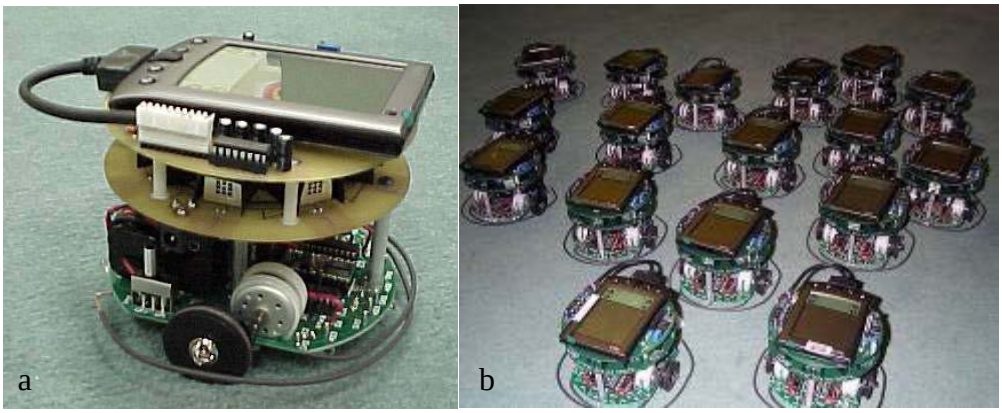

Figure 42. (a) HRL Pherobot and (b) a swarm of HRL Pherobots (Payton, 2010).

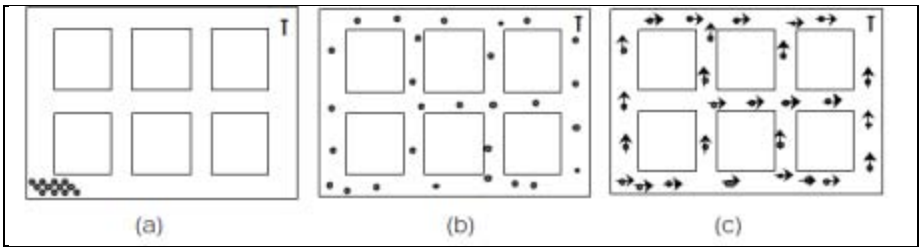

Figure 43. (a) The robots are released into an area, (b) the robots begin their search pattern c-when the "object found" pheromone is released, and (c) all bots converge (Payton, Daily, Hoff, Howard, and Lee, 2001).

A command pheromone can also be used to specify whether a given message should stop with the receiving robot or be relayed to the rest of the swarm. Through this system, individual robots can be commanded separately from the group behavior. Some of the pheromone message primitives developed for this system are shown in table 6 (Payton, Estkowski and Howard, 2003).

Table 6. Pheromone messaging primitives (Payton, Estkowski and Howard, 2003).

Pheromone messaging primitives	
Pheromone data request primitives	Have I sensed type X? Give me all of type X Give me "best" of type X Give me "best" of type X in each bin
Pheromone message-passing primitives	Forward X when Y is true/false Forward X, incrementing (or decrementing) hop-count by P Forward X, setting FOV and pheromone type Forward last X for K time cycles Forward X for K cycles then nothing for T cycles Forward X relative to received direction Forward X or Y depending on which has the max or min hop-counts Forward X or Y, alternating between them
Pheromone sending primitives	Initiate sending X (once, forever, for time T) Send X with priority P Send X in directions (N, S, E, W, etc.)

The potential for variation in the virtual pheromone enables the robots to create a barrier against the others by emitting a repelling virtual pheromone, if the dispersion of the swarm should stop. The robots can use the strength of the IR signal to maintain their formation. If a given robot is in the short-range area of a neighboring robot, then it is repelled from that unit, but if it is in the long-range region, it is attracted. This allows the swarm to maximize the area it covers while maintaining lines of communication (figure 44) (Payton, Daily, Hoff, Howard, and Lee, 2001).

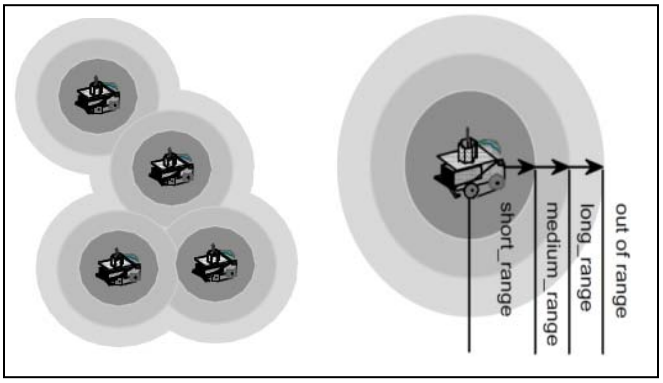

Figure 44. The HRL Pherobots maximize the area that the swarm searches without losing communication with the swarm (Payton, Daily, Hoff, Howard, and Lee, 2001).

4. Tactile

Tactile sensitivity manifests itself in a variety of ways in the animal kingdom. Some species, like the spider, use naked hairs to sense airflow or contact with solid objects. Some marine animals can sense water pressure using hairs encapsulated in gel as part of the lateral line sensing mechanism. The cockroach and cricket also use tactile antennae, which have inspired biomimetic hair sensors.

4.1 Tactile Hairs: Spiders

Spiders have two different types of hair sensors, air-flow hair sensors called trichobothria for long-range sensing, and tactile hairs for regular touch sensing (figure 45).

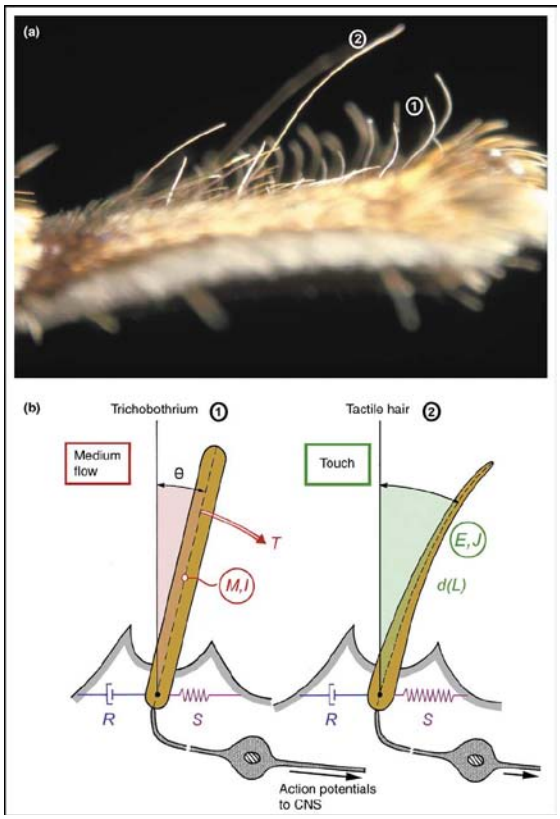

Figure 45. Diagram of a trichobothrium (1) and a tactile hair (2), illustrating some of the key differences in their form and operation (Barth and Dechant, 2003).

Note: Abbreviations: d, diameter; E, Young's modulus; I, inertia; J, second moment of area; L, length of hair shaft; M, mass; R, inertial resistance; S, elastic restoring force.

Trichobothria are some of the most sensitive hairs among arthropods. *Cupiennius salei's* trichobothria have an activation energy threshold of less than 1.5×10^{-19} J (2.5×10^{-20} J -1.5×10^{-19} J). This is comparable to the energy in one photon of visible light (E-18 → E-19 J). They can sense air motion as slight as 1 mm/s and hair deflections as small as 0.001°–0.1° (Barth, Humphrey, and Secomb, 2003, p. 129–130), giving spiders the ability to sense another creature moving up to 30 cm away (Barth and Dechant, 2003). This is only slightly less sensitive than cricket filiform hairs, which have been shown to operate near the limit of sensitivity imposed by thermal Brownian motion (Shimozawa, Murakami, and Kumagai, 2003).

Trichobothria have a very low stiffness at the base of the hair (order of magnitude 10^{-12} N·m/rad), so the force required to deflect the hair is significantly less than the force required to bend the hair. As a result of this, the hair remains straight as it deflects and the motion is dominated by the mass (M) and rotational inertia of the hair (I) (figure $40b_1$) (Barth and Dechant, 2003). Each spider leg has about 90 trichobothria arranged in arrays on each leg. Considering the response of all these hairs together gives the spider a detailed picture of the

airflow as it varies in space and time (Barth, 2004). The spider's hairs range in length from 0.1–1.4 mm (Barth, Wastl, Humphrey, and Devarakonda, 1993). The difference in the lengths of the hairs allows the spider to distinguish the frequency of the signal. Different hair lengths correspond to the different boundary layer thickness of flows at relevant frequencies in the spider's environment. The boundary layers that form on a spider's leg vary from 2600 to 600 μm, corresponding to frequencies that vary from 10 to 960 Hz. (Barth, Wastl, Humphrey and Devarakonda, 1993) At low frequencies, only the longer hairs extend through the thick boundary layer far enough to be stimulated by the fast moving flow. At higher frequencies, the boundary layer is thinner and the shorter hairs are long enough to be stimulated by the viscous flow.

Tactile hairs have some significant differences from flow sensing hairs. Far more numerous than trichobothria, there can be hundreds of thousands of tactile hairs on a spider's body as dense in some places as 400 hairs/mm^2. Spiders use these hairs to sense direct contact with objects in their environment, as well as the movement of their body parts relative to each other. The most significant mechanical difference between tactile hairs and trichobothria is the stiffness of the joint where the hair attaches to the spider's body (figure 45b). The joint in tactile hairs is three to four orders of magnitude stiffer (10^{-9}–10^{-8} N·m/rad) than the joint in trichobothria (10^{-12} N·m/rad), causing the hair to bend (figure 46a) as well as deflect when a load is placed upon it (figure 45b). This bending is critical to their operation. (This means that, unlike trichobothria, the mechanical behavior of tactile hairs are dominated by their Young's modulus [E] and their moment of area [J].) As a vertical load on a hair increases, the hair bends under the load, shifting the action point of the load toward the base of the hair, shortening the moment arm and reducing the rate of moment increase at the base of the hair (figure 46). As a result, while the hair is sensitive to very light loads, this sensitivity decreases as the load increases (figure 47). This significantly increases the load range that the hair can withstand while maintaining sensitivity to very light loads. Remarkably, it limits the deflection of the base to 12° and the maximum bending moment on the base to 4×10^{-9} N·m, keeping the hair from breaking (Barth and Dechant, 2003). The length of the hair also protects the nerves connected to the base of the hair from being over-stimulated. When the hair is struck by a force, even without considering bending, it acts as lever, scaling down the deflection from the tip to the base by a factor of 750:1. This is important because while probing their surroundings in the dark, spiders can hit obstacles with their hairs at speeds of up to 11 cm/s. The trade off for such a dramatic decrease of deflection from the tip to the base is that the nerve cells that sense the motion of the base must be extremely sensitive (Barth, 2004).

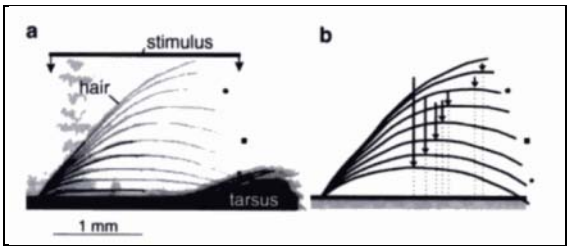

Figure 46. Diagram of a loading being placed on a spider tactile hair. As the load increases, the point of loading shifts towards the base of the hair shortening the moment arm (Barth and Dechant, 2003).

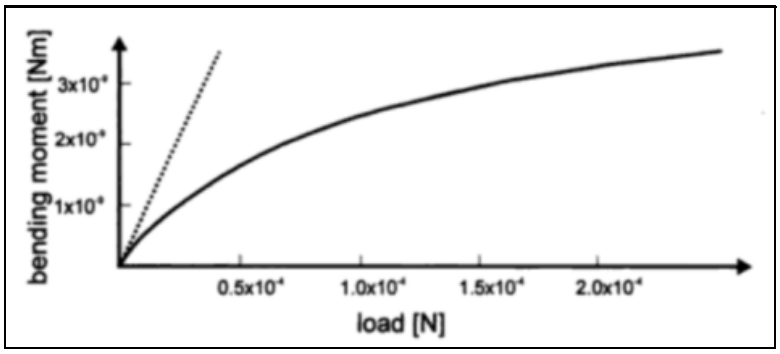

Figure 47. Theoretical bending moment on the base of a tactile hair as a function of the load on the hair (according to Finite Element simulation) (Barth and Dechant, 2003).

Application

A significant amount of research has been done in constructing artificial tactile antenna as well as artificial hair sensor arrays. In chapter 19 of the *Springer Handbook of Robotics*, *Force and Tactile Sensors*, Cutkosky, Howe, and Provancher (2008) give a thorough summary of current tactile sensing technology. Lee et al. (2008) present a model of cockroach wall-following behavior as a proportional-derivative (PD) controller. One of the problems that come with active antenna is that they produce a significant amount of electrical noise that can disrupt the signal. Muraoka presents an active antenna that uses a quartz resonator as a force sensor. This sensor creates a noise-free antenna by applying force to a quartz resonator to produce a phase shift that is inherently noise free (Muraoka, 2005).

The Transducers Science and Technology Group at the MESA Research Institute in the Netherlands has done extensive research in artificial hair sensor arrays (Dijkstra, van Baar, Wiegerink, Lammerink, de Boer, and Krijnen, 2005) presents the construction of an artificial hair sensor modeled after the hairs on the cricket's cerci (Jaganatharaja, Izadi, Floris, Lammerink, Wiegerink, and Krijnen, 2007) presents a theoretical model of a system that can be used to vary structural and geometric parameters in order to increase sensitivity. They demonstrate the accuracy of their model and the ability to tune the system's resonant frequency

(Izadi, Jaganatharaja, Floris, and Krijnen, 2007) present a way to reduce the negative effects of stress on the sensitivity of the hair sensors (Jaganatharaja, et al., 2009) presents the state of the art technology in artificial hair sensor arrays used for detecting airflow. So far, these flow sensor arrays have achieved remarkable sensitivity, demonstrating responses to oscillating airflows (1 kHz) with speeds of only 0.85 mm/s, as well as clearly directional responses to airflow (moving in a figure-of-eight pattern). Bruinink et al. (2009) also presents a discussion of recent design optimizations and improvements to the fabrication process. The Micro and Nanotechnology Laboratory at the University of Illinois at Urbana-Champaign is also working to create artificial hair sensor arrays. (Chen, Tucker, Engel, Yang, Pandya, and Liu, 2007) demonstrates an artificial hair sensor consisting of an epoxy cilium on a silicon cantilever beam with a piezoresistive strain gauge at its base. This sensor was characterized for steady state laminar flow and oscillatory flow and was found to have a sensitivity below 1 mm/s in oscillatory flow and to have a best case angular resolution of 2.16°.

This lab has also constructed artificial hair cell sensors entirely out of polyurethane elastomer. This rubber material makes the hair cell sensors much more resistant to tearing stresses (Engel, Chen, Bullen, and Liu, 2005). (Liu C., 2007) also presents an overview of strategies for creating artificial hair cell sensors including material choices, fabrication methods, and performance. As a sensor system, arrays of hairs demonstrate high sensitivity over a large frequency range (Barth, 2004) and may be applicable to spectral analysis (Krijnen et al., 2006).

4.2 Lateral Line Sensing: Fish and Aquatic Amphibians

Fish and some aquatic amphibians use lateral line sensing to detect changes in pressure of the surrounding water. The blind cave fish (*Astyanax fasciatus mexicanus*), which resides in areas with very little light, is a good example of how these creatures evolved to use touch instead of sight to gather information about their surroundings. The pressure waves that are created by a swimming fish change slightly when the fish approaches an obstacle or when another swimming fish is near. The fish can use this sense to successfully navigate its environment, avoiding obstacles and predators, hunting prey, or swimming in a school (Weeg and Bass, 2002). There is also evidence that suggests sharks may use their lateral line pressure sensitivities to predict severe weather (BBC News, 2008). Using its lateral line system, a fish can sense water flows along its body with velocities on the order of a few μm/s, and distinguish distances of 1 mm (McConney et al., 2008). Lateral line sensing can also be used to detect low frequency vibrations of 100 Hz or less (Weeg and Bass, 2002), follow a hydodynamic trail (a wake), and locate a dipole source created by the tail motion of a swimming fish. Biomimetic improvement of manmade sensors based on the lateral line system could advance technology in a number of fields including; marine and air navigation and control, fluid mechanics studies and underwater imaging (Yang, Chen, Tucker, Engel, Pandya, and Liu, 2007).

Mechanism

The lateral line system (figure 48a) consists of the lateral-line canal (figure 48b) below the skin with external openings to the aquatic environment and neuromasts (figure 48c) that continuously send sensory signals through the lateral-line nerve to the brain. There are two different types of neuromasts: superficial neuromasts and canal neuromasts. Superficial neuromasts measure fluid velocities and are located on the surface of the fish's body. Canal neuromasts are located within the lateral line canal (Yang et al., 2006). Using the aggregate set of canal neuromasts, the fish can sense a pressure gradient, which is proportional to the acceleration of surrounding water (Ćurčić-Blake and van Netten, 2006). Water cycles through the lateral line canal and applies pressure to the cupula, which is the gelatinous upper part of the neuromast. When the cupula is moved, the hairs inside are bent, causing modulation of the frequency of the signals sent by the neuromast sends to the nerve (*Encyclopædia Britannica*, 2009f). These hairs are sensitive to nanometer scale distortions, which explain the high motion sensitivity of the entire system (McConney et al., 2009). The combination of superficial and canal neuromasts creates a spatial-temporal image of the surrounding area using the hydrodynamic signatures of nearby objects (Yang et al., 2006).

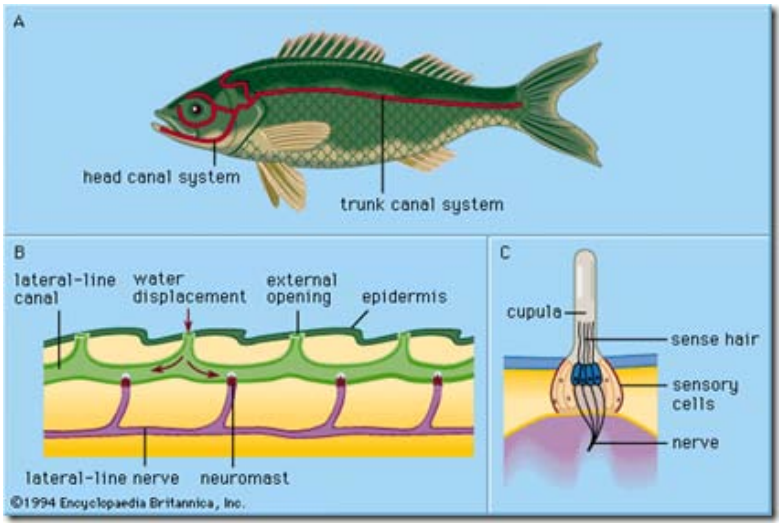

Figure 48. (a) The location of the lateral line system on the fish, (b) image of lateral-line canal, and (c) image of a neuromast (*Encyclopædia Britannica*, 2009f).

Applications

The Micro and Nanotechnology Laboratory at the University of Illinois has built an artificial lateral line system using artificial hair cells (figure 49). The group was inspired by two tactile biological sensors: the arthropod filiform hair cell, which was discussed in section 4.1, and the fish lateral line system. Their system consists of a polymer hair protruding from a paddle-shaped cantilever that has doped silicon strain gauges at the base. This creates an artificial neuromast.

When flow exerts pressure on the polymer hair, it changes the loading conditions on the cantilever, which is reflected in the strain gauges. For the finished artificial hair sensor component of the system, the hair itself has a diameter of 80 µm and length of 500 µm. The cantilever is 2 µm thick with the dimensions 40x100 µm. The sensor is fabricated on a silicon-on-insulator wafer. The hairs can consistently survive 55° deflections, but lose accuracy at 48°. Under conditions of 35° deflection, it was established that the system maintains accuracy well over time. The artificial hair cell sensor can detect deflections of 2.5 micro-strains, which translates to a water velocity sensitivity of 1 mm/s. The sensors were also able to sense both a wake and a dipole field accurately (Yang, Chen, Tucker, Engel, Pandya, and Liu, 2007).

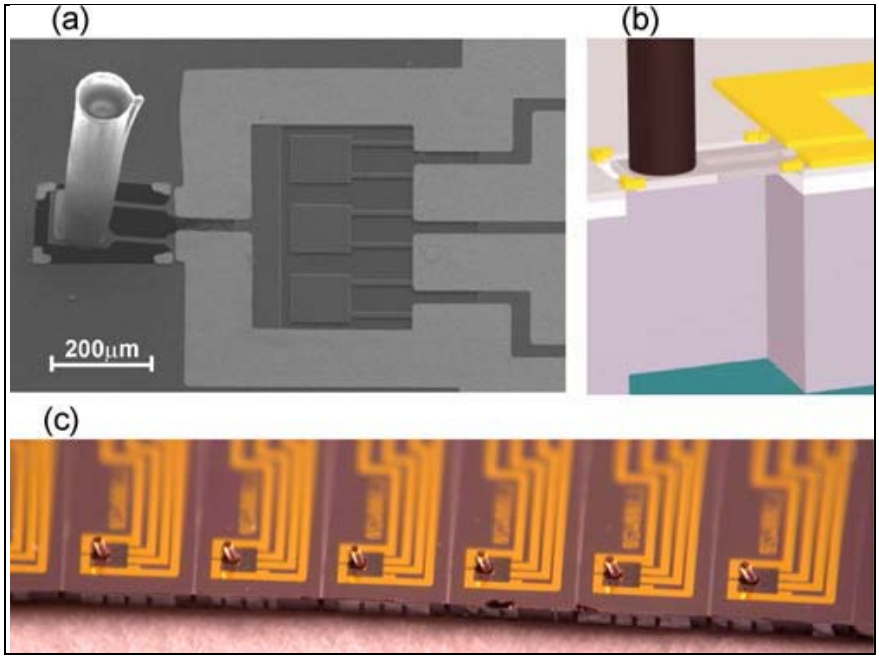

Figure 49. (a) Artificial hair cell sensor (scanning electron microscope [SEM] image), (b) cutaway view of sensor, and (c) artificial hair cell sensor array (Yang, Chen, Tucker, Engel, Pandya, and Liu, 2007).

These individual artificial hair cell sensors were then used in parallel to fabricate an artificial lateral line system. Four sensors were attached to either side of an airfoil (chord 76.2 mm and span 50.8 mm) to form a model fish (figure 50a). This model fish was not tested practically in this study, but a proof-of-concept using commercial anemometers in a similar configuration was. This proof-of-concept fish was attached to a robotic arm and tested in conjunction with advanced decision-making algorithms (figure 50b). The model fish was able to track the vibrating target using only sensory input from the artificial lateral line. The tracking pattern is shown in figure 50c (Yang, Chen, Tucker, Engel, Pandya, and Liu, 2007).

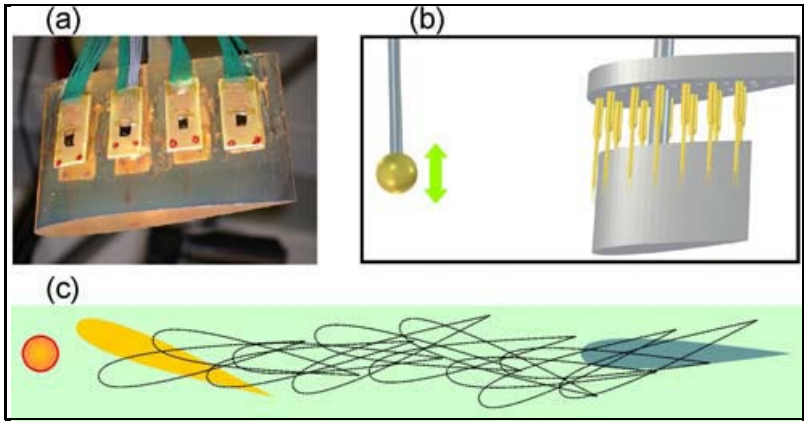

Figure 50. (a) Artificial hair cell sensors attached to airfoil to create an artificial lateral line, (b) proof-of-concept of artificial lateral line tracking vibrating target, and (c) tracking path of model fish (Yang, Chen, Tucker, Engel, Pandya, and Liu, 2007).

Another group took the biomimetic technology one step further, adding a hydrogel cap to the artificial hair cell sensor (figure 51b). The first version of the cap represented canal neuromasts and the way that water "slides" over them. This version had a low aspect ratio of ~1:1 and used a polymer with an elastic modulus of ~10 kPa. The second version of the cap was meant to mimic superficial neuromasts and the way that water bends the cap itself. In this version, the aspect ratio was increased to 5:1, and the elastic modulus decreased to the order of 10Pa (figure 51d). The addition of the hydrogel cap improved the sensitivity of the sensor by a factor of 38. The original sensor, when tested with a 10-nm maximum deflection, had a velocity sensitivity of 1.2 nm/(mm/s) (nm hair deflection per mm/s of flow velocity), which improved to 45 nm/(mm/s). This translated to an equivalent improvement in sensor output: 3.2 mV/(mm/s) to 122 V/(mm/s). Also, the original sensor had a 100 μ/s minimum velocity threshold, which decreased by a factor of 40 to 2.5 μm/s with the addition of the polymer coating McConnery et al., 2008).

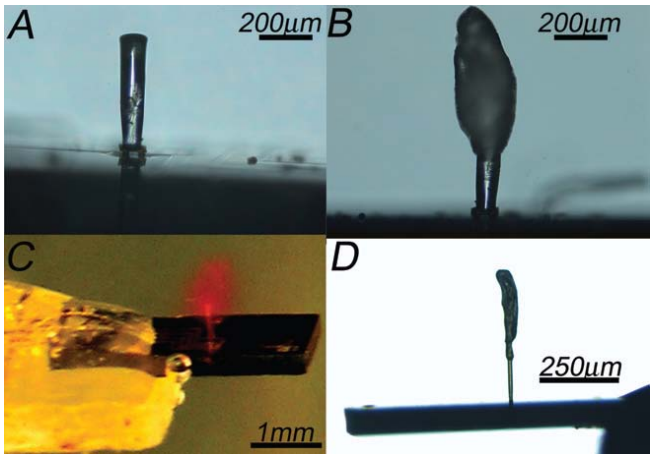

Figure 51. The front-view of a hair sensor (a) before and (b) after being coated with the PEG-based hydrogel material; (c) a swollen cupula on a working sensor (the hydrogel is dyed using rhodamine); and (d) the side view of a sensor with a long SU-8 hair and a long/high aspect ratio cupula in the dry state (McConney et al., 2008).

5. Electromagnetic

Ion-rich environments like bodies of salt water are highly conducive to electromagnetic sensing. Sharks and some fish use ampullae of Lorenzini to sense charges in their surrounding environment, while other weakly electric fishes actually produce their own electric field to perform electrolocation.

5.1 Ampullae of Lorenzini

Sharks and some bony fish use ampullae of Lorenzini (figure 52), a modification of lateral line sensing, to detect electric charges or fields (Martin, 2003). Some marine animals can sense electrical charges as low as 2 nV/cm (Brown, Hughes and Russo, 2002). Behavioral experiments with sharks and rays indicate that their behavioral threshold is approximately 0.01 µV/cm (*Encyclopædia Britannica*, 2010g). To gain perspective on this sensitivity, a newborn Bonnethead shark can detect electric fields less than 1 nv/cm^2, which is equivalent to a flashlight battery being placed underwater and connected to electrodes 16,000 km away (Martin, 2003).

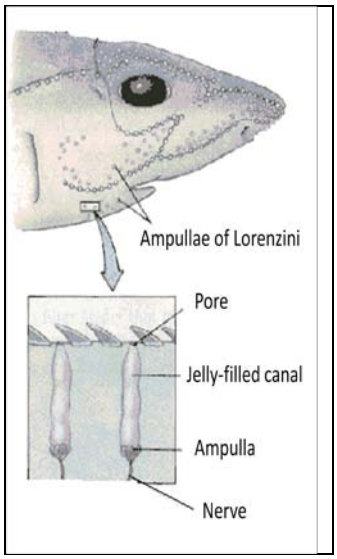

Figure 52. Diagram of the ampullae of Lorenzini (Hickman, 1994).

Ampullae of Lorenzini consist of thousands of small pores called ampullae. The hammerhead shark, on average, has 3,067 of these pores scattered over its head (Kajiura, 2001). Each ampulla has a 1-mm wide canal leading from the surface pores into the skin. The resistance of the canal walls is on the MΩ scale (Brown, Hughes and Russo, 2002). This canal and ampullae are filled with gel and lined with many sensory hair cells. Electrical charge is conducted through the walls of the canal, and the sensory hair cells detect the voltage. When voltage is detected, different neurotransmitters are released depending on the difference in electric potential between the body of the shark and the pore (Davidson College, 2005a). The gel that fills these pores is similar to seawater, but has a much lower voltage noise. It contains water, large sulfated glycoprotein molecules, potassium, and sodium, calcium, and chloride ions in concentrations similar to those found in seawater. The high resistance of this gel maintains the voltage difference between the pore and the ampullae, allowing the shark to sense electrical signals (Brown, Hughes and Russo, 2002).

Animals, including humans, emit an electric field in seawater (Cohen, 2004), which is a good conducting medium given the large number of electrons. These very weak fields are created by movement of muscles, metabolizing cells, nerve signals, and the difference in charge between the organism's body and the water (Martin, 2003). These charges can be sensed easily by the ampullae, which are sensitive to less than 5 nV/cm (Martin, 2003), especially if the organism is wounded and leaking electrolytes (Marks, 2006). A wounded animal is especially vulnerable because a cut emits electrolytes, changing these fields and allowing the shark to detect the creature that is now emitting a signal up to three times as strong as a healthy organism (Martin, 2003). The ampullae of Lorenzini can also detect the Earth's electromagnetic field, a capability that sharks are believed to use for migration and homing (*Encyclopædia Britannica*, 2009b). A study of scalloped hammerhead sharks revealed that they navigate between sites of interest

through their magnetic sensitivity. Electrolytes in the creature's body create electrical currents when the shark moves through Earth's magnetic field, allowing them to follow "magnetic highways" along the sea floor (Martin, 2003). Shark navigation is still being studied, and many current claims regarding their navigation system are controversial.

5.2 Electrolocation: Weakly Electric Fishes

Electrolocation is a type of active location that some species of fish, like the elephantnose fish (*Gnathonema petersii*), use to operate in darkness or in turbid waters where visibility is low. The capability is similar to the dolphin or bat echolocation, except the mode of signal is electricity, not sound. The fish emits a weak electric signal (von der Emde, 2006) on the scale of millivolts (Nelson, 1996), which can be in a pulsed or a wave-like continuous AC signal (figure 53) (Bastian, 1994), and senses the returning signal, which has been distorted by the environment (figure 54). This distortion can provide the fish with the distance and three-dimensional shape of an object. The Mormyrid weakly electric fish uses its electric sensitivity to distinguish between live and dead objects when hunting by measuring the impedance of its target (von der Emde, 2006). They produce about 300 shocks per second, each on the order of a few volts, to create this electric field (*Encyclopædia Britannica*, 2010g).

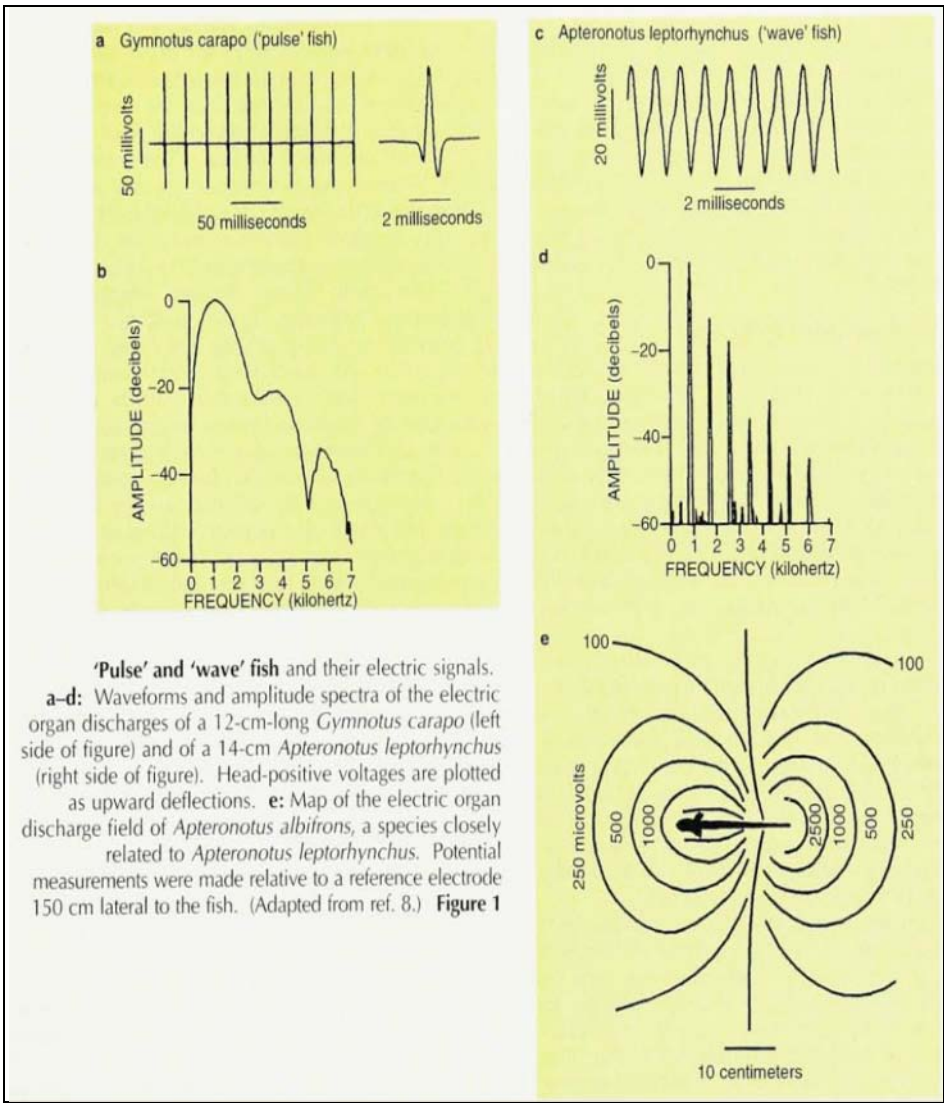

Figure 53. Pulse and wave fish and their electric signals (Bastian, 1994).

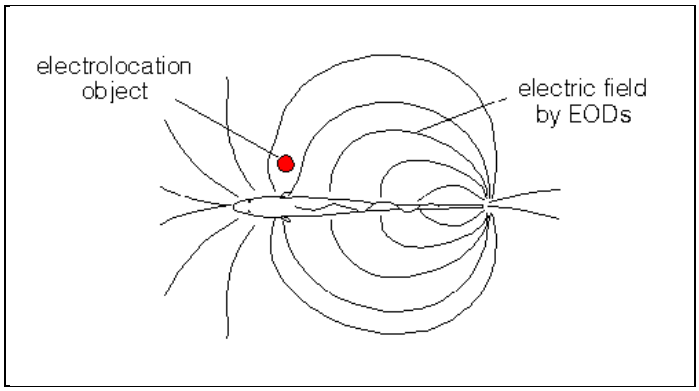

Figure 54. Location of an object through electrolocation (University of Virginia).

Mechanism

The elephantnose fish has specialized electric organs in the tail that produce weak electric organ discharges (EODs), the return signal of which is sensed by electroreceptive skin on the foveal regions on the nasal region and Schnauzenorgan (SO) (figure 55) (Hofmann and Wilkens, 2005).

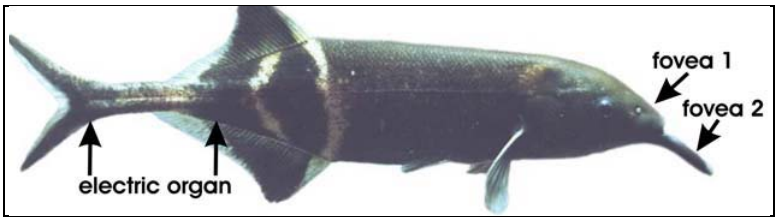

Figure 55. The locations of the electric organ and of the two electric foveae regions: (1) nasal region and (2) Schnauzenorgan (von der Emde, 2006).

The returned signal produces an electrical picture of the surrounding environment for the fish, presenting the size, distance, shape, and material of the surrounding objects. Each discharge builds up an electrical field around the fish, which is sensed by cutaneous electroreceptor organs that are distributed over most of the body surface. Nearby objects distort this electrical field and cause a local alteration in current flow in the electroreceptors closest to the object. By constantly monitoring responses of its electroreceptor organs, the fish can detect, localize, and identify environmental objects. The SO is used for close-range imaging and the nasal region is more suitable for a wider-range image analysis. (von der Emde, 2006).

A visual representation of the signal an object sends to the skin of the *G. petersii* is shown in figure 56. In each diagram, the fish is being acted upon by an electrical dipole (equivalent to a small conductive sphere) whose current density is projected onto the diagram of the fish. The current density depends both on the distance between the object and surface of the fish, and its size. The upper fish displays the current density for a dipole at a distance of 1 cm (corresponding to the dotted line) and the lower fish displays the current density for a dipole at 1.5 cm (corresponding to the solid line) (Engelmann, Pusch, and von der Emde, 2008).

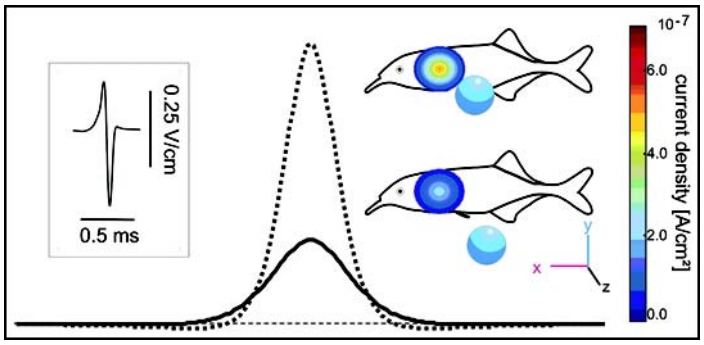

Figure 56. Visual representation of the electrical dipole signal on the fish (Engelmann, Pusch, and von der Emde, 2008).

When searching for prey, *G. petersii* adapts a specialized swimming position: they swim at a constant angle of their body axis of 18° ± 3.6° towards the ground, moving their SO in a rhythmic fashion from left to right. During exploratory and foraging behaviors, the fish can move the SO with a high velocity of up to 800°/s (figure 57). As depicted in figure 57, when the SO is bent by approximately 62°, the amplitude of the EOD decreases by 80%. Interestingly, the amplitude is restored to the previous number when the field is measured at a different tip location. It demonstrates that the internal conductivity of the SO forces the electric field to "move" with it during bending. As a consequence, the local sensory stimuli at the SO's tip do not change when the fish moves (Pusch et al., 2008).

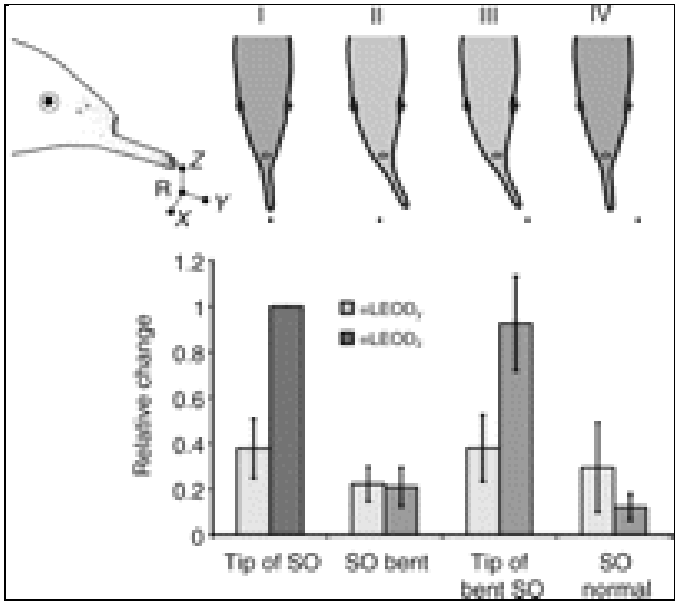

Figure 57. Results from moving SO on the dorsal-ventral component of the local EOD at its tip. All measurements were taken from the position pictured by the black dot in the figures and measured the mean EOD amplitude (N=7; normalized to 1). In I, the SO was straight and black dot placed at the tip. In II, the SO was bent 62°±13.5° to the left and the black dot was in the same position as in I. In III, the black dot was moved to the bent tip position (to find the initial amplitude), and in arrangement IV the SO was returned to the straight position and the black dot was in the same position as in III (von der Emde et al., 2008).

Electric fish also modify their discharge frequency in order to avoid jamming with other signals (figure 58). This jamming avoidance response (JAR) allows multiple fish to discharge in the same area without interfering with each other (Lynch, 2008).

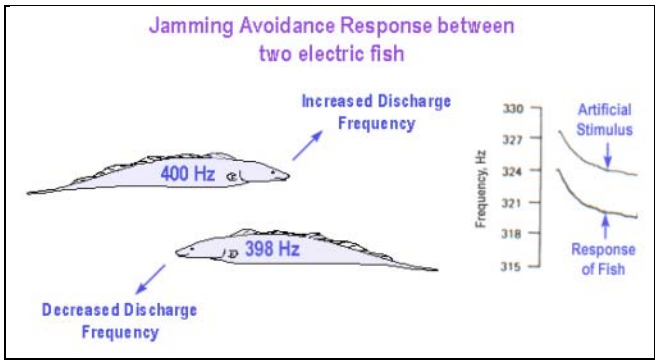

Figure 58. JAR between two electric fish (Lynch, 2008).

Applications

Fish electrolocation has inspired the development of remote object sensing technology for aquatic or ionized gas environments. This technology mimics the fish's system with devices that emit electrical current pulses in a conducting medium while sensing local current. The devices can be used for object detection, the localization of an object in space, remote distance measurement, or measurement of properties such as the material composition, thickness, and material faults. The technology is fairly robust, with the devices proven to be insensitive to environmental instabilities such as heat, pressure, and turbidity, and has a wide range of applications, including material identification, quality control, distance measurements, and medical applications. Research is being conducted on the biological species to further the sensor technology (von der Emde, 2007).

6. Optical

Novel optical communications mechanisms range from the highly sophisticated vision system of the Mantis shrimp to the very simple pinhole IR sensors of the pit viper. The novelty of the pit viper's mechanism lies in the combination of this IR sensor with another simple visual sensor to achieve much higher sensitivity than using either sensor alone. The Jewel beetle has a built-in mechanical noise-reduction system that allows a rudimentary IR sensor to detect very accurately at long range.

6.1 The Mantis Shrimp

The Mantis shrimp (figure 59) has the most sophisticated visual sensory capabilities of any known organism (Kilday 2005). It can see frequencies of light from ultraviolet (UV) to IR, as well as linearly polarized light, and is the only known species capable of detecting circularly polarized light (University of Queensland, 2008), and has exceptional depth perception of each eye independently (Kilday, 2005). Species of the Mantis shrimp can be as small as 1 cm in length (figure 60) (Brauchli, 2008).

Figure 59. The Mantis shrimp (Photo: Roy Caldwell/University of California, Berkeley).

Figure 60. The Mantis shrimp can be smaller than a human finger (Marine Specimens Educate).

The Mantis shrimp has two eyes, each on a stalk that can move independently of the other. There are 10,000 photoreceptor cells in each eye, divided into three regions (Brauchli, 2008): the dorsal hemisphere, the midband, and the ventral hemisphere (figure 61). The dorsal and ventral hemispheres (upper and lower, respectively) detect linearly polarized light, and the midband detects color and circular polarization (Robinson, 2008). Each section has a pupil-like area, shown by the dark spots in figure 61, which independently sense visual inputs and can be used to triangulate the location of any object and result in depth perception for each individual eye (Kilday, 2005).

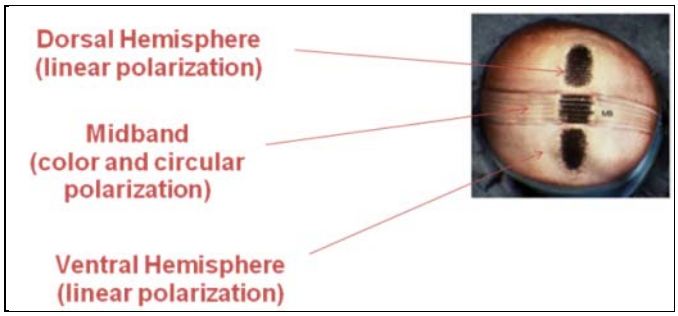

Figure 61. The Mantis shrimp eye (Chiou et al., 2008).

In the midband, there are four rows of cells (rows 1–4) that facilitate color vision, and two (rows 5 and 6) that see UV and green light, and can detect circularly polarized light (figure 62) (Robinson, 2008).

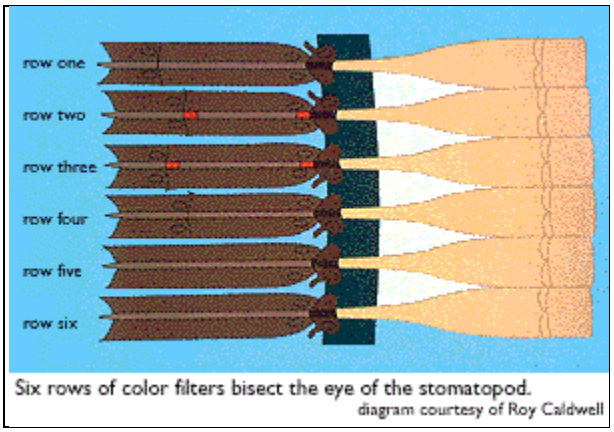

Figure 62. Six rows of color filters bisect the eye of the stomatopod (San Juan, 1998, courtesy of Roy Caldwell).

The arthropod eye is constructed of small transparent rods called rhabdom. Each rhabdom is comprised of 8 cells labeled R1 through R8. The rhabdom in the 5th and 6th rows cells (figure 63) are unique in that their cells are arranged to convert circularly polarized light into linearly polarized light, and then detect the transformed signal. The R8 cells are oriented at a 45° angle to the underlying R1–R7 cells and act as a $\lambda/4$ (quarter-wave) retarder to convert circularly polarized light to linearly polarized light. The R1–R7 cells in rows 5 and 6 have thousands of microvilli (Robinson, 2008), which detect linearly polarized light only when the light is oriented in the same direction as the microvillus (Volpe, 2008). The cells in row 5 are oriented 90° to those in row 6, so the twin cells in each row can see the same polarization of light. The R8 cells overlay the R1–R7 cells, so the light that reaches these cells is linearly polarized. Cells R1, R4, and R5 are sensitive to left-handed polarized light, and cells R2, R3, R6, and R7 are sensitive to right-handed polarized light (Robinson, 2008).

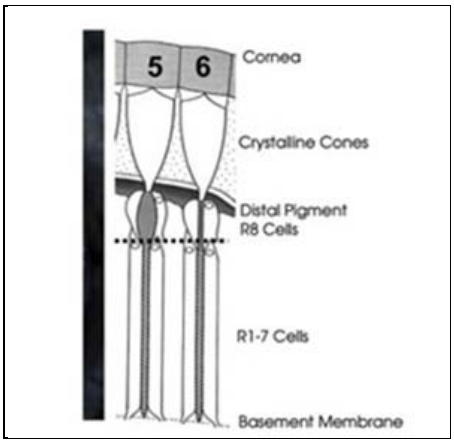

Figure 63. The rhabdom in the 5th and 6th rows cells (Chiou et al., 2008).

It is not yet known exactly how Mantis shrimp use circularly polarized light, but researchers believe that this ability serves as a communication channel that cannot be detected by any other species. There are certain regions of the Mantis shrimp's body that reflect polarized light, which are displayed to other members of the species to communicate, most likely for mating signals (figure 64). Also, many species reflect polarized light, which the Mantis shrimp is able to see. Some of their prey is transparent, and a Mantis shrimp can sense the victim's presence because of the sugars in its body that polarize passing light (Volpe, 2008). Another theory is that Mantis shrimp use their polarization vision to see more clearly in turbid waters. When light is scattered, as in the marine environment inhabited by Mantis shrimp, it can become circularly polarized, so the ability to distinguish this aspect of the light may help the Mantis shrimp to distinguish objects from their background (Chiou et al., 2008).

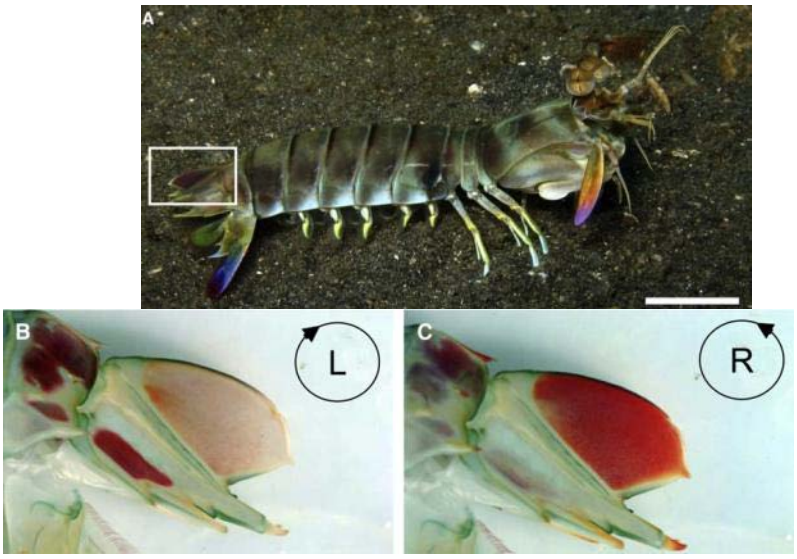

(Chiou, et al., 2008)

Figure 64. The telson keel, located on the tail of the Mantis shrimp (a), appears bright red only when seen with a right-handed circular polarizer (c).

6.2 Infrared Sensory System

Different species have developed unique ways to sense IR radiation to best fit with their survival goals. Snakes sense longer wavelengths, which are produced by their warm-blooded mammalian prey (peak emission ≈10 μm) (Lavers, Franks, Floyd and Plowman, 2005), at a short distance. These reptiles have a thin membrane with many nerves that detects heat directly (Bakken and Krochmal, 2007). Some species of beetle use extremely sensitive mechanosensors, converting IR radiation into a micro-movement, to sense shorter wavelengths (peak sensitivity ≈2–4 μm) at much greater distances (Schmitz and Bleckmann, 1997). The *Melanophila acuminate* beetle uses this highly specialized sensor to find forest fires, where they lay their eggs in the now vulnerable scorched wood (Schmitz, Mürtz, and Bleckmann, 2000). The spectral emittance versus wavelength for forest fires and warm-blooded animals are highlighted in figure 65.

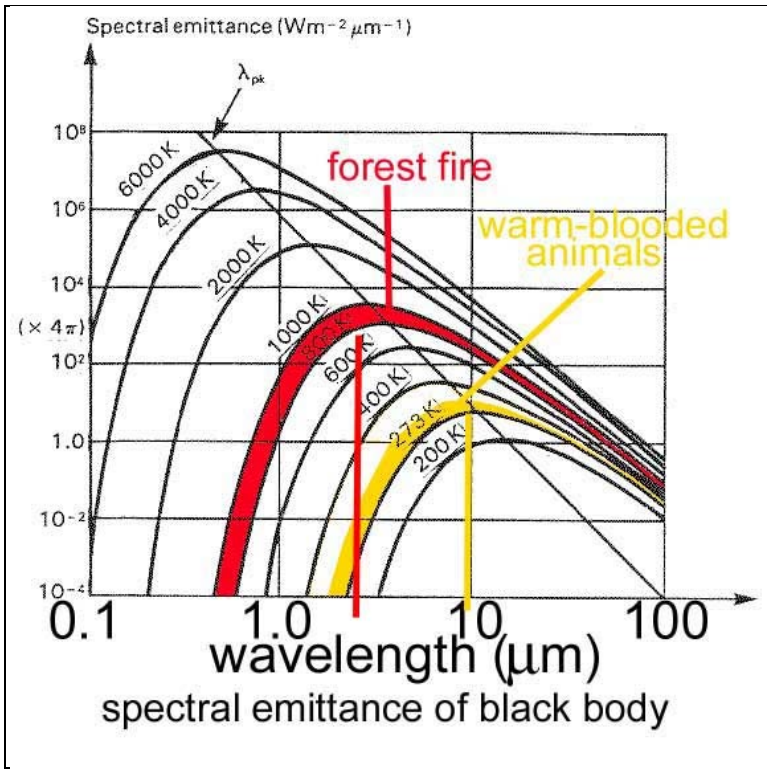

Figure 65. Wavelength vs. spectral emittance of a black body for forest fire and warm-blooded animals (Gronenberg, Pereira, Tibbetts, and Paulk, 2001).

6.2.1 Pit Vipers and Boids (Short Range, Long Wavelength)

Two types of snakes, pit vipers and boids, have small IR sensors called pit organs located between the eyes and nostrils that they use to hunt their warm-blooded prey (figure 66) (Zyga, 2006). These sensors are mushroom-shaped cavities 1–3 mm in diameter (Bakken and Krochmal, 2007) that function similarly to pinhole cameras. Pit vipers, along with their prey, are exceptionally active on moonless nights. The pit organs allow these snakes to hunt even when their vision is impaired (Bakken and Krochmal, 2007).

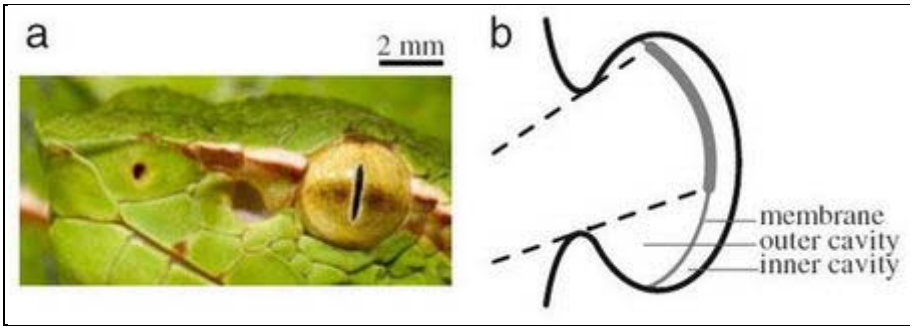

Figure 66. (a) The pit organs are located between the eyes and nostrils and (b) a diagram of the pit organ (Zyga, 2006).

When IR radiation enters the small pit, it is projected as an inverted thermal image, heating the membrane inside. There are thousands of sensors on the membrane that are sensitive to 0.003 °C or less (Bakken and Krochmal, 2007). Pit vipers have 1600 sensory cells on a membrane and a 100° field of view. These sensors create a blurry 3-D thermal image as input from what equates to a pinhole camera spreads from a point to a disc on the membrane. In the case of the pit viper, the point spans out 2.5° when transferred to the membrane. This low-resolution thermal image does not explain the 5° accuracy that snakes exhibit when striking for their prey (Zyga, 2006). The signal passes through the trigeminal nerve to the optic tectum where IR stimuli are processed (Bakken and Krochmal, 2007). The snake's brain reconstructs the image to a quality that depends on the amount of background noise. This low-quality reconstruction is still better than a manmade uncooled IR camera with a comparable number of detector cells (Zyga, 2006). Mathematical models have been developed to illustrate how a snake's brain reconstructs an image and applied it to the image of a rabbit (figure 67) (Sichert, Friedel, and van Hemmen, 2006).

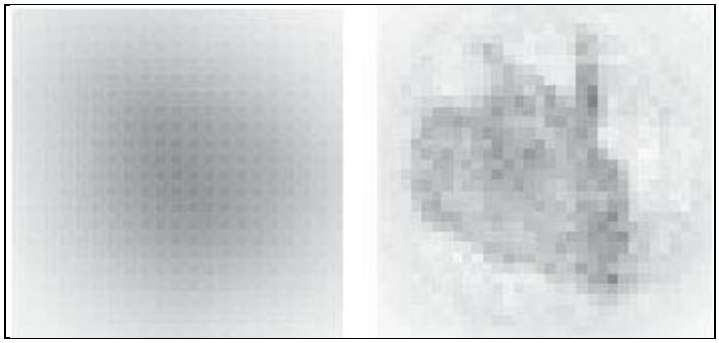

Figure 67. Reconstructed image with low level of noise (mathematical model of how snake brain reconstructs image (Sichert, Friedel, and van Hemmen, 2006).

There is strong evidence that the eyes and pit organs work in tandem (Bakken and Krochmal, 2007). The optic tectum receives input from both the IR and visual sensors and creates a spatiotopical image based on data from both. A signal is then sent to premotor areas (brainstem) and motor areas (spinal cord), preparing the snake to strike (Kardong and Berkhoudt, 1999). Figure 68 illustrates the visual and IR projections in a rattlesnake brain.

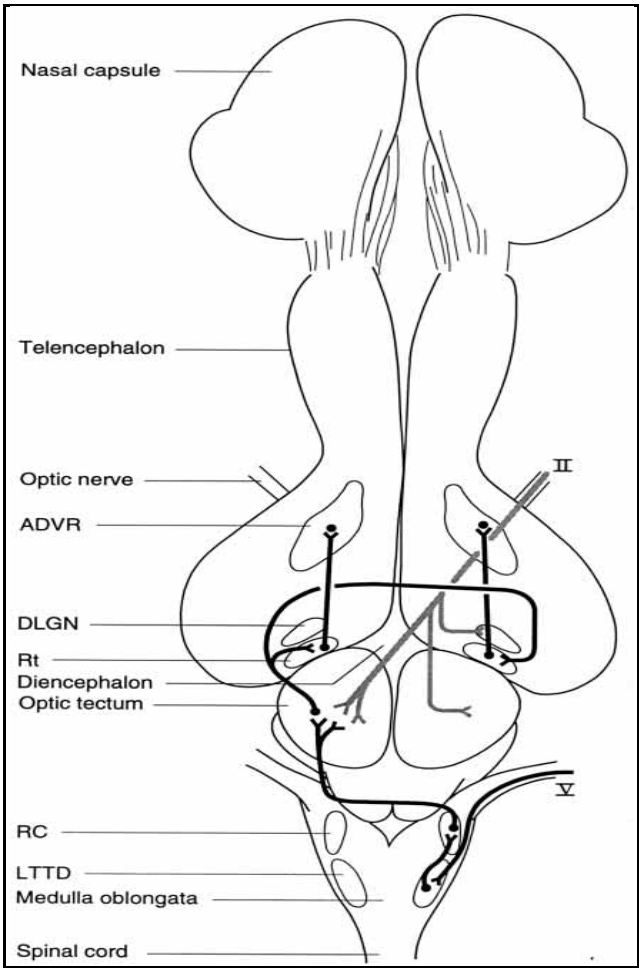

Figure 68. Dorsal view diagram of visual (gray) and IR (black) projections in rattlesnake brain (Kardong and Berkhoudt, 1999).

Note: ADVR = Anterior dorsal ventricular ridge; DLGN = dorsal lateral geniculate nucleus; LTTD = nucleus descendens lateralis trigemini; RC = nucleus reticularis caloris; Rt = nucleus rotundus.

6.2.2 Jewel Beetle (Long Range, Short Wavelength)

The 1-cm-long Jewel beetle (*Melanophila acuminate*) (figure 69a) has been reported to sense forest fires from a distance of 80 km (Schmitz and Bleckmann, 1997). They sense the IR radiation with two pit organs, located on the sides of the thorax (figure 69b) (Universität Bonn, 2010). Each pit organ has a depth and diameter of approximately 0.1 mm (Pain, 1999) and 100 µm, respectively, and contains approximately 70 individual IR sensilla receptors (figure 69c) (caesar, 2010).

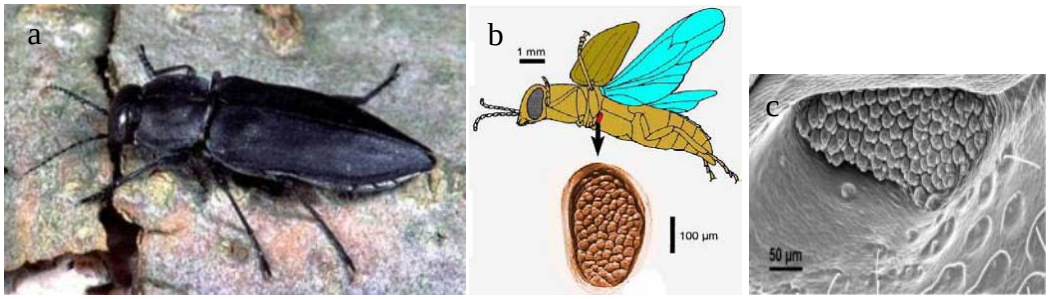

Figure 69. (a) The Jewel beetle (caesar, 2010), (b) the location of the IR sensor on the beetle and a magnified view of the pit organ (Gronenberg, Pereira, Tibbetts, and Paulk, 2001), and (c) a magnified image of the sensilla receptors in the pit organ (Schmitz, Sehrbrock, and Schmitz, 2007).

Mechanism

The individual sensilla (figure 70) are comprised of several layers that convert IR radiation into a pressure change, then to a micro-movement that triggers the nerve. IR radiation is absorbed by the cuticle, and the temperature of the fluid inside the spongy intermediate masocuticular layer increases. This causes a thermal expansion, which increases the pressure in the inner pressure chamber. The pressure expansion slightly deforms the membrane of the dendritic tip of the mechanosensory cell, which opens stretch-activated ion-channels. This process is not triggered by the gradual changes in environmental temperature that occur throughout the day because nanocanals in the exocuticle neutralize the pressure difference that would otherwise cause a false signal (Universität Bonn, 2010).

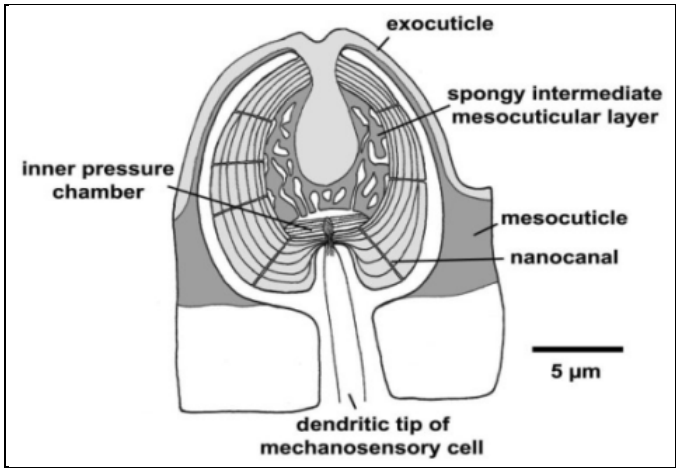

Figure 70. A diagram of the sensilla (Schmitz, Sehrbrock, and Schmitz, 2007).

Forest fires typically burn between 500 and 1000+ °C with a maximum emission of radiation being in the wavelength range of 2.2–4 µm (Schmitz and Bleckmann, 1997). The beetle's sensitivity capabilities peak at a wavelength of 2–4 µm, which makes their pit organs ideal for finding forest fires (Hazel, Fuchigami, Gorbunov, Schmitz, Stone, and Tsukruk, 2001).

Experimentation

A number of experiments have been conducted over the past few decades to characterize these unique sensors, with the purpose of using the information in the development of biomimetic technologies. The advantage of this type of system is that the sensor does not need a cooling system to function (Pisano, 2005). In one study, individual sensilla from *Melanophila* pit organs were subjected to IR radiation from a thermal radiator with an emission similar to that of a forest fire. When the sensilla were radiated with a power of 24 mW/cm^2, they responded with 7 potential spikes in about 10–40 ms. Under these conditions, a single spike could be produced with a signal of only 2 ms. When the power was reduced to 5 mW/cm^2, there were only 2–3 spikes observed and the response time increased by 5–6 ms. Calculations from this data led to the conclusion that this species of beetle can be expected to detect a 10-hectare fire from 12 km away. Given the large number of sensors, researchers suspect that this significantly underestimates what the actual beetle can sense (Schmitz & Bleckmann, 1997). A later study demonstrated that the best sensitivity for these individual cells occurred when radiated with 2.8–3.5 µm wavelength. At this wavelength, an intensity of 14.7 mW/cm^2 produced single action potentials. Increasing the intensity was found to decrease the reaction time and increase the number of spikes produced (Schmitz, Mürtz, & Bleckmann, 2000). Another research group investigated characteristics of individual parts of the receptor and estimated the local thermal expansion coefficient to be below $1.5x10^{-4}$ $grad^{-1}$ (Hazel, Fuchigami, Gorbunov, Schmitz, Stone, and Tsukruk, 2001). In an experiment to test the spectral range of the pit organ, the sensor responded to wavelengths of 2–6 µm and was classified as a broadband detector. This study did find a much stronger response to smaller IR signals of wavelength = 2.8–3.5 µm, the Fourier transform IR spectroscopy of which showed an increased absorbance (Hammer, Seigert, Stone, Rylander, and Welch, 2001).

Applications

A number of research groups have developed sensors inspired by the Jewel beetle. Table 7 shows the results of a parameter analysis of the Jewel beetle that was the basis of a biomimetic sensor's development. This sensor consisted of two Teflon plates, which acted as the absorbing material, with a piezoelectric component in between. The device was demonstrated to detect a human hand at a distance of approximately 30 cm (Schmitz, 2002).

Table 7. Summary of results from sensilla testing using broadband and monochromatic IR radiation (Schmitz, 2002).

Parameter examined	**Action potentials [AP´s]** Generation and number
Threshold (Sensitivity)	5 mW/cm^2 (broadband) 14,7 mW/cm^2 (at 3,4 µm)
Latencies	5 – 9 ms at 15 mW/cm^2 2 – 3 ms at 100 mW/cm^2 < 2 ms at 270 mW/cm^2
Saturation	At about. 250 mW/cm^2 (8 - 9 AP´s evoked)
Dynamic range	14,7 – 250 mW/cm^2 = **12 dB**
Dependence of receptor response on wavelength	Between 2,8 – 3,5 µm **no** dependence on wavelength detectable at 5 µm number of AP´s reduced by 20 %; latencies increased by 55 %
Repetitive Stimulation (chopperwheel)	AP´s up to about 100 Hz at each **ON**-event within the dynamic range (broadband)

The Center of Advanced European Studies and Research (caesar, 2010) used silicon technology to develop a biomimetic sensor that more closely followed the design of the pit organ sensilla (figure 71). IR radiation enters the system through the window, heating the water. The water then expands and deforms the condenser membrane, thus changing its capacity. The pressure balance chamber is used to neutralize slow temperature changes. The sensor itself is approximately 0.9 mm thick, with 2x5 mm dimensions, but is expected to be easily reduced in size using silicon technology. The finished chip consists of 408 sensors on a 4-in wafer (caesar, 2010).

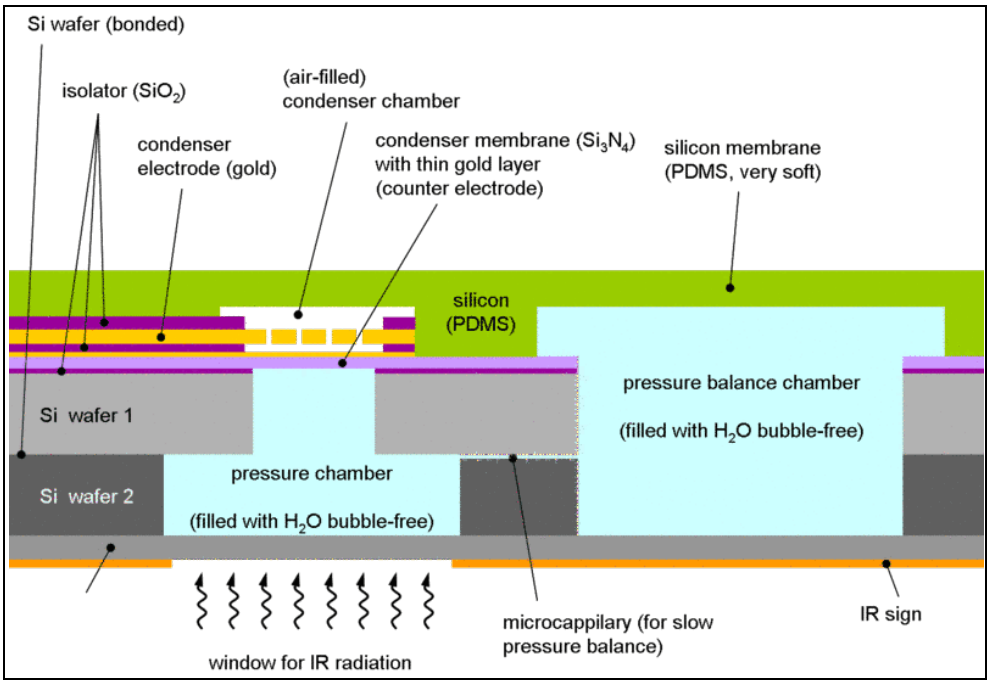

Figure 71. Biomimetic sensor based on the pit organ sensilla of the Jewel beetle (caesar, 2010).

Comparing the artificial device to its natural counterpart, one can clearly see how the researchers adapted the concept of the pit organ to fit their own purposes and resources (figure 72).

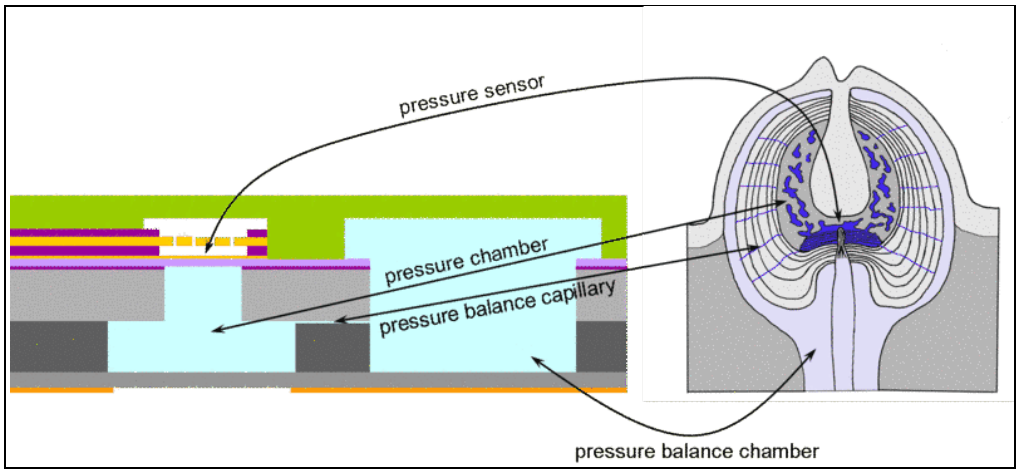

Figure 72. The biomimetic IR sensor compared to the biological sensor of the Jewel beetle (caesar, 2010).

The Pisano group at University of California at Berkeley is currently working on an uncooled, photomechanical IR sensor modeled after this same beetle's pit organs (figure 73). They expect their device performance to equal or exceed a standardized detectivity (D*) of 1e8 cm*sqrt(Hz)/W, a noise equivalent difference temperature (NEDT) equal or less than 20 mK, pixel size equal or less than 20 µm, and field of view equal or greater than 180° (Pisano, 2005).

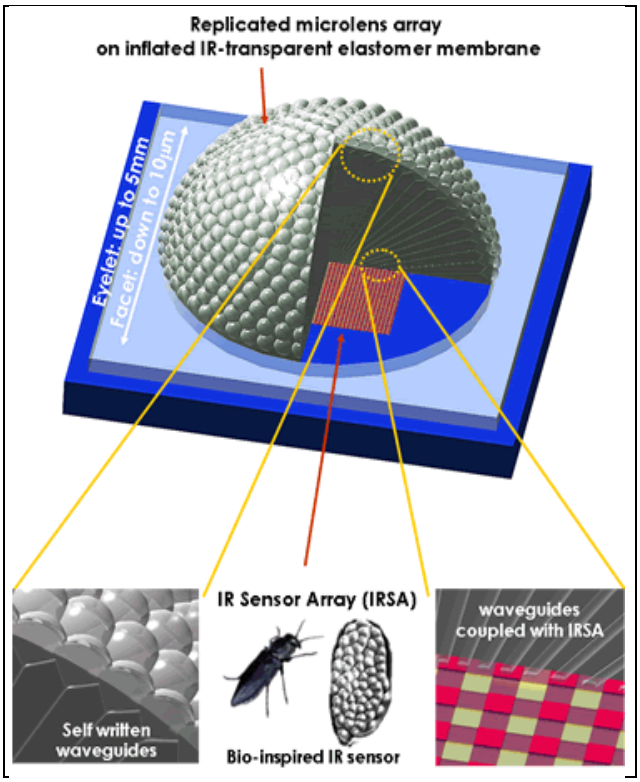

Figure 73. The Pisano group's biomimetic uncooled photomechanical IR sensor (Pisano, 2005).

8. Conclusion

A variety of low-power communications mechanisms are reviewed in this report. They have been selected to be representative of a broad range of biological mechanisms that may hold potential for engineered analogs. Recurrent themes of interest from biological systems include dual usage of structural components, fusion of multiple low-resolution sensor inputs to yield higher precision localization capability, and structural noise reduction characteristics. For example, mosquito antennae are sensitive mechanical receptors of incoming sound frequencies that also contain thermoreceptors that generate spike frequencies in the antennae to enable tracking of prey. Enhanced target strike precision is enabled in the snake by the combined use of relatively low resolution IR and chemical sensory input. Mitigation of environmental factors that could lead to false alarms in the sensory response is observed in the integrated structural mechanism of the jewel beetle, which dynamically normalizes its IR sensor response to the ambient temperature. A number of engineered analogs are presented that not only present direct biomimetic solutions (e.g., artificial hair sensors and IR sensors), but also adapt one mechanistic behavior to another mechanistic approach (e.g., the application of pheromone gradient tracking to controlled robotic swarm behavior).

The biological communications devices and mechanisms discussed in this report are presented as a foundation for further research efforts in engineered communication devices applicable to millimeter- to centimeter-scale engineered autonomous systems.

9. References

Alcock, J.; Bailey, W. J. Acoustical Communication and the Mating System of the Australian Whistling Moth Hecastesia Exultans (Noctuidae: Agaristinae). *J. of Zoology, London* **1995**, *237*, 337–352.

Alexander, R. D. Sound Production and Associated Behavior in Insects. *The Ohio J. of Science* **1957**, *57* (2), 101.

Bailey, W. J. The Mechanics of Stridulation in Bush Crickets (Tettigonioidea, Orthoptera): I. The Tegminal Generator. *J. of Experimental Biology* **1970**, *52*, 495–505.

Bailey, W. J. Resonant Wing Systems in the Australian Whistling Moth Hecastesia (Agarasidae, Lepidoptera). *Nature* **1978**, *272*, 444–446.

Bailey, W. J. *Acoustic Behaviour of Insects: An Evolutionary Perspective*; New York: Chapman and Hall, 1991.

Bakken, G. S.; Krochmal, A. R. The Imaging Properties and Sensitivity of the Facial Pits of Pitvipers as Determined by Optical and Heat-Transfer Analysis. *J. of Experimental Biology* **2007**, 2801–2810.

Barclay, R. M. Interindividual Use of Echolocation Calls: Eavesdropping by Bats. *Behavioral Ecology and Sociobiology* **1982**, *10*, 271–275.

Barth, F. G. Spider Mechanoreceptors. *Current Opinion in Neurobiology* **2004**, *14*, 415–422.

Barth, F. G.; Dechant, H.-E. Arthropod Cuticular Hairs: Tactile Sensors and the Refinement of Stimulus Transformation. In F. G. Barth, J. A. Humphrey, and T. W. Secomb, *Sensors and Sensing In Biology And Engineering*, New York: Springer, 2003, p. 159–169.

Barth, F. G.; Humphrey, J. A.; Secomb, T. W. *Sensor and Sensing in Biology and Engineering;* New York: Springer, 2003.

Barth, F. G.; Wastl, U.; Humphrey, J. A.; Devarakonda, R. Dynamics of Arthropod Filiform Hairs. II. Mechanical Properties of Spider Trichobothria (Cupiennius salei Keys.). *Philosophical Transactions: Biological Sciences* **1993**, *340* (1294), 445–461.

Bassler, B. (Presenter). Bacterial Quorum Sensing. *iBioSeminars* [ONLINE], **2008**. http://www.ibioseminars.org/index.php?option=com_contentandview=articleandid=6andItemid=37 (accessed 2010).

Bastian, J. Electrosensory Organisms. *Physics Today* **1994**, 30–37.

Sharks ‘may predict the storms’. *BBC News* [ONLINE], 25 March 2008. http://news.bbc.co.uk/2/hi/uk_news/scotland/north_east/7311847.stm (accessed 2010).

Bennet-Clark, H. C. Size and Scale Effects as Constraints in Insect Sound Communication. *Philosophical Transactions of the Royal Society London. B.* **1998**, *353*, 407–419.

Bennet-Clark, H. C. Resonators in Insect Sound Production: How Insects Produce Loud Pure-Tone Songs. *J. of Experimental Biology* **1999**, *202*, 3347–3357.

Bennet-Clark, H. C. Wing Resonances in the Australian Field Cricket Teleogryllus Oceanicus. *J. of Experimental Biology* **2003**, *206*, 1479–1496.

Boughman, J. W. Vocal Learning by Greater Spear-nosed Bats. *Proceedings of the Royal Society London B* **1998**, *265*, 227–233.

Brauchli, F. *Peacock Mantis Shrimps - Pugnacious Predators. uemis DiveWorld* [ONLINE], 23 January 2008. http://www.uemis.org/en/magazin/natur_und_wissenschaft/fangschreckenkrebse_blitzschnelle_raeuber, (accessed 20 August 2009).

Brown, A. S. From Simple Rules, Complex Behavior. *Mechanical Engineering* **2009, July**, pp. 22–27.

Brown, B.; Hughes, M.; Russo, C. Infrastructure in the Electric Sense: Admittance Data from Shark Hydrogels. *J. of Comparative Physiology A* **2005**, *191* (2), 115–123.

Bruinink, C. M.; Jaganatharaja, R. K.; de Boer, M. J.; Berenschot, J. W.; Kolster, M. L.; Lammerink, T. S.; et al. Advancements in Technology and Design of Biomimetic Flow-sensor Arrays. *22nd IEEE International Conference on Micro Electro Mechanical Systems (MEMS 2009).* Sorrento, Italy, 2009.

caesar (Center of Advanced European Studies and Research) Web site. The Pyrophilous Jewel Beetle as a Model for Micro Technological Infrared Sensors, 2010. http://www.caesar.de/infrarotsensor.html?&L=2 (accessed 5 January 2010).

Chen, N.; Tucker, C.; Engel, J. M.; Yang, Y.; Pandya, S.; Liu, C. Design and Characterization of Artificial Haircell Sensor for Flow Sensing With Ultrahigh Velocity and Angular Sensitivity. *J. of Microelectromechanical Systems* **2007**, *16* (5), 999–1014.

Chiou, T.-H.; Kleinlogel, S.; Cronin, T.; Caldwell, R.; Loeffler, B.; Siddiqi, A. et al. Circular Polarization Vision in a Stomatopod Crustacean. *Current Biology* **25 March 2008**, 429–434.

Chiu, C.; Xian, W.; Moss, C. F. Adaptive Echolocation Behavior in Bats for the Analysis of Auditory Scenes. *J. of Experimental Biology* **2009**, *212* , 1392–1404.

Cohen, D. DC Magnetic Fields from the Human Body Generally: A Historical Overview. *Neurology, Neurophysiology and Neuroscience* **2004**.

Conner, W. E. 'Un Chant D' Appel Amoureux': Acoustic Communication in Moths. *J. of Experimental Biology* **1999**, *202*, 1711–1723.

Cotton, S. Bombykol: The Sex Pheromone of the Silk Moth. University of Bristol School of Chemistry, May 2009. http://www.chm.bris.ac.uk/motm/bombykol/bombykolh.htm (accessed 24 July 2009).

Ćurčić-Blake, B.; van Netten, S. M. Source Location Encoding in the Fish Lateral Line Canal. *J.l of Experimental Biology* 2006, 1548–1559.

Currano, L. J.; Liu, H.; Gee, D.; Yang, B.; Yu, M. Microscale Implemetation of a Bio-inspired Acoustic Localization Device. *Proc. SPIE 7321, 73210B*, DOI: 10.1117/12.821675, 2009.

Cutkosky, M. R.; Howe, R. D.; Provancher, W. R. "Force and Tactile Sensors." In *Springer Handbook of Robotics*; Siciliano, B; Khatib, O., eds., Springer Berlin Heidelberg, 2008, pp. 455–476.

Davidson College (n.d.). "Electro-reception." In *The Physiology of the Ampullae of Lorenzini in Sharks*. http://www.bio.davidson.edu/people/midorcas/animalphysiology/websites/2005/DiLuzio/electro-reception.htm (accessed 14 July 2009).

Davidson College (n.d.). "Structure of the Ampullae." In *The Physiology of the Ampullae of Lorenzini in Sharks*, 2005a http://www.bio.davidson.edu/people/midorcas/animalphysiology/websites/2005/DiLuzio/structurs%20of%20ampullae.htm (accessed 14 July 2009)..

Davidson College (n.d.). "The Compass Sense" In *The Physiology of the Ampullae of Lorenzini in Sharks*, 2005b. http://www.bio.davidson.edu/people/midorcas/animalphysiology/websites/2005/DiLuzio/compass%20sense.htm (accessed 20 July 2009).

Davidson College (n.d.). "The Function of the Gel in the Ampullae".In*The Physiology of the Ampullae of Lorenzini in Sharks*, 2005c. http://www.bio.davidson.edu/people/midorcas/animalphysiology/websites/2005/DiLuzio/gel.htm (accessed 21 January 2010).

Deisboeck, T. S.; Couzin, I. D. Collective Behavior in Cancer Cell Populations. *BioEssays* **2009**, 190–197.

Dijkstra, M.; van Baar, J. J.; Wiegerink, R. J.; Lammerink, T. S.; de Boer, J. H.; Krijnen, G. J. Artificial sensory Hairs Based on the Flow Sensitive Receptor Hairs of Crickets. *J. Micromech. Microeng* **2005**, *15*, S132–S138.

Dutta, R.; Hines, E. L.; Gardner, J. W.; Boilot, P. Bacteria Classification Using Cyranose 320 Electronic Nose. *BioMedical Engineering OnLine* **2002**.

Elliott, C. J.; Koch, U. T. The Clockwork Cricket. *Naturwissenschaften* **1985**, *72*, 150.

Encyclopædia Britannica. lateral line system, 2009a. http://www.search.eb.com.proxy-um.researchport.umd.edu/eb/article-9047277 (accessed 14 July 2009).

Encyclopædia Britannica, sound reception, 2010a. http://www.search.eb.com.proxy-um.researchport.umd.edu/eb/article-38408 (accessed 10 June 2010).

Encyclopædia Britannica. resilin, 2010b. http://www.britannica.com/EBchecked/topic/499225/resilin (accessed 4 June 2010).

Encyclopædia Britannica. silkworm moth, 2010c. http://www.search.eb.com.proxy-um.researchport.umd.edu/eb/article-9067779 (accessed 6 January 2010).

Encyclopædia Britannica. olfactory receptor, 2010d. http://www.britannica.com/EBchecked/topic/549520/olfactory-receptor (accessed 11 January 2010).

Encyclopædia Britannica. snake, 2010e. http://www.search.eb.com.proxy-um.researchport.umd.edu/eb/article-64827 (accessed 12 January 2010).

Encyclopædia Britannica. Jacobson's organ, 2010f. http://www.search.eb.com.proxy-um.researchport.umd.edu/eb/article-9043211 (accessed 12 January 2010).

Encyclopædia Britannica. mechanoreception, 2010g. http://www.search.eb.com.proxy-um.researchport.umd.edu/eb/article-64720 (accessed 10 June 2010).

Encyclopædia Britannica. olfactory bulb, 2010h. http://www.search.eb.com.proxy-um.researchport.umd.edu/eb/article-9471169 (accessed 11 June 2010).

Engel, J.; Chen, J.; Bullen, D.; Liu, C. Polyurethane Rubber as a MEMS Material: Characterization and Demonstration of an All-Polymer Two-Axis Artificial Haircell Flow Sensor. *18th IEEE International Conference on Micro Electro Mechanical Systems, MEMS 2005.* Miami Beach, FL: IEEE, 2005.

Engelmann, J.; Pusch, R.; von der Emde, G. Active Sensing: Pre-receptor Mechanisms and Behavior in Electric Fish. *Communicative and Integrative Biology* **2008**, 29–31.

Fletcher, N. H. Acoustic Systems in Biology: From Insects to Elephants. *Proceedings of ACOUSTICS 2005*, 29–33.

Furry, K.; Swain, T.; Chiszar, D. Strike-Induced Chemosensory Searching and Trail following by Prarie Rattlesnakes (Crotalus viridis) Preying upon Deer Mice (Peromyscus maniculatus): Chemical Discrimination among Individual Mice. *Herpetologica* **1991**, 69–78.

Gopfert, M. C.; Briegel, H.; Robert, D. Sound-induced Antennal Vibrations in the Mosquito Aedes Aegypti. *J. of Experimental Biology* **1999**, *202*, 2727–2738.

Gopfert, M. C.; Humphris, A. D.; Albert, J. T.; Robert, D.; Hendrich, O. Power Gain Exhibited by Motile Mechanosensory Neurons in Drosophila Ears. *Proceedings of the National Academy of Sciences (PNAS), National Academy of Sciences* **2005**, *102* (2), 325–330.

Gopfert, M. C.; Robert, D. Active Auditory Mechanics in Mosquitoes. *Proceedings of the Royal Society London B* **2001**, *268*, 333–339.

Gopfert, M. C.; Robert, D. Motion Generation by Drosophilia Mechanosensory Neurons. *Proceedings of the National Academy of Sciences (PNAS), National Academy of Sciences* **2003**, *100* (9), 5514–5519.

Gopfert, M. C.; Robert, D. Nanometre-range Acoustic Sensitivity in Male and Female Mosquitoes. *Proceedings of the Royal Society London B* **2000**, *267*, 453–458.

Greenfield, M. D. *Signalers and Receivers: Mechanisms and Evolution of Arthropod Communication;* New York: Oxford University Press, 2002.

Gronenberg, W.; Pereira, J.; Tibbetts, L.; Paulk, A. Perception of Infrared Radiation. Arizona Research Laboratories Division of Neurobiology, 7 September 2001. http://web.neurobio.arizona.edu/gronenberg/nrsc581/powerpoint%20pdfs/infrared.pdf, (accessed 4 January 2010).

Halpern, M.; Cinelli, A. R.; Wang, D. Prey Chemical Signal Transduction in the Vomeronasal System of Garter Snakes. *Chemmical Signals in Vertebrates* **2006**, 242–255.

Hammer, D. X.; Seigert, J.; Stone, M. O.; Rylander, H. G.; Welch, A. J. Infrared spectral sensitivity of Melanophila acuminata. *J. of Insect Physiology* **2001**, 1441–1450.

Hazel, J.; Fuchigami, N.; Gorbunov, V.; Schmitz, H.; Stone, M.; Tsukruk, V. V. Ultramicrostructure and Microthermomechanics of Biological IR Detectors: Materials Properties from a Biomimetic Perspective. *BioMacromolecules* **2001**, 304–312.

Hickman. Fig 28-10 ampullae of Lorenzini. Memorial University Biology, 1994. http://www.mun.ca/biology/scarr/Fig28-10_ampullae_of_Lorenzini.gif (accessed 22 July 2009).

Higgins, D. A.; Pomianek, M. E.; Kraml, C. M.; Taylor, R. K.; Semmelhack, M. F.; Bassler, B. L. The Major Vibrio Cholerae Autoinducer and its Role in Virulence Factor Production. *Nature* **2007**, 883–886.

Hill, J. E.; Smith, J. D. Bats-A Natural History. *University of Texas Press, Austin Texas,* 1984.

Hofmann, M. H.; Wilkens, L. A. Temporal Analysis of Moving dc Electric Fields in Aquatic Media. *Physical Biology* **2005**, 23–28.

Holderied, M. W.; Baker, C. J.; Vespe, M.; Jones, G. Understanding Signal Design During the Pursuit of Aerial Insects by echolocating Bats: Tools and Applications. *Integrative and Comparative Biology Advance Access* **2008**.

Holland, R. A.; Waters, D. A.; Rayner, J. M. Echolocation Signal Structure in the Megachiropteran Bat Rousettus Aegyptiacus Geoffroy 1810. *J. of Experimental Biology* **2004**, *207*, 4361–4369.

Hölldobler, B.; Wilson, E. O. *The Ants;* Cambridge: Harvard University Press, 1990.

Hopkins, C. D.; Friedman, M. A. Tracking Individual Mormyrid Electric Fish in the Field using Electric Organ Discharge Waveforms. *Animal Behaviour* **1996**, 391–407.

Interrupting Cholera's Conversation. Howard Hughes Medical Institute, 15 November 2007. http://www.hhmi.org/news/bassler20071115.html (accessed 13 January 2010).

Ishida, H.; Nakamoto, T.; Moriizumi, T.; Kikas, T.; Janaka, J. Plume-Tracking Robots: A New Application of Chemical Sensors. *Biological Bulletin* **2001**, 222-226.

Izadi, N.; Jaganatharaja, R. K.; Floris, J.; Krijnen, G. Optimization of Cricket-Inspired, Biomimetic Artificial Hair Sensors for Flow Sensing. *DTIP 2007.* Stresa, Italy: EDA Publishing, 2007.

Jackson, D. E.; Ratnieks, F. L. Communication in Ants. *Current Biology* **2006**, R570-R574.

Jaganatharaja, R. K.; Bruinink, C. M.; Hagedoorn, B. M.; Kolster, M. L.; Lammerink, T. S.; Wiegerink, R. J. et al. Highly-Sensitive, Biomimetic Hair Sensor Arrays for Sensing Low-Frequency Air Flows. *Transducers 2009*, Denver, CO: IEEE, 2009, 1541–1544.

Jaganatharaja, R. K.; Izadi, N.; Floris, J.; Lammerink, T. S.; Wiegerink, R. J.; Krijnen, G. J. Adaptive, cricket-inspired artificial hair sensor arrays. *10th Annual Workshop on Semiconductor Advances for Future Electronics and Sensors (SAFE).* Veldhoven, The Netherlands, 2007.

Johnson, A. T. *Biology for Engineers*, CRC Press, 2010, http://www.amazon.com/Biology-Engineers-Arthur-T-Johnson/dp/1420077635.

Jones, G. Scaling of Echolocation Call Parameters in Bats. *J. of Experimental Biology* **1999**, *202*, 3359–3367.

Josephson, R. K.; Halverson, R. C. High Frequency Muscles Used in Sound Production by a Katydid. I. Organization of the Motor System. *The Biological Bulletin* **1971**, *141*, 411–433.

Kaissling, K.-E. "Pheromone-controlled Anemotaxis in Moths." In *Orientation and Communication in Arthropods*; Lehrer, M., ed., Birkhauser Verlag: Base, pp. 343–374.

Kaissling, K.-E. Insect Olfaction. Former Research Group Kaissling, 30 April 2001. http://www.orn.mpg.de/~kaisslin/ (accessed 6 January 2010).

Kaissling, K.-E. "The Sensitivity of the Insect Nose: The Example of Bombyx Mori." In, *Biologically Inspired Signal Processing for Chemical Sensing*; Gutiérrez, A.; Marco, S., eds., Springer Berlin/Heidelberg, 2009, pp. 45–52.

Kajiura, S.M. Head morphology and electrosensory pore distribution of carcharhinid and sphyrnid sharks. *Environmental Biology of Fishes* **2001**, *61*(2), http://www.ingentaconnect.com/content/klu/ebfi/2001/00000061/00000002/00322294.

Kardong, K. V.; Berkhoudt, H. Rattlesnake Hunting Behavior: Correlations between Plasticity of Predatory performance and Neuroanatomy. *Brain, Behavior and Evolution* **1999**, 20–28.

Karp, G. *Cell and molecular biology*, 5th edition; John Wiley and Sons, Inc.: Atlantic Highland, NJ, 2008.

Keuper, A.; Weidemann, S.; Kalmring, K.; Kaminski, D. Sound Production and Sound Emission in Seven Species of European Tettigoniids. I. The Different Parameters of the Song; Their Relation to the Morphology of the Bushcricket. *Int. J. Anim. Sound and Record* **1988**, *1*, 31–48.

Kilday, P. Mantis Shrimp Boasts Most Advanced Eyes. The Daily Californian, 28 September 2005. http://www.dailycal.org/article/19671/mantis_shrimp_boasts_most_advanced_eyes (accessed 20 August 2009).

Kimball, J.W. The Sense of Smell. Kimball's Biology Pages, 30 December 2009. http://users.rcn.com/jkimball.ma.ultranet/BiologyPages/O/Olfaction.html (accessed 11 January 2010).

Klarreich, E. The mind of the swarm. *Science News* **25 November 2006**, *170* (22), 347–349.

Krijnen, G. J.; Djkstra, M.; van Baar, J. J.; Shankar, S. S.; Kuipers, W. J.; de Boer, R. J. et al. MEMS Based Hair Flow-sensors as Model Systems for Acoustic Perception Studies. *Nanotechnology*, 2006, S84–S89.

Lavers, C.; Franks, K.; Floyd, M.; Plowman, A. Application of Remote Thermal Imaging and Night Vision Technology to Improve Endangered Wildlife Resource Management with Minimal Animal Distress and Hazard to Humans. *J. of Physics: Conference Series* **2005**, *15*, 207–212.

Lee, J.; Sponberg, S. N.; Loh, O. Y.; Lamperski, A. G.; Full, R. J.; Cowan, N. J. Templates and Anchors for Antenna-Based Wall Following in Cockroaches and Robots. *IEEE Transactions on Robotics* **2008**, *24* (1), 130–143.

Lewis Research Group Web site. Research: Electronic Nose. (n.d.). Lewis Research Group, Division of Chemistry and Chemical Engineering. http://nsl.caltech.edu/research.en.html (accessed 7 January 2010).

Liu, C. Micromachined Biomimetic Artificial Haircell Sensors. *Bioinsp. Biomim* 2007, *2*, S162–S169, doi: 10.1088/1748-3182/2/4/S05.

Liu, H.; Currano, L.; Gee, D.; Yang, B.; Yu, M. Fly-ear Inspired Acoustic Sensors for Gunshot Localization. *Proc. SPIE 7321* **2009**, *73210A* , DOI: 10.1117/12.821212.

Lynch, R. Jamming Avoidance Response Between Two Electric Fish. University of Colorado at Boulder: Auditory, Chemical and Special Senses, 24 April 2008: http://www.colorado.edu/intphys/Class/IPHY3730/image/figure8-29.jpg (accessed 12 January 2010).

Ma, E. A Highly Compliant Passive Antenna for Touch Mediated Maneuvering of a Biologically Inspired Hexapedal Robot. *Stanford Undergraduate Research Journal* **2003**, 13–17.

Marconi, E. M. *The 'Nose' Knows a Sweet Smell of Success.* NASA, 16 August 2004. http://www.nasa.gov/missions/science/f_e-nose.html (accessed 7 January 2010).

MarineBuzz.com. Marine Robots use Intelligence of Fish to Navigate at Sea, 8 January 2008. http://www.marinebuzz.com/2008/01/08/marine-robots-use-intelligence-of-fish-to-navigate-at-sea/ (accessed 17 July 2009).

Marine Specimens Educate Web Page. http://marinespecimenseducate.googlepages.com/marinespecimenseducate (accessed 2010).

Marks, R. In-depth: shark senses. PBS, 5 July 2006. http://www.pbs.org/kqed/oceanadventures/episodes/sharks/indepth-senses.html (accessed 2010).

Martin, R. A. Electroreception. Biology of Sharks and Rays, 2003 http://www.elasmo-research.org/education/white_shark/electroreception.htm#ampulla (accessed 14 July 2009).

McConney, M. E.; Chen, N.; Lu, D.; Hu, H. A.; Coombs, S.; Liu, C. et al. Biologically inspired Design of Hydrogel-capped Hair Sensors for Enhanced Underwater Flow Detection. *The Royal Society of Chemistry* **2008**, 292–295.

Meredith, M. (n.d.). Snake vomeronasal Organ (Jacobson's Organ).Florida State University program in Neuroscience. http://www.neuro.fsu.edu/~mmered/vomer/snake.htm (accessed 12 January 2010).

Michelsen, A.; Nocke, H. Biophysical Aspects of Sound Communication in Insects. *Advanced Insect Physiology* **1974**, *10*, 247–296.

Milius, S. Swarm Savvy. *Science News* **9 May 2009**, 16–21.

Milius, S. Screaming Bats Make Big Noise. *Science News* **24 May 2000**, 10.

Miller, K. Electronic Nose. *Science@NASA* **6 October 2004**.

Moss, C. F.; Bohn, K.; Gilkenson, H.; Surlykke, A. Active Listening for Spatial Orientation in a Complex Auditory Scene. *PLoS Biology 4(4)* **2006**, e79.

Muraoka, S. Environmental Recognition Using Artificial Active Antenna System with Quartz Resonator Force Sensor. *Measurement* **2005**, *37*(2) , 157–165.

Myers, P. Museum of Zoology, University of Michigan, 2008. http://animaldiversity.ummz.umich.edu/site/resources/phil_myers/blattaria/hissing_cockroach2.jpg/view.html (accessed 2010),

Nakano, R.; Ishikawa, Y.; Tatsuki, S.; Skals, N.; Surlykke, A.; Takanashi, T. (2009). Private Ultrasonic Whispering in Moths. *Communicative and Integrative Biology* 2009, *2:2*, 123–126.

NASA Jet Propulsion Laboratory Web site. Electronic Nose to Return from Space Station. California Institute of Technology, 10 September 2009. http://www.jpl.nasa.gov/news/features.cfm?feature=2309 (accessed 7 January 2010).

NASA Jet Propulsion Laboratory Web site. Frequently Asked Questions. Claifornia Institute of Technology, 2010a. http://enose.jpl.nasa.gov/faq.html (accessed 7 January 2010).

NASA Jet Propulsion Laboratory Web site. The JPL Electronic Nose. California Institute of Technology, 2010b. http://enose.jpl.nasa.gov/publications/Poster.gif (accessed 7 January 2010).

NASA Jet Propulsion Laboratory Web site. An Introduction to JPL's ENose. California Institute of Technology, 2010c. http://enose.jpl.nasa.gov/intro.html (accessed 7 January 2010).

NASA Jet Propulsion Laboratory Web site. ENose in Space. California Institute of Technology, 2010d. http://enose.jpl.nasa.gov/flightmission.html (accessed 7 January 2010).

Nelson, M. Jamming Avoidance Respone in Weakly Electric Fish. Electrosensory Signal Processing Lab, September 1996. http://nelson.beckman.illinois.edu/courses/neuroethol/models/jamming_avoidance/JAR.html (accessed 11 January 2010).

Nelson, M. C. Sound Production in the Cockroach, Gromphadorhina Portentosa: The Sound-Producing Apparatus. *J. of Comparative Physiology* **1979**, *132*, 27–38.

Pain, S. Burning Desire. *NewScientist* [ONLINE], 7 August 1999. http://www.newscientist.com/article/mg16321985.100-burning-desire.html?full=true (accessed 5 January 2010).

Parmentola, J. Micro Autonomous Systems and Technology. *Desktop Manufacturing as a Distruptive Technology* . U.S. Army: College Park, MD, 15 October 2008.

Payne, R. Lecture0322; BSCI330, College Park, MD, University of Maryland, 2010.

Payton, D.; Estkowski, R.; Howard, M. Compound Behaviors in Pheromone Robotics. *Robotics and Autonomous Systems* **2003**, *44* (3–4), 229–240.

Payton, D. *Pheromone Robotics.* HRL Laboratories: http://www.swarm-robotics.org/SAB04/presentations/payton-review.pdf (accessed 7 January 2010).

Payton, D.; Daily, M.; Hoff, B.; Howard, M.; Lee, C. Pheromone Robotics. *SPIE* **2001**, 67–75.

Pisano, A. Research. Biomimetic Infrared Nanosystems Project, 12 August 2005. http://www-bsac.eecs.berkeley.edu/groups/bmad/BIRN/research.htm (accessed 4 January 2010).

Pusch, R.; von der Emde, G.; Hollmann, M.; Bacelo, J.; Nobel, S.; Grant, K. et al. Active Sensing in a Mormyrid Fish: Electric Images and Peripheral Modifications of the Signal Carrier Give Evidence of Dual Foveation. *J. of Experimental Biology* **2008**, 921–934.

Pyk, P.; Berm´udez i Badia, S.; Bernardet, U.; Kn¨ usel, P.; Carl, M.; Gu, J. et al. An Artificial Moth: Chemical Source Localization using a Robot Based Neuronal Model of Moth optomotor Anemotactic Search. *Auton Robot* **2006**, 197–213.

Robert, D. Innovative Biomechanics for Directional Hearing in Small Flies. *Biological Bulletin 200* **2001**, 190–194.

Robert, D. Projects. Bionanoscience, School of Biological Sciences, University of Bristol, 2009. http://bionano.bris.ac.uk/projects.htm (accessed 13 August 2009).

Robert, D.; Gopfert, M. C. Acoustic Sensitivity of Fly Antennae. *J. of Insect Physiology* **2002**, *48*, 189–196.

Robert, D.; Jackson, J. C. Nonlinear Auditory Mechanism Enhances Female Sounds for Male Mosquitoes. *Proceedings of the National Academy of Sciences* **2006**, *103 (45)*, 16734–16739.

Robinson, K. Mantis shrimps see circularly polarized light. photonics.com May 2008: http://www.photonics.com/Content/ReadArticle.aspx?ArticleID=33641 (accessed 19 August 2009).

Suhr, S. H.; Song, Y. S.; Lee, S. J.; Sitti, M. Biologically Inspired Minature Water Strider Robot. *Proceedings of the Robotics: Science and Systems I* **2005**, 319–325.

Schmitz, H. *Infrared Sensory Systems in Insects.* Airforce Office of Scientific Research: Arlington, VA, 2002.

Schmitz, H.; Bleckmann, H. The Photomechanic Infrared Receptor for the Detection of Forest Fires in the Beetle Melanophila Acuminata (Coleoptera: Buprestidae). *J. of Comparative Physiology A* **1997**, 647–657.

Schmitz, H.; Mürtz, M.; Bleckmann, H. Responses of the Infrared Sinsilla of Melanophila Acuminata (Coleoptera: Buprestidae) to Monochromatic Infrared Simulation. *J. of Comparative Physiology A* **2000**, 543–549.

Shimozawa, T.; Murakami, T.; Kumagai, T. Cricket Wind Receptors: Thermal Noise for the Highest Sensitivity Known. In *Sensors and Sensing in Biology and Engineering*, Barth, F. G.; Humphrey, J. A. ; Secomb, T. W., eds., Springer: New York, NY, 2003, pp. 145–157.

Shin, B.; Kim, H-Y.; Cho, K-J. Towards a Biologically Inspired Small-scale Water Jumping Robot. *Proceedings of the 2nd Biennial IEEE/RAS-EMBS International Conference on Biomedical Robotics and Biomechatronics*, 2008, 127–131.

Shope, R.; Fisher, D. Enose is Enose is Enose. NASA Space Place, September 2000. http://spaceplace.jpl.nasa.gov/en/educators/enose_web.pdf (accessed 7 January 2010).

Sichert, A. B.; Friedel, P.; van Hemmen, J. L. Snake's Perspective on Heat: Reconstruction of Input Using an Imperfect Detection System. *Physical Review Letters* **2006**.

Simmons, J. A.; Stein, R. A. Acoustic Imaging in Bat Sonar: Echolocation Signals and the Evolution of Echolocation. *J. of Comparative Physiology* **1980**, 61–84.

Speakman, J. R.; Anderson, M. E.; Racey, P. A. The Energy Cost of Echolocation in Pipistrelle Bats (Pipistrettus pipistrellus). *J. of Comparative Physiology A: Neuroethology, Sensory, Neural, and Behavioral Physiology* **1989**, *165*, *5*, 679–685.

Stephen, R. O.; Bennet-Clark, H. C. The Anatomical and Mechanical Basis of Stimulation and Frequency Analysis in the Locust Ear. *J. of Experimental Biology* **1982**, *99*, 279–314.

Sueur, J.; Aubin, T. When Males Whistle at Females: Complex FM Acoustic Signals in Cockroaches. *Naturwissenschaften* **2006**, 500–505.

Sueur, J.; Windmill, J. F.; Robert, D. Tuning the Drum: The Mechanical Basis for Frequency Discrimination in a Mediterranean Cicada. *J. of Experimental Biology* **2006**, *209*, 4115–4128.

Surlykke, A. Hearing in Notodontid moths: a Tympanic Organ with a Single Auditory Neurone. *J. of Experimental Biology* **1984**, 323–335.

Tallarovic, S.; Zakoh, H. Electric Organ Discharge Frequency Jamming During Social Interactions in Brown Ghost Knifefish. *Animal Behavior* **2005**, 1355–1365.

The University of Nottingham Quorum Sensing Research Group. Vibrio fischeri. The quorum sensing site, 12 August 2009. http://www.nottingham.ac.uk/quorum/fischeri2.htm (accessed 13 January 2010).

TrekNature Web site. Photo by meng meng, 27 February 2008. http://www.treknature.com/gallery/Asia/Thailand/photo154910.htm (accessed 2010).

UniSci Web page. Fish's Sixth Sense Could Help Robots Navigate Oceans. 24 July 2002. http://www.unisci.com/stories/20022/0624024.htm (accessed 16 July 2009).

UniversitätBonn. The Melanophila infrared organ. insect-inspired biomimetic infrared sensors: http://www.zoologie.uni-bonn.de/Neurophysiologie/home/Schmitz/BMBF-HP/models.html (accessed 5 January 2010).

University of Queensland. Weird Shrimp Has Astounding Vision. Science Daily [ONLINE], 15 May 2008. http://www.sciencedaily.com/releases/2008/05/080513210456.htm (accessed 19 August 2009).

USDA-Forest Service. Town Ants (Atta texana). Southern Research Station: http://www.srs.fs.usda.gov/idip/spb_ii/photos_ants.html (accessed 6 January 2010).

Volpe, G. Super-Vision for Mr. Shrimp. Optics and Photonics Focus, 25 June 2008. http://opfocus.org/index.php?topic=story&v=1&s=3 (accessed 19 August 2009).

von der Emde, G. Non-Visual Environmental Imaging and Object Detection Through Active Electrolocation in Weakly Electric Fish. *J. of Comparative Physiology A* **2006**, 601–612.

von der Emde, G. Biomimetic Sensors: Active Electrolocation of Weakly Electric Fish as a Model for Active Sensing in Technical Systems. *J. of Bionic Engineering* **2007**, 85–90.

von der Emde, G.; Amey, M.; Engelmann, J.; Fetz, S.; Folde, C.; Hollmann, M. et al. Active Electrolocation in Gnathonemus petersii: Behaviour, Sensory Performance, and Receptor Systems. *J. of Physiology-Paris* **2008**, 279–290.

Walsh, D. D. The Chemistry of Moth Pheromones. *Agrichemical and Environmental News* **April 2000**, 12–13.

Weeg, M. S.; Bass, A. H. Frequency Response Properties of Lateral Line Superficial Neuromasts in a Vocal Fish, With Evidence for Acoustic Sensitivity. *J. of Neurophysiology* **2002**.

University of Virginia Web site. What is an electric fish? http://people.virginia.edu/~mk3u/mk_lab/electric_fish_E.htm (accessed 11 January 2010).

Wilcox, R. S. Communication by Surface Waves: Mating Behavior of Water Strider (Gerridae). *J. comp. Physiol* **1972**, 255–257.

Wilcox, R. S. (1989). Vibratory Signals Enhance Mate-Guarding in a Water Strider (Hemiptera: Gerridae). *J. of Insect Behavior*, 43–45.

Windmill, J. F.; Bockenhauer, S.; Robert, D. Time-resolved Tympanal Mechanics of the Locust. *J. of the Royal Society Interface 5* **2008**, 1435–1443.

Windmill, J. F.; Fullard, J. H.; Robert, D. Mechanics of a 'simple' Ear: Tympanal Vibrations in Noctuid Moths. *J. of Experimental of Biology 210* **2007**, 2637–2648.

Windmill, J. F.; Gopfert, M. C.; Robert, D. Tympanal Travelling Waves in Migratory Locusts. *J. of Experimental Biology 208* **2005**, 157–168.

Windmill, J. F.; Jackson, J. C.; Tuck, E. J.; Robert, D. Keeping up with Bats: Dynamic Auditory Tuning in a Moth. *Current Biology 16* **2006**, 2418–2423.

WooriSystems. Electronic Nose. Gas Monitors, 2001. http://www.gasmonitors.co.kr/cynose.htm (accessed 7 January 2010).

Wyatt, T. D. *Pheromones and Animal Behaviour.* Cambridge: Cambridge University Press, 2003.

San Juan, A. A Lurker's Guide to Stomatopods, 3 February 2008. http://www.blueboard.com/mantis/bio/vision.htm (accessed 2010).

Song, Y. S.; Suhr, S. H.; Sitti, M. Modeling of the Supporting Legs for Designing Biomimetic Water Strider Robots. *Proceedings 2006 IEEE International Conference on Robotics and Automation*, 2006, 2303–2311.

Song, Y. S.; Suhr, S. H.; Sitti, M. STRIDE: A Highly Maneuverable and Non-Tethered Water Strider Robot. *2007 IEEE International Conference on Robotics and Automation*, 2007, 980–984.

Yang, Y.; Chen, J.; Engel, J.; Pandya, S.; Chen, N.; Tucker, C. et al. Distant touch hydrodynamic imaging with an artificial lateral line. *Proceedings of the National Academy of Sciences of the United States of America*, 2006, 18891–18895.

Yang, Y.; Chen, N.; Tucker, C.; Engel, J.; Pandya, S.; Liu, C. *From Artificial Hair Cell Sensor To Artificial Lateral Line System Development and Application.* Urbana: University of Illinois at Urbana-Champaign, 2007.

Young, D. Do Cicadas Radiate Sound Through Their Ear-Drums? *J. of Experimental Biology* **1990**, *151*, 41-56.

Young, D.; Bennet-Clark, H. C. The Role of the Tymbal in Cicada Sound Production. *J. of Experimental Biology 198* **1995**, 1001–1019.

Zyga, L. Snakes' heat vision enables accurate attacks on prey. Physorg.com, 31 August 2006. http://www.physorg.com/news76249412.html (accessed 11 January 2010).

Appendix A. Neuron Signal Transmission Mechanism

The previous report highlights several systems that provide data input to a biological platform in a variety of ways. For actionable response, the sensory input is processed in a system specifically designed for the sensor and intended response. Three mechanisms on the cellular level are presented here to provide the reader with a biological systems perspective. Further reading is recommended in the textbook *Cell and Molecular Biology* (Karp, 2008).

The neuron signal transmission mechanism describes exactly how a signal gets from the sensor to the brain. Looking at the mechanoreceptor in a finger-pinch scenario, these particular neurons stretch from the spinal cord to the tip of the finger. The part of the neuron at the tip of the finger is the dendrite, which actually senses the pinch (or olfactory molecule or thermal change, etc., in other neurons). The dendrite sends an action potential up the axon, along the plasma membrane of the cell, until it reaches the terminal near the spinal cord. The message is transmitted from the nerve terminals to other neurons in the spinal cord, which transmit the signal to the brain. The cell body carries out critical cellular processes to keep the neuron itself alive and functional (figure A-1) (Payne, 2010).

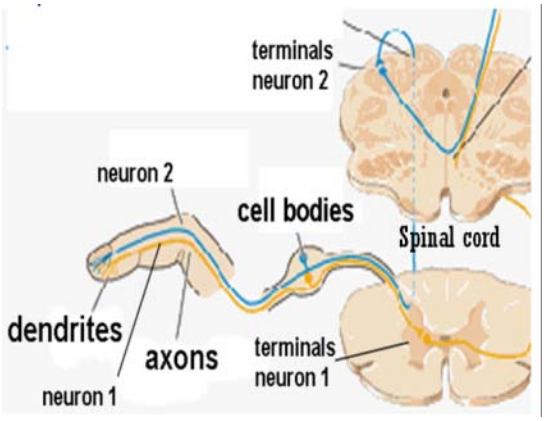

Figure A-1. Critical cellular processes involved in neuro-based messages (Payne, 2010).

Sodium-potassium pumps throughout the cell membrane maintain a high concentration of sodium (Na+) outside the cell (low inside the cell) and a high concentration of potassium (K+) inside the cell (low outside the cell). There are also calcium (Ca2+) pumps throughout the cell membrane that maintain a very low concentration of Ca2+ inside the cell. The neuron starts out with a membrane potential of –70 mV, caused by a number of potassium leak channels that allow K+ ions to continuously leak out of the cell (figure A-2: Time 1). With positive charge continuously leaking out, the membrane potential decreases until it is negative enough to prevent further outflow of K+ ions, which occurs at –70 mV. When the skin is pinched,

mechanosensitive sodium ion channels in the dendrite open, allowing Na+ ions to rush into the cell. This causes a local decrease in polarization (depolarization) of the membrane in the dendrite (Payne, 2010).

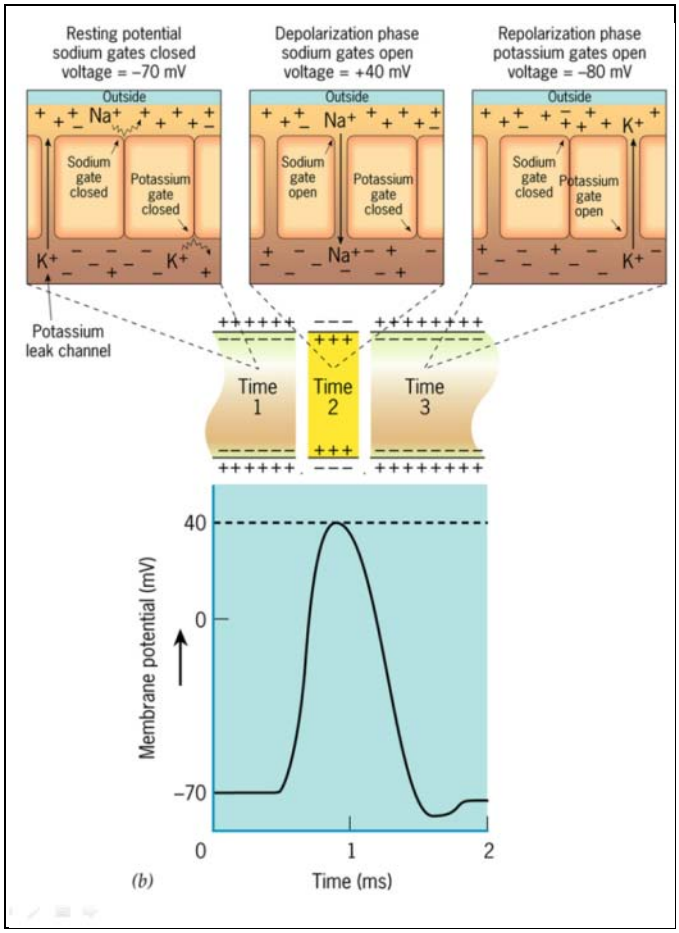

Figure A-2. Sodium-potassium pumps in neurons (Karp, 2008).

The local depolarization of the dendritic membrane causes voltage-gated sodium channels in the axon to open, allowing sodium to enter that part of the cell (figure A-2: Time 2), which depolarizes the corresponding section of membrane to approximately +40 mV (figure A-2b). This action potential propagates up the axon (figure A-3) until it reaches the terminal. Approximately 1 ms after a section of membrane has been depolarized, the voltage-gated sodium channels close and voltage-gated potassium channels open, causing the addition of sodium into the cell to cease and potassium to rush out of the cell. This repolarizes the membrane to about –80 mV, at which point the voltage-gated potassium channels close as well (figure A-2: Time 3). Then, the sodium-potassium pumps and potassium leak channels return the membrane to its original state. The action potential travels from dendrite to the terminal at the spinal cord on the order of tens of milliseconds (Payne, 2010).

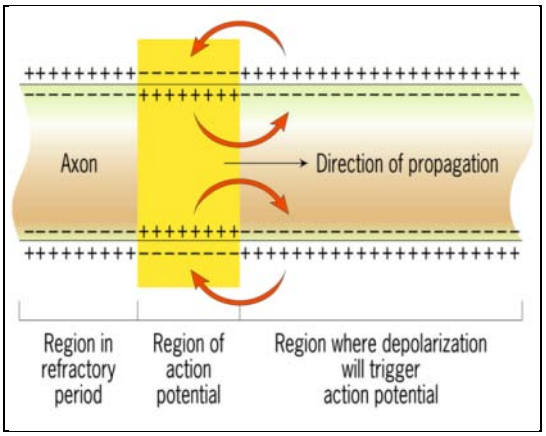

Figure A-3. The action potential as it propagates up the axon (Karp, 2008).

When the action potential reaches the terminal, the voltage-gated calcium channels in the membrane of the terminal open. The steep concentration gradient of calcium causes Ca2+ ions to rush into the cell. The increase in Ca2+ concentration causes synaptic vesicles containing acetylcholine (a neurotransmitter) to fuse with the cell membrane and release the acetylcholine into the synaptic cleft (the space between the terminal and the spinal cord nerve cell). Acetylcholine diffuses across the synaptic cleft and comes in contact with the dendrite of a spinal cord neuron, sending an action potential up that neuron's axon to the brain (figure A-4) (Payne, 2010).

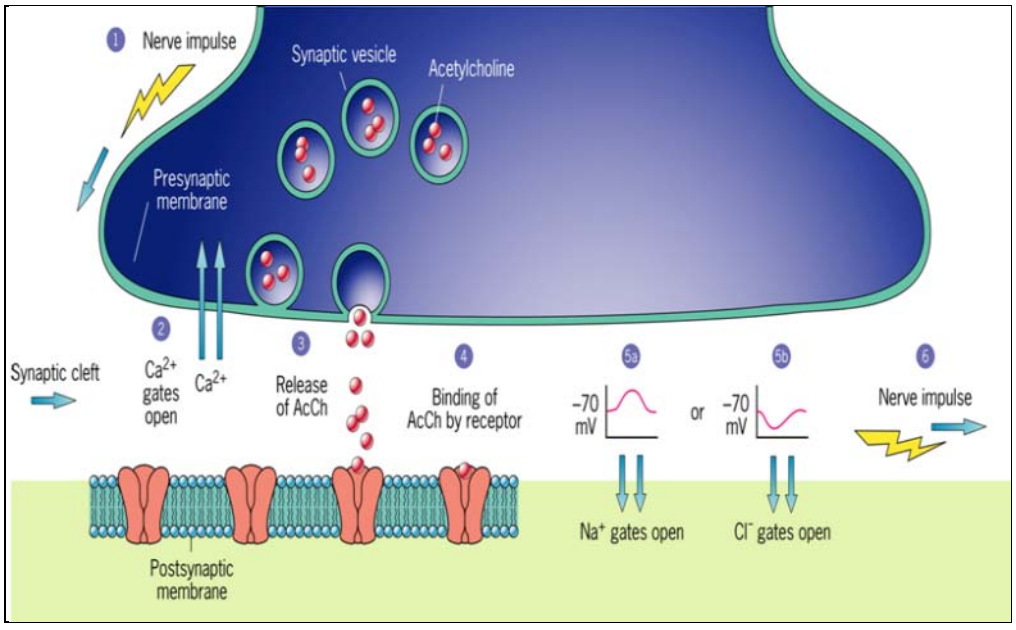

Figure A-4. Acetylcholine diffusing across the synaptic cleft and coming in contact with the dendrite of a spinal cord neuron, sending an action potential up that neuron's axon to the brain (Karp, 2008).

INTENTIONALLY LEFT BLANK.

Appendix B. Signal Amplification Mechanism in Stimulus Response

Systems with very small signal inputs often require amplification before the signal is processed. An example of biological amplification is the ryanodine receptor in the phosphoinositide cascade. Calcium ions are an impetus for many cellular processes. The cytosolic concentration of Ca2+ is kept very low (≈0.1 µM) in a resting state by pumps in the cell plasma membrane that pump Ca2+ out of the cell, and pumps in the smooth endoplasmic reticulum (SER) membrane, that pump Ca2+ out of the cytoplasm and into the smooth endoplasmic reticulum. When an event occurs that requires a calcium-initiated process, Ca2+ channels in the cell membrane can open to bring in extracellular Ca2+ (e.g., signal propagation at the nerve terminal from appendix A) or Ca2+ can flow into the cytosol from the SER through a channel called the ryanodine receptor (ex: when acetylcholine activates smooth muscle cells). When the cytosolic Ca2+ concentration raises slightly, the ryanodine receptor releases a lot of calcium from the SER into the cell, amplifying the Ca2+ signal (figure B-1) (Payne, 2010).

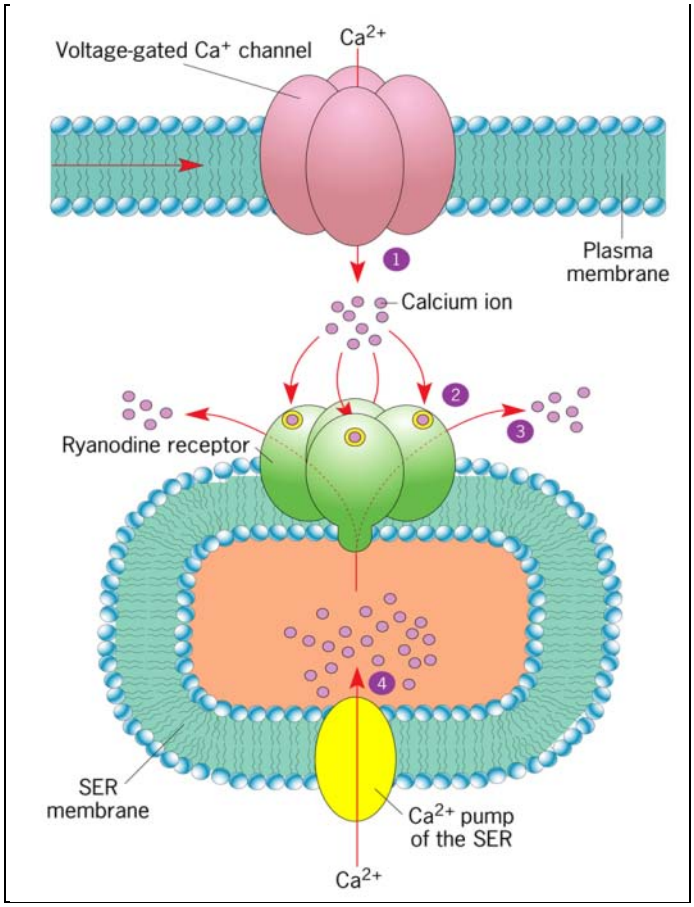

Figure B-1. When the cytosolic Ca2+ concentration raises slightly, the ryanodine receptor releases a lot of calcium from the SER into the cell, amplifying the Ca2+ signal (Karp, 2008).

The phosphoinositide cascade is one mechanism used to generate a response to a stimulus by causing vast amounts of Ca2+ to enter the cytosol and by activating an enzyme called protein kinase C (PKC). One example of the body's use of this cascade is the contraction of smooth and skeletal muscle. The phosphoinositide cascade begins when a ligand binds to a receptor on the extracellular side of the cell membrane. This activates a G-Protein, which activates the enzyme phospholipase C – beta (PLC- ß) on the intracellular side of the membrane. (PLC- ß) catalyzes the split of PIP_2 into inositol 1,4,5-triphosphate (IP_3)and diacylglycerol (DAG). DAG stays in the plasma membrane to activate PKC, and IP_3 goes to the IP_3 receptor (a ligand-gated Ca2+ channel) on the SER membrane and causes Ca2+ to be released into the cytosol (figure B-2). This small amount of Ca2+ activates the local calcium-gated ryanodine receptors on the SER membrane (figure B-1), which activate ryanodine receptors further away, and the signal propagates in the manner along the SER membrane, resulting in a large spike of cytosolic Ca2+ concentration (Payne, 2010).

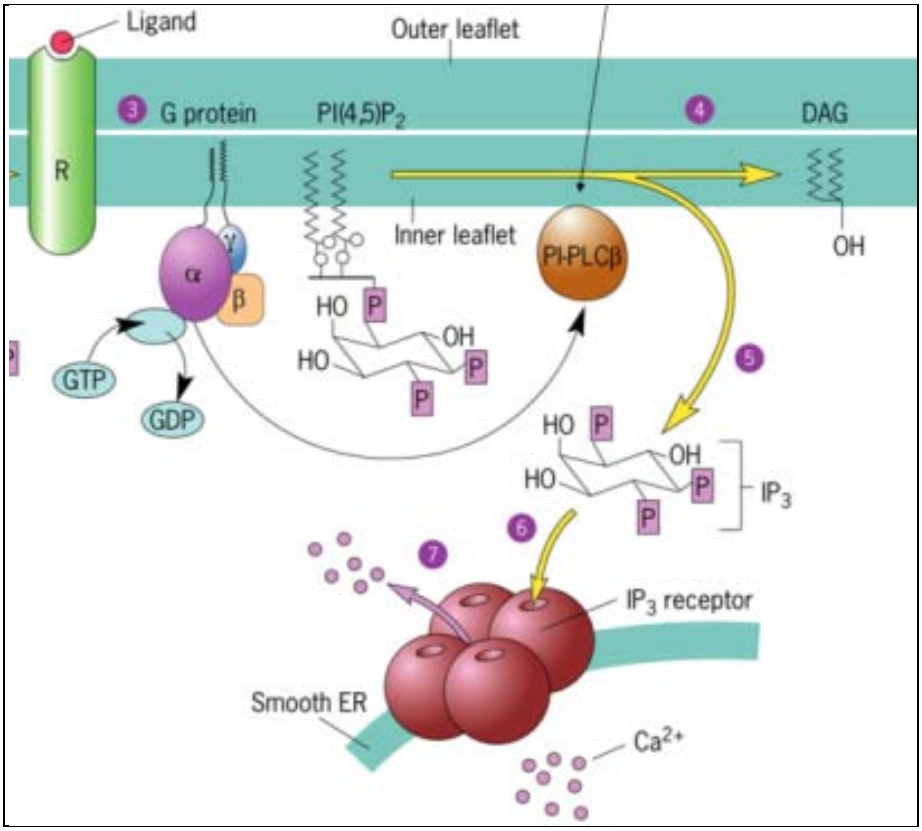

Figure B-2. This small amount of Ca2+ activates the local calcium-gated ryanodine receptors on the SER membrane (Karp, 2008).

Appendix C. Olfaction Mechanism

Olfaction (figure C-1) provides an excellent example of how a signal can be pre-processed before it reaches higher regions of the brain. Air laden with odorant molecules comes in contact with the dendrites of olfactory receptor cells. There are odorant receptor proteins in the membrane of the dendrite that bind to the odorant. Each olfactory receptor binds to only one molecule or class of molecules, and each olfactory receptor cell only expresses one type of receptor. There are hundreds of different types of receptors (≈400 in humans) and olfactory cells that express them (Karp, 2008). Smells can be identified by the combination of olfactory receptor cells that send signals to the brain. Given that the epithelium (skin inside) of the nose has millions of olfactory receptor cells, the amount of information processed by the olfactory system is huge (Payne, 2010).

When an odorant molecule binds to an odorant receptor, the odorant receptor is activated through a cascade and an action potential is sent through the axon to the olfactory bulb in the brain (Payne, 2010). The olfactory bulb has structures called glomeruli that begin the processing of olfactory information. All of the axons of nerve cells that express the same or similar odorant receptors terminate in the same glomerulus. From the glomerulus, the signal is transmitted no neurons that lead to higher parts of the brain over synapses (as seen in appendix A) (olfactory bulb, 2010).

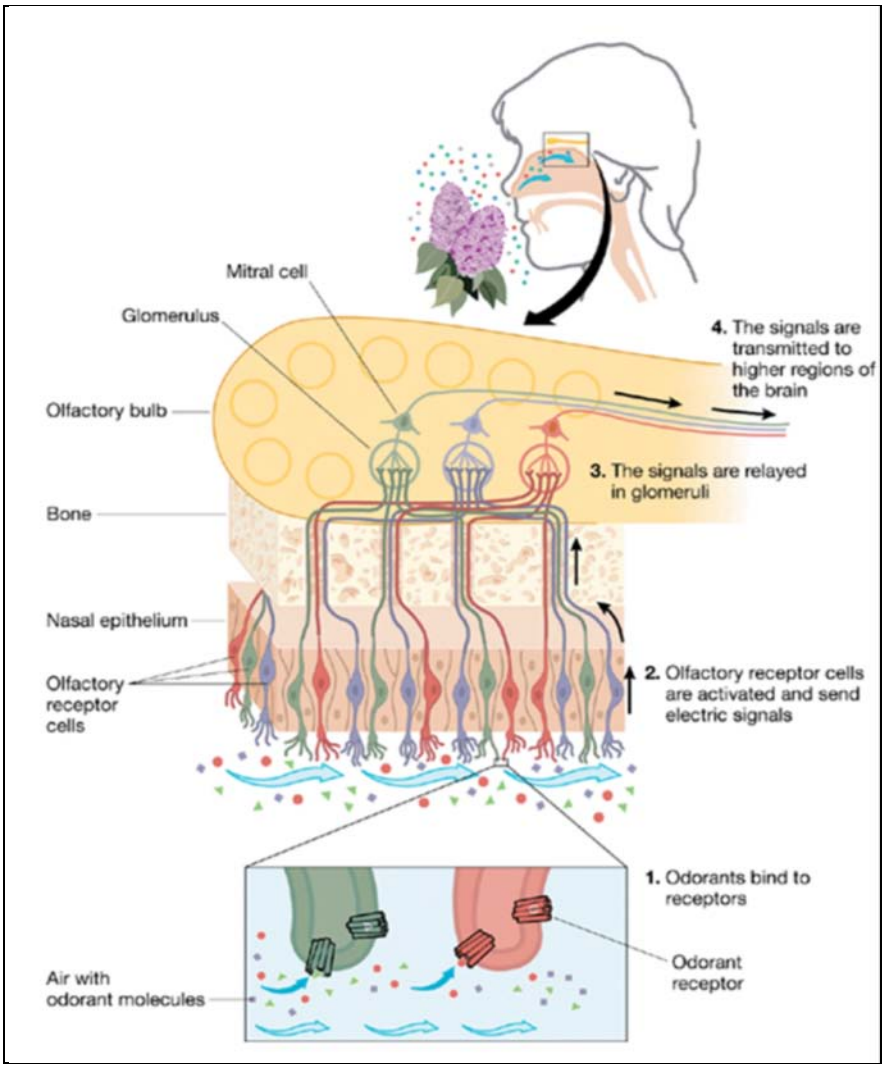

Figure C-1. A schematic of the human olfactory system (Payne, 2010).

List of Symbols, Abbreviations, and Acronyms

3-D	three dimensional
AC	alternating current
ADVR	anterior dorsal ventricular ridge
amoth	artificial moth
BBC	British Broadcasting Corporation
caesar	Center of Advanced European Studies and Research
CAI-1	Cholerae Autoinducer 1
CAI-2	Cholerae Autoinducer 2
DAG	diacylglycerol
DLGN	dorsal lateral geniculate nucleus
Enose	electronic nose (note… not in report)
EOD	electric organ discharge
HRL	Hughes Research Laboratories
IP_3	inositol 1,4,5-triphosphate
IR	infrared
ISS	international space station
JAR	jamming avoidance response
JPL	Jet Propulsion Laboratory
LGMD	lobula giant movement detector
LTTD	nucleus descendens lateralis trigemini
MEMS	micro-electromechanical system
NASA	National Aeronautics and Space Administration
NEDT	noise equivalent difference temperature
PD	proportional-derivative

PDA	personal digital assistant
PKC	protein kinase C
PLC- ß	phospholipase C – beta
RC	nucleus reticularis caloris
Rt	nucleus rotundus
SER	smooth endoplasmic reticulum
SO	schnauzenorgan
SPL	sound pressure level
STRIDE	Surface Tension Robotic Insect Dynamic Explorer
USDA	United States Department of Agriculture
UV	ultraviolet
VO	vomeronasal organ

NO. OF COPIES	ORGANIZATION
1 ELEC	ADMNSTR DEFNS TECHL INFO CTR ATTN DTIC OCP 8725 JOHN J KINGMAN RD STE 0944 FT BELVOIR VA 22060-6218
1 CD	OFC OF THE SECY OF DEFNS ATTN ODDRE (R&AT) THE PENTAGON WASHINGTON DC 20301-3080
1	US ARMY INFO SYS ENGRG CMND ATTN AMSEL IE TD A RIVERA FT HUACHUCA AZ 85613-5300
1	COMMANDER US ARMY RDECOM ATTN AMSRD AMR W C MCCORKLE 5400 FOWLER RD REDSTONE ARSENAL AL 35898-5000
1	UNIVERSITY OF MICHIGAN CENTER FOR WIRELESS INTEGRATED MICROSYSTEMS ATTN PROF K NAJAFI (2 HCS) ANN ARBOR MI 48109-2122
5	DANIEL CALDERONE 2335 EUNICE STR BERKELEY CA 94708
1	US ARMY RSRCH LAB ATTN RDRL HR L ALLENDER ABERDEEN PROVING GROUND MD 21005
1	US ARMY RSRCH LAB ATTN RDRL WM (A) BLDG 4600 ABERDEEN PROVING GROUND MD 21005
1	US ARMY RSRCH LAB ATTN RDRL CIM G T LANDFRIED BLDG 4600 ABERDEEN PROVING GROUND MD 21005-5066
1	US ARMY RSRCH LAB ATTN RDRL VT M NIXON ABERDEEN PROVING GROUND MD 21005-5066

NO. OF COPIES	ORGANIZATION
1	DIRECTOR US ARMY RSRCH LAB ATTN RDRL SL P TANENBAUM BLDG 328 ABERDEEN PROVING GROUND MD 21005-5068
83	US ARMY RSRCH LAB ATTN IMNE ALC HRR MAIL & RECORDS MGMT ATTN RDRL CI J GOWENS ATTN RDRL CII A S H YOUNG ATTN RDRL CIM L TECHL LIB ATTN RDRL CIM P TECHL PUB ATTN RDRL CIN B SADLER (2 HCS) ATTN RDRL SE J PELLEGRINO ATTN RDRL SED E SHAFFER ATTN RDRL SED E B MORGAN T ALEXANDER ATTN RDRL SEE G WOOD ATTN RDRL SEE M M WRABACK ATTN RDRL SEE O J SUMNER N FELL ATTN RDRL SER P AMIRTHARAJ J MAIT (2 HCS) ATTN RDRL SER E B HUEBSCHMAN G BIRDWELL R DEL ROSARIO R KAUL R RAO ATTN RDRL SER L A WICKENDEN (10 HCS) B PIEKARSKI (2 HCS) E ZAKAR J PULSKAMP L CURRANO R POLCAWICH W NOTHWANG (2 HCS) K JORDAN (20 HCS) A RUBIN (5 HCS) ATTN RDRL SER M E ADLER ATTN RDRL SER U C FAZI K KAPPRA ATTN RDRL SES J EICKE ATTN RDRL SES P A EDELSTEIN D HULL M SCANLON ADELPHI MD 20783-1197

TOTAL: 98 (1 ELEC, 1 CD, 96 HCS)

INTENTIONALLY LEFT BLANK.